PPARγ in myeloid cells controls CNS autoimmunity

DISSERTATION

zur

Erlangung des Doktorgrades (Dr. rer. nat.)

der

Mathematisch-Naturwissenschaftlichen Fakultät

der

Rheinischen Friedrich-Wilhelms-Universität Bonn

vorgelegt von

Stephanie Hucke

aus

Lindlar

Ahlen, Juli 2011

Angefertigt mit der Genehmigung der Mathematisch-Naturwissenschaftlichen Fakultät
der Rheinischen Friedrich-Wilhelms-Universität Bonn

Die vorliegende Arbeit wurde an den Instituten für Molekulare Medizin und
Experimentelle Immunologie am Universitätsklinikum Bonn angefertigt.

1. Gutachter: Prof. Dr. Percy Knolle
2. Gutachter: Prof. Dr. Waldemar Kolanus

Tag der Promotion: 14.12.2011
Erscheinungsjahr: 2012

Erklärung

Diese Dissertation wurde im Sinne von § 4 der Promotionsordnung vom 7.1.2004 im Zeitraum von Februar 2008 bis Januar 2011 von Herrn Prof. Dr. Percy Knolle betreut.

Eidesstattliche Erklärung

Hiermit versichere ich, dass ich die vorliegende Arbeit persönlich, selbstständig und unter Offenlegung der erhaltenen Hilfen angefertigt habe.

Ahlen, den 13. Juli 2011,

Stephanie Hucke

Meiner Familie

Auszüge dieser Arbeit waren Bestandteile folgender Publikationen und Kongressbeiträge:

Publikationen

1) *Zur Publikation eingereicht*

Hucke S* and Floßdorf J*, Dunay I, Mack M, Klockgether T, Prinz M, Knolle P, Klotz L.

„The Nuclear Receptor PPARγ Controls T Cell-mediated Licensing of CNS-macrophages and Critically Contributes to Local Control of CNS Autoimmunity"

(*contributed equally)

2) J Exp Med. 2009 Sep 28;206(10):2079-89

Klotz L, Burgdorf S, Dani I, Saijo K, Flossdorf J, **Hucke S**, Alferink J, Nowak N, Beyer M, Mayer G, Langhans B, Klockgether T, Waisman A, Eberl G, Schultze J, Famulok M, Kolanus W, Glass C, Kurts C, Knolle PA.

"The Nuclear Receptor PPAR Gamma Selectively Inhibits Th17 Differentiation in a T Cell-Intrinsic Fashion and Suppresses CNS Autoimmunity"

3) J Immunol. 2009 Jul 1;183(1):129-36

Klotz L* and **Hucke S***, Thimm D, Classen S, Gaarz A, Schultze J, Edenhofer F, Kurts C, Klockgether T, Limmer A, Knolle P, Burgdorf S.

"Increased Antigen Cross-Presentation But Impaired Cross-Priming After Activation of Peroxisome Proliferator-Activated Receptor Gamma is Mediated by Up-Regulation of B7H1"

(*contributed equally)

Kongressbeiträge

September 10	Posterpräsentation auf dem 40th Annual Meeting of the German Society for Immunology, Leipzig "PPARγ Activation Ameliorates EAE by Reducing Immunogenicity of CNS Macrophages and Microglia."
September 09	Posterpräsentation auf dem 2nd European Congress of Immunology, Berlin "Increased Antigen Cross-Presentation But Impaired Cross-Priming After Activation of Peroxisome Proliferator-Activated Receptor Gamma is Mediated by Up-Regulation of B7H1."
September 08	Vortrag auf dem Joint Annual Meeting of Immunology of the Austrian and German Societies (ÖGAI, DGFI) "PPARγ Enhances Uptake and Cross-presentation of Soluble Antigen in Dendritic Cells."

Abstract

The nuclear receptor peroxisome proliferator-activated receptor gamma (PPARγ) is a ligand-activated transcription factor that regulates the immunogenicity of myeloid cells such as dendritic cells (DCs), macrophages, and microglia. In this thesis, we investigated two novel aspects of PPARγ-mediated modulation of immune responses.

First, we characterised the impact of PPARγ activation on cross-presentation of soluble antigen by DCs and subsequent cross-priming of naive $CD8^+$ T cells. We demonstrated that treatment with the synthetic PPARγ agonist PIO significantly increased MR expression in DCs *in vitro* and *in vivo* which in turn resulted in enhanced MR-mediated uptake of the soluble model antigen OVA and elevated levels of cross-presented OVA. Importantly, after PPARγ-activation, DCs significantly upregulated the coinhibitory molecule B7H1 which impaired activation of naive $CD8^+$ T cells and resulted in strongly reduced $CD8^+$ T cell effector functions. Importantly, these data unveil a new mechanism of antigen-specific $CD8^+$ T cell inactivation by DCs that results from increased cross-presentation and concomitant coinhibitory signalling via B7H1.

In the second part of this thesis, we revealed that during the effector phase of experimental autoimmune encephalomyelitis (EAE), PPARγ limits myeloid cell-mediated autoimmune inflammation. We identified $CCR2^+$Ly-$6C^{hi}$ inflammatory monocytes as the key myeloid cell population regulated by PPARγ and showed that a distinct population of inflammatory monocytes differentiated into microglial cells after infiltration of the central nervous system (CNS). PPARγ-mediated modulation of CNS myeloid cell immunogenicity resulted in dampening of both directions of myeloid cell – encephalitogenic $CD4^+$ T cell interaction. Firstly, activation of PPARγ in CNS macrophages and microglia reduced the expression of MHC-II and CD40, both of which are important for local reactivation of autoreactive T cells. In line with this, we observed that T_H1 and T_H17 responses were diminished in the CNS. Secondly, PPARγ activation in myeloid cells increased the threshold towards T cell-mediated licensing resulting in reduced T cell-induced innate immune responses, i.e. production of nitric oxide or tumor necrosis factor-alpha. Hence, these data demonstrate that modulation of

myeloid cell immunogenicity during ongoing CNS inflammation is a very effective strategy to interefere with reciprocal interaction of autoreactive T cells and CNS myeloid cells which critically contributes to cessation of CNS autoimmunity.

Taken together, the studies presented in this thesis identify PPARγ in myeloid cells as a promising candidate for the development of therapeutic approaches aimed at the control of excessive autoimmune responses. Importantly, we provide evidence that targeting PPARγ in myeloid cells interferes with ongoing inflammation in multiple aspects, namely with T cell priming and/or local reactivation but also with T cell-mediated licensing of myeloid cells.

Zusammenfassung

Der nukleäre Peroxisom-Proliferator-aktivierte Rezeptor gamma (PPARγ) ist ein durch Liganden aktivierter Transkriptionsfaktor, der die Immunogenität von myeloiden Zellen, wie zum Beispiel dendritischen Zellen (DZ), Makrophagen und Mikroglia reguliert. In der vorliegenden Arbeit wurden zwei bislang unbekannte Aspekte der PPARγ-vermittelten Modulation von Immunantworten untersucht.

Im ersten Teil der Arbeit konnten wir zeigen, dass PPARγ die Fähigkeit von DZ zur Kreuzpräsentation von löslichem Antigen und die anschließende Aktivierung von naiven $CD8^+$ T Zellen reguliert. Die Aktivierung von PPARγ in DZ durch den synthetischen Liganden PIO führte zu einer signifikant erhöhten Expression des Mannoserezeptors (MR) *in vitro* und *in vivo*, was in einem Anstieg sowohl der MR-vermittelten Aufnahme des löslichen Modellantigens Ovalbumin (OVA) als auch der Menge an kreuzpräsentiertem OVA resultierte. Weiterhin konnte beobachtet werden, dass eine PPARγ-Aktivierung in DZ eine starke Hochregulation des koinhibitorischen Moleküls B7H1 induzierte, welche die Aktivierung von naiven $CD8^+$ T Zellen und deren Differenzierung in Effektorzellen verhinderte. Zusammenfassend lässt sich sagen, dass in dieser Studie ein neuer Mechanismus der antigen-spezifischen $CD8^+$ T Zell-Inaktivierung durch DZ aufgezeigt werden konnte, der durch die Kombination aus erhöhter Kreuzpräsentation mit gleichzeitiger Hochregulation des koinhibitorischen Moleküls B7H1 vermittelt wird.

Im zweiten Teil dieser Arbeit konnte gezeigt werden, dass PPARγ in myeloiden Zellen während der Effektorphase der experimentellen autoimmunen Enzephalomyelitis (EAE) eine wichtige Rolle spielt, da PPARγ die durch myeloide Zellen verursachte autoimmune Entzündungsreaktion hemmt. Des Weiteren konnten wir zeigen, dass die Population der $CCR2^+Ly\text{-}6C^{hi}$ inflammatorischen Monozyten die zentrale myeloide Zellpopulation darstellt, die durch PPARγ reguliert ist und dass inflammtorische Monozyten nach Einwanderung ins zentrale Nervensystem (ZNS) zu Mikroglia differenzieren können. Die PPARγ-vermittelte Modulation der Immunogenität von myeloiden Zellen des ZNS führte zu einer Abschwächung beider Richtungen der

Interaktion von myeloiden und enzephalitogenen T Zellen. Zum Einen reduzierte die Aktivierung von PPARγ in myeloiden Zellen die Expression von MHC-II Molekülen und CD40, die bei der lokalen Reaktivierung von autoreaktiven T Zellen eine wichtige Rolle spielen, und wir konnten zeigen, dass gleichzeitig die T_H1 und T_H17 Antworten im ZNS reduziert waren. Auf der anderen Seite erhöhte die Aktivierung von PPARγ in myeloiden Zellen die Reizschwelle gegenüber T Zell-vermittelter Aktivierung, was zu einer Reduktion der T Zell-induzierten innaten Immunantworten, wie z.B. der Produktion von Stickoxid und Tumornekrosefaktor-alpha, führte. Zusammengenommen zeigen diese Daten, dass die Modulation der Immunogenität von myeloiden Zellen während einer Inflammation des ZNS einen sehr effektiven Ansatz darstellt, um die wechselseitige Aktivierung von myeloiden Zellen und enzephalitogenen T Zellen zu hemmen.

Die hier präsentierten Studien zeigen auf, dass die Aktivierung von PPARγ in myeloiden Zellen einen erfolgversprechenden Ansatz für die Entwicklung von Therapien ist, die die Behandlung von Autoimmunerkrankungen zum Ziel haben. Ein wichtiger Aspekt, der in dieser Arbeit gezeigt werden konnte, ist, dass die Aktivierung von PPARγ in myeloiden Zellen in mehrerer Hinsicht abschwächend auf anhaltende Inflammation wirkt: Zum einen hemmt es T Zell (Re-)Aktivierung, zum anderen verhindert es die durch T Zellen vermittelte Aktivierung von myeloiden Zellen.

1 Introduction

1.1 The immune system

The mammalian immune system is responsible for the host defence against invading pathogens and is traditionally divided into two parts, namely the innate and the adaptive immune system[1]. While the innate immune system is highly conserved among species, only vertebrates are able to mount antigen-specific and long-lasting adaptive immunity[2]. The innate immune system is the first line of host defence and includes cellular and biochemical defense mechanisms that are in place before infection and mediate fast activation of the innate immune response after exposure to pathogens. In contrast, the highly specific adaptive immune system is involved in the elimination of the infection at a later phase of the immune response as antigen-specific clones first need to proliferate and differentiate into effector cells before they can mediate protection. Furthermore, the adaptive immune system is involved in the generation of immunological memory[3].

1.1.1 The innate immune system

The innate immune system consists of several distinct components that are rapidly activated after exposure to pathogens and limit the infection. These components include:

- Epithelial surfaces, e.g. the skin or mucosal epithelia, which function as physical barriers to prevent intrusion of microbes[2].
- Circulating cells, including dendritic cells (DCs) or macrophages, which are important for detection and elimination of pathogens[2].
- Soluble mediators which include peptides that act as natural antibiotics, members of the complement system that play a role in opsonisation and lysis of microorganisms, as well as cytokines that regulate and coordinate the activity of innate as well as adaptive immune cells[3].

Cells of the innate immune system express germ line-encoded pattern-recognition receptors (PRRs) that recognise conserved structures expressed by many microorganisms. Although these pathogen-associated molecular patterns (PAMPs) are distinct with regard to their chemical structure, all share some general characteristics.

Firstly, they are only produced by pathogens and not by the host. Secondly, PAMPs are often essential for the survival or pathogenicity of the microorganism. Thirdly, structures are invariant and common to many pathogens[1]. Upon recognition of a PAMP by its specific PRR, the PRR-expressing cell becomes activated and performs effector functions, like phagocytosis or activation of proinflammatory signalling pathways resulting in production of proinflammatory cytokines like interleukin-6 (IL-6), IL-12, or tumor necrosis factor-alpha (TNF-α). Furthermore, the production of nitric oxide (NO) or reactive oxygen species (ROS) contributes to efficient clearance of phagocytosed pathogens[2-4].

DCs are professional antigen-presenting cells (APCs) that represent a critical link between innate and adaptive immunity as they play a central role in the activation and differentiation of naive T lymphocytes which belong to the adaptive immune system. Immature DCs are present in most tissues where they act as sentinels, continuously sampling the environment. Upon encounter with a powerful immunological stimulus, e.g. the recognition of PAMPs by PRRs[5], the DC matures which leads to phenotypical and functional changes that are the prerequisite for the activation of antigen-specific T cells. During maturation, DCs loose the ability to take up and process antigen from the environment while the surface expression levels of molecules important for effective T cell activation are upregulated, namely major histocompatibility complexes (MHC) and the costimulatory molecules CD80, CD86, and CD40[6]. Furthermore, the expression of chemokine receptors (CCRs), which are responsible for homing to peripheral tissues, are downregulated and the expression of CCR7 is upregulated[7]. Expression of CCR7 mediates DC migration towards and entry into the T cell areas of secondary lymphoid organs which allows close contact of antigen-presenting DCs with naive T cells. Recognition of the specific antigen complexed to the MHC molecule results in activation of the T cell[8].

1.1.2 The adaptive immune system

The adaptive immune response is divided into a B cell-mediated humoral and a T cell-mediated cellular immune response[3]. Every B and T cell, respectively, carries a unique, highly antigen-specific receptor on the surface that is not germ line-encoded but generated during the development of each cell by a process termed somatic

recombination[1,2]. The B cell receptor (BCR) is expressed membrane-bound or as its soluble form, the antibody, and recognises diverse three-dimensional structures. Extracellular microbes and their toxins are targets of the humoral immune response. Binding of foreign antigens by antibodies and subsequent recognition of these complexes by innate immune cells results in activation and induction of effector mechanisms like phagocytosis or production of proinflammatory cytokines in these cells[3].

The cellular immune response is mediated by T lymphocytes and is important for the clearance of infections with intracellular pathogens. In contrast to the BCR, the T cell receptor (TCR) recognises its specific antigen only as antigen-derived peptide presented on MHCs on the surface of APCs. T cells are divided into $CD4^+$ and $CD8^+$ T cells which carry out different effector functions and recognise peptides in the context of different MHC molecules. $CD4^+$ T cells recognise peptides bound to MHC class II molecules (MHC-II) and differentiate into T helper cells which play an important role in full activation of B cells and in licensing of DCs to activate naive $CD8^+$ T cells. In contrast, $CD8^+$ T cells respond to peptides in the context of MHC class I molecules (MHC-I) and differentiate into cytotoxic T lymphocytes that efficiently eliminate infected cells[3,9].

After recognition of the specific antigen, B and T cells strongly proliferate and differentiate into effector cells which clear the infection. After the elimination of the pathogen, numbers of effector cells strongly decline. Some of the antigen-specific lymphocytes differentiate into long-living memory cells which remain in a quiescent state for years after the antigen has been cleared. Upon reexposure to the specific antigen, memory cells get activated and are able to mediate a rapid and enhanced adaptive immune response[10,11].

1.1.3 Antigen presentation

$CD4^+$ and $CD8^+$ T cells recognise their specific peptide antigens only if these are presented by APCs on MHC-II and MHC-I molecules, respectively. MHC-I molecules are expressed by all nucleated cells whereas MHC-II molecules are expressed by APCs of the immune system.

MHC-I molecules present mainly endogenous peptides which are of cytosolic origin where proteins are degraded by the proteasome. However, in case of an infection, the

cell also presents pathogen-derived peptides which results in recognition and elimination of the infected cell by cytotoxic $CD8^+$ T cells finally leading to the clearance of infection[9,12].

MHC-II molecules are expressed by professional APCs like DCs and present extracellular-derived antigens. For the generation of MHC-II-restricted antigens, extracellular antigens are internalised, degraded in lysosomes by lysosomal proteases, and loaded on MHC-II molecules[9,13,14]. Recognition of the antigen by antigen-specific $CD4^+$ T cells results in activation and differentiation into T helper cells that are essential for full activation of macrophages, B cells, and $CD8^+$ T cells *in vivo*[3]. In addition to this "classical antigen presentation", DCs are capable of presenting extracellular antigens on MHC-I molecules, a process termed cross-presentation, that enables DCs to activate naive $CD8^+$ T cells to become cytotoxic effector cells (cross-priming)[15,16]. It was shown that DCs are the main cell-type *in vivo* that is capable of cross-priming $CD8^+$ T cells[13] which plays a role in a variety of processes, including the induction of immune responses against viruses that do not directly infect DCs[16-19].

In vivo, several subsets of DCs have been described that exhibit different capabilities to cross-present antigens probably due to differential gene expression[20]. Among these subsets, splenic $CD8\alpha^+$ DCs are the most efficient in cross-priming $CD8^+$ T cells[20,21]. However, so far, intracellular compartments involved in cross-presentation are not well defined although there is strong evidence that phagocytosed antigen reaches the cytosol after internalisation and that antigen processing occurs there[22,23]. Recently, Burgdorf et al. demonstrated that the route by which antigen is taken up determines the way of subsequent presentation of antigen-derived peptides, i.e. whether antigen is presented via the classical route on MHC-II or cross-presented on MHC-I molecules[24,25]. In their study they demonstrated that the soluble model antigen ovalbumin (OVA) was presented on MHC-II molecules when it was taken up via pinocytosis or scavenger receptor-mediated endocytosis whereas OVA-derived peptides were cross-presented on MHC-I molecules when OVA was endocytosed via the mannose receptor (MR)[24-26]. Importantly, cross-presentation of OVA depended on the MR as MR-deficient DCs were not capable of cross-presenting OVA[25]. Following MR-mediated uptake of OVA, the antigen was targeted into a special type of stable early endosomal compartments

which did not mature into lysosomes. In these endosomal compartments OVA-derived peptides were loaded onto MHC-I molecules for efficient cross-presentation[24].

1.1.4 T cell activation

The recognition of the cognate antigen presented on MHC molecules by APCs by the TCR of a naive T cell is a prerequisite for its activation and generally referred to as signal 1[10]. However, signal 1 alone promotes T cell inactivation, e.g. by induction of anergy or deletion as for full activation, T cells depend on additional signals, i.e. costimulation via CD80 and CD86 (signal 2) as well as cytokines (signal 3) which are provided by the antigen-presenting APC. Delivery of these three signals results in the induction of a potent adaptive immune response[27]. In addition to indirect tolerance induction due to lack of signals 2 and 3, APCs are capable to induce tolerance directly by signalling through coinhibitory molecules like B7H1 or B7DC which bind to PD1 on the surface of T cells resulting in T cell inactivation[28].

Furthermore, APC-derived cytokines, i.e. signal 3, influence the differentiation of naive $CD4^+$ T cells into distinct T helper (T_H) cell subsets with different effector mechanisms. Initially two T_H subsets had been described: T_H1 cells, which produce interferon (IFN)-γ and induce strong cell-mediated immunity e.g. by activation of macrophages, and T_H2 cells, which secrete IL-4, IL-13, and IL-25 and support B cell antibody production[10]. In addition to these classical T_H cell subsets, a third subset of T_H cells has been identified, namely T_H17 cells, which are characterised by production of IL-17A, IL-17F, and IL-22. Although T_H17 cells mediate protection against a variety of pathogens, they also have been linked to the development and pathology of autoimmune diseases such as multiple sclerosis (MS) and collagen-induced arthritis[29-31].

1.1.5 Autoimmunity

During lymphocyte development also self-reactive lymphocytes develop which express receptors that recognise self antigens and could mediate immune responses against non-harmful self-antigens. However, during their development, all B and T cell precursors undergo different processes of selection during which self-reactive lymphocytes are eliminated or inactivated, resulting in a state that is referred to as self-tolerance[3]. Central tolerance of T cells is induced in the thymus and results in depletion of the vast majority

of autoreactive T cells. In a first step, immature T cells undergo a positive selection process that ensures that only those T cells survive that recognise self-MHC molecules whereas T cells that cannot recognise MHC molecules die by apoptosis. This ensures that surviving T cells will recognise antigenic-peptides bound to MHC molecules on APCs in the periphery and thus be able to efficiently mount an immune response. In a second step, T cells that bind with high affinity to self-antigens presented on MHC molecules are depleted by induction of apoptosis resulting in a pool of mature non-self-reactive $CD4^+$ or $CD8^+$ T cells that egress to the periphery.

Self-reactive T cells that escape central tolerance are subject to peripheral tolerance induction which is mediated in several ways: Antigen recognition without adequate costimulation or in the presence of inhibitory signals induces clonal anergy, which is the incapability to respond to the antigen, and repeated recognition of the antigen in this context results in apoptosis. In addition, regulatory T cells (T_{regs}) play an essential role in peripheral tolerance induction as T_{regs} produce transforming growth factor-beta and IL-10 which suppresses activity of effector T cells. Deficiency in or dysfunction of these cells causes systemic autoimmunity, thus demonstrating the crucial importance of regulatory T cells for maintenance of peripheral tolerance[32,33].

Breakdown of self-tolerance results in autoimmune diseases which can be broadly divided into systemic autoimmune diseases, like systemic lupus erythematosus, or organ-specific, localised autoimmune disorders, like type I diabetes mellitus, thyroiditis, and MS, depending on the principal pathology of disease[3,34].

1.2 Central nervous system autoimmunity

1.2.1 Multiple sclerosis

MS is a chronic disease of the central nervous system (CNS) that is the leading cause of nontraumatic disability in young adults in the United States and Europe[35]. The etiology of MS is unknown. However, genes like certain human leukocyte antigen (HLA) class II alleles involved in antigen presentation to $CD4^+$ T cells as well as environmental factors, e.g. viral infections or migration from low- to high-risk areas before adolescence, have been associated with the risk of developing disease[36-39].

About 80 % of patients have a relapsing-remitting disease course which typically starts in the second or third decade of life and has a female predominance of about 2:1. The course of MS in an individual patient is unpredictable. However, sensory disturbances, limb weakness, unilateral optic neuritis, neurogenic bladder, and bowel symptoms are some of the typical symptoms described during onset of disease. During a relapse, clinical symptoms establish within several days, stabilise, and improve in response to corticosteroids but also spontaneously. Persistent signs of CNS dysfunction may remain after such a relapse and furthermore, the disease may progress between acute relapses which is referred to as secondary progressive MS. It is estimated that about 50 % of the patients will need help walking within 15 years after disease onset[40].

Up to now, IFN-β is a prominent treatment for relapsing-remitting MS although IFN-β-based drugs are limited in their efficacy as they reduce the frequency of relapses only by about 30 %[41]. Furthermore, as IFN-β therapy is accompanied by serious side effects like flu-like symptoms, skin reactions, or depression, many patients terminate the therapy. Although the precise action of IFN-β is largely unknown, it could be demonstrated in mice that CNS myeloid cells are the main cell population targeted by IFN-β-administration resulting in reduced myeloid cell activation which regulated the effector phase of CNS autoimmunity[42]. Glatiramer acetate (GA) is a random polymer of four amino acids found in the MS-associated antigen myelin basic protein. Treatment with GA reduces the frequency of relapses in patients with relapsing-remitting MS and promotes the development of T_H2 cells in humans[43,44] It is assumed that these T_H2 cells infiltrate the CNS during MS where they cross-react with myelin autoantigens and release anti-inflammatory cytokines like IL-4 or IL-10[45]. Novel treatment strategies which are currently under investigation comprise strategies that prevent neurodegeneration or disable a component of the immune system. One example for such treatment is the antibody Natalizumab, which binds to the α4β1 integrin, also known as very late antigen-4, expressed by activated lymphocytes and monocytes. Binding of Natalizumab to α4β1 results in inhibition of inflammatory cell trafficking to the CNS and reduces the risk of relapses by 70 % as well as the risk of sustained accumulation of disability[46]. However, despite strong efforts in pharmaceutical research, up to now no drug compound has been identified that completely prevents disease progression or stably reverses disability.

The neuropathology of MS in early stages is characterised by the formation of acute inflammatory lesions following a breakdown of the blood-brain barrier (BBB)[47]. Studies of human tissue derived from MS patients show that in early inflammatory lesions microglia and macrophages exhibit an activated phenotype characterised by expression of HLA class II. Although only few cell infiltrates are present in early inflammatory lesions, such infiltrates increase with time[48] and are characterised by the accumulation of monocyte-derived and perivascular macrophages as well as the presence of T cells[49]. Several weeks after initiation, lesions are characterised by a leaky BBB, demyelinated areas, and the presence of cytokines and chemokines. Following remission phases, remyelination takes place, however it is usually incomplete[48,50].

MS is thought to be a T cell-mediated autoimmune disease and it is hypothesised that the initial event, which leads to the onset of MS, is the activation of autoreactive T cells in peripheral lymphoid tissues. CNS-derived antigens are mainly presented by APCs in cervical lymph nodes which are considered to be the draining lymph nodes of the brain. Responding T cells proliferate and migrate to the CNS where they reencounter their specific antigen on local APCs which are located at the perivascular space surrounding blood vessels of the CNS[51]. Local reactivation of encephalitogenic T cells results in induction of effector functions, such as cytokine and chemokine production, that lead to further recruitment and activation of additional immune cells such as inflammatory monocytes and B cells, thereby contributing to the perpetuation of disease[52,53].

1.2.2 Experimental autoimmune encephalomyelitis

The animal model experimental autoimmune encephalomyelitis (EAE) has been used to investigate the disease of MS in rodents and some monkeys. To initiate disease, susceptible animals are immunised with peptide epitopes derived from myelin proteins in complete Freund's adjuvant. After 1 to 2 weeks, animals develop clinical and neuropathologic signs characterised by cell infiltration of lymphocytes and macrophages which resemble the alterations observed in MS patients[52]. The disease course of EAE is divided into a T cell-mediated induction phase, which comprises the initial events of T cell priming and T cell-mediated initiation of disease, and the effector phase, which is characterised by CNS infiltration of leukocytes, establishment of local inflammation, and demyelination. EAE is, like MS, a T cell-mediated disease that can

be induced in naive animals by transfer of $CD4^+$ T cells derived from diseased animals[54]. Among activated $CD4^+$ T cells, cells of the T_H17 lineage which express CCR6 have been demonstrated to be essential for the induction of disease. After entry of $CCR6^+$ T cells into the CNS, more T cells, including $CCR6^-$ T_H1 cells, are recruited to the CNS in a CCR6-independent manner[55]. Within the CNS, encephalitogenic T cells interact with myeloid cells, i.e. microglial cells and recruited inflammatory monocytes and macrophages, which results in local reactivation of T cells. Moreover, interaction also leads to reciprocal activation of myeloid cells e.g. by T cell-derived granulocyte macrophage colony-stimulating factor (GM-CSF)[56] or IFN-γ[57] or via CD40-CD40 ligand (CD40L) interaction[58,59], a process referred to as licensing of myeloid cells. Upon activation, macrophages and microglia produce proinflammatory cytokines and neurotoxic mediators which strongly contribute to perpetuation of disease[60,61].

1.2.3 Role of myeloid cells in CNS inflammation and autoimmunity

Although autoreactive T cells are important for the initiation of EAE, many studies provide evidence that the main effector mechanisms leading to demyelination and CNS-inflammation are mediated by other cell types[60]. Especially myeloid cells, including CNS-resident microglia and infiltrating inflammatory monocytes and macrophages, respectively, have been identified to play a crucial role in perpetuation of disease[62-64] as they actively contribute to inflammatory processes within the CNS and disease pathology, i.e. demyelination and axonal damage, by production of proinflammatory cytokines, like TNF-α or IL-12, and neurotoxic mediators, such as NO and ROS, resulting in perpetuation of disease[60,61].

Microglia are CNS-resident immune cells that exhibit a ramified morphology and express low levels of molecules associated with macrophage function in the steady state[65]. They constantly screen the surrounding area without disturbing neuronal structures. However, if an injury is detected, microglia rapidly change their phenotype and migrate to the place of injury[66]. During EAE, microglial paralysis results in amelioration of disease demonstrating that microglia actively contribute to disease pathology[62] and it has been shown that microglia interact with infiltrating autoreactive T cells by T cell-derived GM-CSF, IFN-γ, or via CD40 which results in activation of microglia[56,57,59]. Furthermore, inflammatory monocytes which are characterised by

expression of CCR2 and high levels of Ly-6C play a crucial role during the effector phase of EAE. After recruitment to the CNS, inflammatory monocytes differentiate into mature macrophages and upregulate inflammatory mediators like IL-12, TNF-α, or inducible nitric oxide synthase (iNOS)[64]. Ablation of inflammatory monocytes reduces numbers of macrophages and diminishes expression of inflammatory mediators in the CNS which results in amelioration of EAE[63]. Moreover, it has been shown that disease severity correlates with the absolute number of macrophages invading the CNS parenchyma[67] and that repetitive depletion of macrophages by clodronate liposome-treatment abrogates EAE[68]. Thus, myeloid cells, i.e. microglia, monocytes, and macrophages, play a critical role during ongoing CNS inflammation.

1.3 Peroxisome proliferator-activated receptor gamma

Peroxisome proliferator-activated receptor gamma (PPARγ), which belongs to the PPAR superfamily of nuclear hormone receptors, is involved in modulation of metabolism and inflammation[69]. PPARγ is a ligand-activated transcription factor that, after ligand binding, heterodimerises with the retinoid X receptor. This heterodimer subsequently recruits a protein complex consisting of coactivators or corepressors to direct transcriptional activation or repression[70]. PPARγ influences gene transcription by binding to PPAR response elements in the promoter region of target genes[71] or by negatively interfering with proinflammatory transcription factors like nuclear factor-κB (NF-κB) which results in inhibition of gene transcription for example of proinflammatory cytokines[72-74]. Several endogenous and synthetic ligands have been identified for PPARγ. Endogenous ligands include unsaturated fatty acids like linoleic acid metabolites generated by the enzyme 12/15 lipoxygenase or 15-deoxy-$\triangle^{12,14}$-prostaglandin J_2. The class of thiazolidinediones (TZDs) represents an important group of synthetic PPARγ ligands and one of the members, i.e. pioglitazone (PIO), was used in this study[69,70,75,76].

PPARγ has gained medical importance in treatment of diabetes type II as high-affinity ligands for PPARγ like PIO mediate improved insulin sensivity[70]. Due to their immunomodulatory effects, PPARγ agonists have also been postulated to be promising agents for therapeutical strategies against autoimmune diseases such as MS and rheumatoid arthritis[77].

1.3.1 PPARγ in inflammation

PPARγ has been demonstrated to regulate DC[78,79], macrophage[69,73], and microglial[80,81] immunogenicity. Nencioni et al. investigated the effect of PPARγ activation on maturation of human monocyte-derived DCs. They demonstrated that PPARγ activation rendered DCs to a less stimulatory mode which was characterised by decreased expression of costimulatory molecules and decreased cytokine production in response to inflammatory stimulation[78]. In addition, our group could show that PPARγ is a negative regulator of DC maturation and function as PPARγ activation impaired inflammation-induced upregulation of the costimulatory molecules CD40, CD80, and CD86, as well as IL-12 production in murine bone marrow-derived DCs (BM-DCs) resulting in impaired activation of naive $CD4^+$ T cells *in vitro* and *in vivo*. Importantly, absence of PPARγ in DCs resulted in enhanced $CD4^+$ T cell activation indicating a constitutive regulatory function of PPARγ in DCs[79].

Several reports show that also in macrophages and monocytes PPARγ inhibits transcription of proinflammatory genes like iNOS or IL-6 in response to inflammatory stimulation *in vitro*[72,73,82]. Importantly, treatment of macrophages and monocytes with the T_H2 cytokine IL-4 results in induction of 12/15-lipoxygenase, an enzyme that produces endogenous PPARγ ligands[82]. This indicates that the environment can directly influence the phenotype of macrophages by modulating PPARγ activity.

In line with this, production of proinflammatory cytokine production upon inflammatory stimulation is also reduced in microglial cells by PPARγ through suppression of signalling molecules like myeloid differentiation primary-response gene 88[83]. Furthermore, PPARγ activation in microglia inhibits also production of different chemokines which play an important role in attracting immune cells during ongoing CNS inflammation[81] including chemokine ligand 2 (CCL2) that attracts inflammatory monocytes.

1.3.2 PPARγ as a pharmaceutical target to limit inflammatory diseases

Insulin-sensitising antidiabetic TZDs are high affinity ligands for PPARγ that are in clinical use for treatment of type 2 diabetes. The discovery that TZDs, like PIO, troglitazone, or rosiglitazone perform antiinflammatory and immunomodulatory effects

on cells of the immune system led to the assumption that PPARγ ligands may effectively treat chronic inflammatory diseases beyond diabetes and indeed several studies have demonstrated that TZDs are effective in treatment of diseases unrelated to insulin resistance[84]. Psoriasis is a common chronic skin disease that involves epidermal inflammation and hyperproliferation of keratinocytes. Treatment of psoriasis patients with troglitazone resulted in improvement or clearance of lesions. Importantly, ligands for PPARγ inhibited keratinocyte proliferation and ameliorated the abnormal phenotype of human psoriatic skin[85]. Inflammatory bowel disease is a chronic inflammation of the gastrointestinal tract. In mice, administration of three different TZDs, i.e. PIO, troglitazone, and rosiglitazone, demonstrated beneficial dose-related treatment effects when administered prior to the onset of experimental colitis. Amelioration was associated with decreased levels of TNF-α and IFN-γ while levels of IL-4 and IL-10 were increased, indicating a shift towards a more antiinflammtory T_H2 response[86]. Myocarditis is an important cause of heart failure among adolescents and young adults. In the experimental mouse model of myocarditis, delivery of PIO resulted in amelioration of disease that was accompanied by inhibition of the initial expansion and activation of T cells as well as reduced numbers of infiltrating macrophages, $CD4^+$ and $CD8^+$ T cells in the myocardium[87]. Furthermore, PPARγ interfered with NF-κB signalling by increasing the expression of inhibitor of κB which resulted in decreased cytokine production[88]. In line with these findings, also in the animal model of MS, EAE, TZDs have proven to ameliorate disease when administered before or after onset of disease[89-91]. PIO-mediated amelioration of EAE was characterised by suppression of T_H17 differentiation[89] and improved neurological symptoms[91].

Hence, it has been concluded that the beneficial effects of PPARγ activation are not restricted to type 2 diabetes but can be extended to other chronic inflammatory diseases. However, the details how these agonists mediate amelioration of such diseases are poorly understood.

2 Aims of the thesis

The nuclear transcription factor peroxisome proliferator-activated receptor gamma (PPARγ) is involved in the regulation of immune responses by myeloid cells, i.e. dendritic cells (DCs), macrophages, and microglia.

We and others have shown that PPARγ in DCs impairs maturation in response to inflammatory stimulation. If PPARγ is activated, DCs exhibit reduced inflammation-induced expression of costimulatory molecules and production of proinflammatory cytokines which results in $CD4^+$ T cell anergy. However, the impact of PPARγ in DCs on cross-priming of $CD8^+$ T cells is not known. Therefore, the first part of this thesis dealt with the following questions:

- Does activation of PPARγ in DCs influence uptake and cross-presentation of soluble antigens?
- Do PPARγ-mediated changes in cross-presentation affect cross-priming of naive $CD8^+$ T cells by DCs?
- What is the molecular mechanism that mediates PPARγ-induced changes in cross-priming capacity of DCs?

At least *in vitro*, it has been demonstrated that the immunogenicity of macrophages and microglia is regulated by PPARγ. As these myeloid cells play an important role in perpetuation of CNS inflammation during multiple sclerosis (MS) and its animal model experimental autoimmune encephalomyelitis (EAE), we investigated whether PPARγ acts as a cell-intrinsic regulator of myeloid cells during EAE:

- Does PPARγ in myeloid cells play a protective role during active EAE?
- How does PPARγ activation in myeloid cells influence the reciprocal interaction of myeloid cells and autoreactive T cells during ongoing CNS inflammation?

3 Materials and methods

3.1 Materials

3.1.1 General laboratory equipment

Autoclave	Belimed, Köln
AutoMACS	Miltenyi Biotec, Bergisch Gladbach
Balances	U4100-OD2.2 and MC BA 100 (Sartorius, Göttingen)
Beakers	5 ml, 10 ml, 25 ml, 50 ml, 100 ml, 150 ml, 250 ml, 500 ml (Schott, Mainz)
Centrifuges	Multifuge 3SR, Biofuge fresco, Biofuge pico (Heraeus, Braunschweig)
Counting Chamber	Neubauer (Brand, Wertheim)
Digital camera	CCD-1300 (Vosskuehler, Osnabrück)
ELISA Reader	SpectraMax 250 (Molecular Devices, Sunnyvale, USA)
ELISpot Reader	Bioreader-2000 (Biosys, Karben)
Erlenmeyer flasks	50 ml, 100 ml, 250 ml, 500 ml (Schott, Mainz)
Flow cytometer	FACSCantoII (BD Biosciences, Heidelberg)
Freezers (-20°C)	Liebherr, Biberach
Freezers (-80°C)	Hera freeze (Heraeus, Braunschweig)
Freezing container	Nalge Nunc Cryo (Nunc, Wiesbaden)
Heating block	ThermoStat plus (Eppendorf, Hamburg)
Ice machine	Icematic (Scotsman®, Frimont Bettolinc, Pogliano, Italy)
Incubators	HERAcell (Heraeus, Braunschweig)
Magnet stirrer	IKA® Laboratory Equipment, Staufen

Measuring cylinders	50 ml, 100 ml, 250 ml, 500 ml, 1l (Schott Mainz)
Microscope	IX81 (Olympus, Hamburg)
Microtiter plate washing device	Nunc-Immuno^{TM} Wash12 (Nalge Nunc International, Thermo Fisher Scientific, Wiesbaden)
Microwave	Panasonic, Wiesbaden
pH-meter	pH 523 (Wissenschaftlich-Technische Werkstätten, Weilheim)
Pipette-Boy	Pipetus (Hirschmann Labortechnik, Eberstadt)
Pipettes	Gilson, Heidelberg and Eppendorf, Hamburg
Preparation Instruments	Labotec, Göttingen
Real-time PCR System	AbiPrism 7900 HT cycler
Refrigerators (+4°C)	Bosch, Stuttgart and Liebherr, Biberach
Sieves, steel	University of Bonn, Department "Feinmechanik"
Sonificator	UW2070/Sonoplus (Bandeln electronic, Berlin)
Spectrophotometers	LB 940 Multilabel Reader Mithras (Berthold Technologies)
NanoDrop™	ND 1000 (NanoDrop Products, Wilmington, USA)
Threaded bottles	100 ml, 250 ml, 500 ml, 1l, 2l (Schott, Mainz)
Ultra-pure water system	NANOpure Diamond, Barnstead (Werner, Reinstwassersysteme, Leverkusen)
Waterbath	TW8 (Julabo, Seelbach)
Workbench, sterile	HERAsafe (Heraeus, Hanau)

3.1.2 Software

Cell^R	Olympus, Hamburg
FACS Diva V6.1.1	BD Biosciences, Germany
FlowJo V8.8.4	Tree Star, Inc., USA
Illustrator CS4	Adobe, USA
Microsoft Office 2008	Microsoft, USA
Prism 4	GraphPad Software, USA
SPF ELISA Software	Molecular Devices, USA
Scan^R	Olympus, Hamburg

3.1.3 Consumables

384-well plate	Applied Biosystems
4-well chamber culture dishes	Nunc, Langenselbold
BeadChip Array	MouseWG-6 v2 Expression BeadChip, Illumina, USA
Cryo vials	VWR International, Darmstadt
Cryomolds	VWR International, Darmstadt
ELISA plates	Microlon, 96-well, flat-bottom, high-binding (Greiner Bio-one, Solingen)
ELISpot	R&D Systems, Minneapolis, USA
FACS tubes	polystyrene, 12/75 mm (Sarstedt, Nümbrecht)
Filtergauze (40 μm)	TechFab, Geldern
Injection needles	27G, 25G , 20G (BD Microlance, Heidelberg)
Microtiter plates	96-well, round and flat bottom (Greiner bio-one, Solingen)
Nylon wool	Kisker GbR (by Labomedic GmbH, Bonn)
Parafilm	Parafilm “M”® (American National Can TM,

	Greenwich, USA)
Pasteur pipettes	150 mm and 230 mm (Roth, Karlsruhe)
PD-MidiTrap™ G-25	GE Healthcare, München
Petri dishes	10 cm (Greiner bio-one, Solingen)
Pipette tips	10 µl, 200 µl, 1000 µl (Greiner bio-one, Solingen)
Plastic Pipettes	5 ml, 10 ml, 25 ml (Sarstedt, Nümbrecht)
Polyamide tissue	"Gaze" (Labomedic, Bonn)
Polypropylene tubes	sterile, 15 ml and 50 ml (Greiner bio-one, Solingen)
Reaction tubes	0.5 ml, 1.5 ml, 2 ml (Eppendorf, Hamburg)
Scalpel	Feather (Osaka, Japan)
Syringes	2 ml, 5 ml, 10 ml, 20 ml BD Discardit™ (BD Bioscience, Heidelberg)
Tissue culture flasks	25 cm^2, 75 cm^2, or 150 cm^2 (TPP, St.Louis, USA or Sarstedt, Nümbrecht)
Tissue culture plates	6-, 12-, 24-, 48-, or 96-well (TPP, St. Louis, USA or Sarstedt, Nümbrecht)

3.1.4 Chemicals and reagents

Ammonium chloride (NH_4Cl)	Merck, Darmstadt
B-27 supplement	Invitrogen, Karlsruhe
β-mercaptoethanol	Sigma Aldrich, München
BME medium	Sigma Aldrich, München
Bovine serum albumin (BSA)	Roth, Karlsruhe
BrefeldinA	BD Biosciences, Heidelberg
Carboxy-fluorescein diacetate succinimidyl ester (CFSE)	Molecular Probes, Leiden, Netherlandes
Carboxymethylcellulose (CMC)	Sigma Aldrich, München

Chlorophenol red-β-galactosidase (CPRG)	Roche, Mannheim
Collagenase A	Roche, Mannheim
Complete Freund's Adjuvant	Difco Laboratories, Detroit, USA
Cytofix/Cytoperm™ Fixation/ Permeabilisation Kit	BD Biosciences, Heidelberg
DEPC treated water (RNase free)	Invitrogen, Karlsruhe
Dimethylsulfoxide (DMSO)	Merck, Darmstadt
DMEM medium	Sigma Aldrich, München
Ethanol, absolute	Merck, Darmstadt
Ethylene diamine tetraacetic acid (EDTA)	Sigma Aldrich, München
EDTA-Disodium (Na_2EDTA)	Sigma Aldrich, München
Fetal calf serum (FCS)	PAA, Cölbe
Fluoresbrite FITC-dyed polystyrene beads (0.5 μm)	Polysciences, Eppelheim
G418 sulfate	PAA, Cölbe
Grey's Balanced Salt Solution (GBSS)	PAN Biotech, Passau
Griess Reagent Kit	Invitrogen, Kralsruhe
H_2DCFA	Molecular Probes, Leiden, Netherlands
Heparin	Ratiopharm, Ulm
Hoechst 33342	Molecular Probes, Leiden, Netherlands
IMDM medium	Lonza, Köln
Ionomycin (IONO)	Sigma Aldrich, München
Laminin	Sigma Aldrich, München
L-Glutamine (200 mM)	PAA, Cölbe
Liquid nitrogen	Linde, Wiesbaden
Liposomes (clodronate or PBS)	Dr. Nico van Rooijen, Amsterdam, Netherlands

Lymphocyte separation medium	PAA, Cölbe
Milk powder	Sigma Aldrich, München
Monensin	BD Biosciences, Heidelberg
Mowiol	Roth, Karlsruhe
Mycobacterium tuberculosis H37RA	Difco Laboratories, Detroit, USA
N2-supplement	Invitrogen, Karlsruhe
Natural silk 5.0	Catgut, Markneukirchen
Neutralised streptavidin-peroxidase	Uptima, Interchim, France
Non-essential amino acids (NEAA)	PAA, Cölbe
Normal goat serum	generated in the lab
Normal mouse serum	generated in the lab
Normal rat serum	generated in the lab
Optimem medium	Gibco, BRL, Karlsruhe
Ovalbumin (OVA)	Serva, Heidelberg
Ovalbumin^{Alexa647}	Invitrogen, Karlsruhe
Paraformaldehyde (PFA)	Fluca, Buchs
Penicillin/Streptomycin (100x)	PAA, Cölbe
Percoll	Amersham Pharmacia, Freiburg
Phosphate buffered saline (PBS)	Biochrom, Berlin
PBS solution	Sigma Aldrich, München
Pioglitazone tablets (30 mg)	Actos, Takeda Pharmaceuticals, USA
Pioglitazone (*in vitro* application)	Axxora, Lörrach
Phorbol myristate acetate (PMA)	Sigma Aldrich, München
Poly-l-ornithine	Sigma Aldrich, München
Potassium bicarbonate ($KHCO_3$)	Sigma Aldrich, München
PowerSYBR Green PCR Mastermix	Applied Biosystems, Carlsbad, USA
RNeasy Kit	Quiagen, Hilden
RPMI 1640 medium	Sigma Aldrich, München

Sodium azide (NaN_3)	Sigma Aldrich, München
Sulfuric acid (H_2SO_4), 96%	Merck, Darmstadt
Superscript III	Invitrogen Life Technologies, Frederick, USA
Taqman Gene Expression Mastermix	Applied Biosystems, Carlsbad, USA
TMB substrate	Uptima, Interchim, France
TritonX	Sigma Aldrich, München
TRIzol	Invitrogen Life Technologies, Frederick, USA
Trypan blue (0.4%)	Lonza, Köln
Trypsin/EDTA	Lonza, Köln
Tween20	Roth, Karlsruhe

3.1.5 Buffers, media, and solutions

3.1.5.1 Fetal calf serum (FCS)

FCS was heat-inactivated at 56°C for 30 min and stored à 50 ml aliquots at -20°C.

3.1.5.2 Phosphate buffered saline (PBS)

1x PBS was adjusted to pH 7.4, aliquoted à 500 ml, autoclaved, and stored at 4°C.

3.1.5.3 0.5 M EDTA

186.1 g EDTA and 20 g NaOH were dissolved in 1000 ml ultra-pure water and the pH was adjusted to 7.8 - 8.0. The solution was autoclaved and stored at room temperature.

3.1.5.4 5 mM β-mercaptoethanol

178 µl of 14.3 M β-mercaptoethanol was added to 500 ml 1x PBS and kept under sterile conditions at 4°C.

3.1.5.5 Ag8653 medium

IMDM medium was supplemented with 10 % (v/v) FCS, 2 mM L-glutamine, 1 % (v/v) penicillin/streptomycin, 50 µM β-mercaptoethanol and kept under sterile conditions at 4°C.

3.1.5.6 Bone marrow-derived dendritic cell (BM-DC) medium

IMDM medium was supplemented with 10 % (v/v) FCS, 2mM L-glutamine, 1 % (v/v) penicillin/streptomycin, 50 μM β-mercaptoethanol and kept under sterile conditions at 4°C. For BM-DC differentiation, 30 % (v/v) of Ag8653-conditioned medium containing granulocyte macrophage colony-stimulating factor (GM-CSF) was freshly added.

3.1.5.7 L929 medium

RPMI 1640 medium was supplemented with 10 % (v/v) FCS, 2 mM L-glutamine, 1 % (v/v) penicillin/streptomycin, 50 μM β-mercaptoethanol and kept under sterile conditions at 4°C.

3.1.5.8 Bone marrow-derived macrophage (BM-M) and T cell culture medium

RPMI 1640 medium was supplemented with 10 % (v/v) FCS, 2 mM L-glutamine, 1 % (v/v) penicillin/streptomycin, 50 μM β-mercaptoethanol and kept under sterile conditions at 4°C. For BM-M differentiation, 30 % (v/v) L929-conditioned medium containing macrophage colony-stimulating factor (M-CSF) was freshly added.

3.1.5.9 Primary microglia medium

DMEM medium was supplemented with 10 % (v/v) FCS, 2 mM L-glutamine, 1 % (v/v) penicillin/streptomycin, 50 μM β-mercaptoethanol, and 1 % (v/v) NEAA and kept under sterile conditions at 4°C.

3.1.5.10 Neuronal medium

BME-based neuronal medium was supplemented with 2 % B-27 supplement, 1 % glucose, and 1 % FCS and kept under sterile conditions at 4°C.

3.1.5.11 FACS buffer

1x PBS containing 1 % (v/v) FCS and 0.1% (v/v) NaN_3. Stored at 4°C.

3.1.5.12 MACS buffer

1x PBS containing 1 % (v/v) FCS and 2 mM EDTA. Stored under sterile conditions at 4°C.

3.1.5.13 ACK lysis buffer

16.58 g NH_4Cl, 2 g $KHCO_3$, 74.4 mg Na_2EDTA was dissolved in 2000 ml ultra-pure water and the pH was adjusted to 7.2 - 7.4. Stored under sterile conditions at room temperature.

3.1.5.14 ELISA coating buffer

0.1 M $NaHCO_3$ in ultra-pure water, the pH was adjusted to 8.2, autoclaved, and stored at 4°C.

3.1.5.15 ELISA blocking buffer

1 % BSA (w/v) in 1x PBS, prepared freshly.

3.1.5.16 0.18 M H_2SO_4 TMB stopping solution

5 ml 96 % H_2SO_4 was added to 500 ml ultra-pure water and kept at room temperature.

3.1.5.17 ELISA washing buffer

1x PBS containing 0.01 % (v/v) Tween20.

3.1.5.18 4% (w/v) PFA solution

8 g PFA was dissolved in 200 ml 1x PBS by gradual heating. The pH was adjusted to 7.4. Stored at room temperature.

3.1.5.19 Permeabilisation buffer

1 x PBS containing 0.5 % (w/v) BSA + 0.25 % Triton X.

3.1.5.20 Blocking solution I

1x PBS containing 50 mg/ml milk powder, 1 % normal mouse serum, 1 % normal rat serum, and 1 % monoclonal antibody 2.4G2. The solution was freshly prepared and used for microscopical analysis of S8L presentation (3.2.13.1).

3.1.5.21 Blocking solution II

1x PBS containing 5 % BSA, 0.5 % normal goat serum, and 0.125 % TritonX used for immunohistochemical staining of neuron-microglial cocultures (3.2.13.2).

3.1.5.22 Percoll solutions

30 %, 37 %, and 70 % Percoll solutions were freshly prepared by diluting 100 % Percoll solution with PBS to the required concentration.

3.1.5.23 Chlorophenol red-β-galactoside (CPRG) solution

250 ml DMEM medium and 250 ml GBSS were mixed and supplemented with 5 % (v/v) FCS, 2mM L-glutamine, 1 % (v/v) penicillin/streptomycin, 50 µM β-mercaptoethanol, and 0.2 mM CPRG. The solution was kept under sterile conditions at 4°C.

3.1.6 Primers for quantitative real-time RT-PCR

	FW	**RV**
IFN-γ	5′-GAACTGGCAAAAGGATGGTGA-3′	5′-TGTGGGTTGTTGACCTCAAAC-3′
IL-1β	5′-GCCCATCCTCTGTGACTCAT-3′	5′-AGGCCACAGGTATTTTGTCG-3′
IL-12p40	5′-CCTGAAGTGTGAAGCACCAA-3′	5′-TCAGGGGAACTGCTACTGCT-3′
IL-23p19	5′-GACTCAGCCASCTCCTCCAG-3′	5′-GGCACTAAGGGCTCAGTCAG-3′
TNF-α	5′-CATCTTCTCAAAATTCGAGTGACAA-3′	5′-TGGGAGTAGACAAGGTACAACCC-3′

3.1.7 Peptides

Peptide	*Company*	*Application*
MOG_{35-55}	Biotrend	*in vivo*
MOG_{35-55}	Pineda	*in vitro*
$OVA_{257-264}$ (SIINFEKL/S8L)	Pineda	*in vitro*

3.1.8 Recombinant cytokines and chemokines

For long-term storage, recombinant cytokines and chemokines for ELISA standard were kept at -80°C. Working aliquots were stored at -20°C.

Cytokine / chemokine	*Company*
IL-2	eBioscience, USA
IL-6	eBioscience, USA
IFN-γ	eBioscience, USA
TNF-α	eBioscience, USA
CCL2	eBioscience, USA

3.1.9 Antibodies

3.1.9.1 Antibodies for flow cytometric analysis

Fluorochrome-labelled antibodies for flow cytometric analysis of expression of diverse surface antigens and for intracellular cytokine staining were obtained from eBioscience or BD Pharmingen except for the mannose receptor (MR) which was ordered from AbD serotec. All antibodies were used in previously titrated concentrations.

Antigen	*Isotype*	*Clone*
B7DC	rat IgG2a,κ	TY25
B7H1	rat IgG2a,λ	M1H5
CD4	rat IgG2b,κ	GK1.5
CD8α	rat IgG2b,κ	53-6.7
CD11b	rat IgG2b,κ	M1/70
CD11c	hamster IgG	N418
CD115	rat IgG2a,κ	AFS98
CD16/32	rat IgG2b,κ	2.4G2
CD40	rat IgG2a,κ	1C10
CD45	rat IgG2b,κ	30-F11
CD45.1	mouse IgG2a,κ	A20
CD45.2	mouse IgG2a,κ	104
CD80	hamster IgG	16-10A1
CD86	rat IgG2b,κ	P03.1
ICOSL	rat IgG2a,κ	HK5.3
I-A^b	mouse IgG2a,κ	AF6-120.1
IFN-γ	rat IgG1,κ	XMG1.2
IL-6	rat IgG1,κ	MP5-20F3
IL-17A	rat IgG2a,κ	eBio17B7
Ly-6C	rat IgG2c	HK1.4

Ly-6G	rat IgG2a,κ	1A8
MR	rat IgG2a,κ	MR5D3
TNF-α	rat IgG1,κ	MP6-XT22

3.1.9.2 Antibodies for ELISA

All antibodies used in cytokine and chemokine ELISAs were purchased from eBioscience as matching antibody pairs which included a primary unlabelled capture antibody and a biotinylated detection antibody and each antibody was applied in previously titrated amounts. For detection of CCL2, the antibodies were ordered as ELISA Ready-Set-Go!® and antibodies were used according to the manufacturer's instructions.

Cytokine	*Clone capture antibody*	*Clone detection antibody*
IFN-γ	AN-18	RA-6A2
IL-2	JES6-1A12	JES6-5H4
IL-6	MP5-20F3	MP5-32C11
TNF-α	TN3-19.12	Polyclonal
CCL2	4E2	2H5

3.1.9.3 Antibodies for *in vitro* activation of T cells

Antigen	*Clone*	*Source*
CD3	145.C11	generated in the lab
CD28	37.52	eBisociences

3.1.9.4 Antibodies for immunohistochemical staining

Antigen	*Clone*	*Source*
S8L complexed to H-2K^b	25D1.16	R. Germain + J. Yewdell
β-tubulin 3	polyclonal mouse	Sigma Aldrich, München
Goat-anti-mouse	polyclonal goat	Jackson Immuno Research, Suffolk, UK
Iba1	polyclonal rabbit	Wako Chemicals, Neuss
Goat-anti-rabbit	polyclonal goat	Invitrogen, Karlsruhe
amyloid precursor protein (APP)	polyclonal goat	Chemicon, Temecula, USA
CD3	CD3-12	Serotec, Düsseldorf
MAC-3	M3/84	BD Biosciences, Heidelberg

3.1.9.5 Antibodies coupled to magnetic beads ("MACS Beads")

Murine αCD4, αCD11b, αCD11c, αCD90.2, and αbiotin antibodies conjugated to magnetic beads as well as CD8$^+$ T cell isolation kit were obtained from Miltenyi Biotech, Bergisch Gladbach, Germany.

3.1.9.6 PD1 blocking antibody for *in vitro* application

To block interaction of B7H1 with PD1 in cocultures of BM-DCs and OT-I T cells, 20 μg/ml antibody against PD1 (clone J43)[92] or the isotype control was added (Hamster IgG).

3.1.9.7 Antibody for *in vivo* depletion of CCR2$^+$ inflammatory monocytes

The αCCR2 antibody MC-21 was a kind gift from Prof. Dr. M. Mack (University of Regensburg, Germany). Rat IgG2b (BD Bioscience) served as Isotype control antibody.

3.1.10 Inhibitors

Inhibitor	*Company*
Monensin	eBioscience, USA
BrefeldinA	eBioscience, USA

3.1.11 Virus

Virus	*Description*	*Source*
AdOVA	E1- and E3-deleted recombinant adenoviral vector expressing the full length OVA protein under the CMV promoter	Dr. Andreas Untergasser; Prof. Dr. Ulrike Protzer

3.1.12 Cell lines

3.1.12.1 Ag8653

Ag8653 is a hybridoma cell line that is used to produce GM-CSF-containing supernatant which was used for the generation of bone marrow-derived dendritic cells[93,94] (3.2.1.2).

3.1.12.2 L929

L929 is a hybridoma cell line that is used to produce M-CSF-containing supernatant which was used for the generation of bone marrow-derived macrophages[95] (3.2.1.5).

3.1.12.3 B3Z

B3Z is a $CD8^+$ T cell hybridoma that recognises the OVA-derived peptide SIINFEKL (S8L) in the context of $H\text{-}2K^b$ molecules[96]. Following activation of the T cell, the *β-galactosidase* gene is expressed under the control of the IL-2 promotor and activation can be assessed by measuring the conversion of the chromogenic substrate CPRG by absorbance spectrophotometry at 595 nm.

3.1.12.4 RMA

Lymphoblast cell line derived from C57BL/6N mice obtained from LGC Standards GmbH, Wesel.

3.1.13 Mouse strains

All mice were bred under pathogen free conditions in accordance with the institutional guidelines of the local animal facility House of Experimental Therapy at the University of Bonn. For all experiments, mice between 6 and 18 weeks of age were used.

Strain	*Source*	*Description*
C57BL/6	Charles River	wild type strain (H-2K^{b})
MR$^{-/-}$	Dr. Michel Nussenzweig	mice that lack the mannose receptor (MR)[97]
OT-I Rag-1$^{-/-}$	Dr. William R. Heath	TCR transgenic line which produces MHC-I-restricted, OVA-specific CD8^{+} T cells; mice lack mature T and B cells due to deficiency in recombination-activating gene 1 (Rag-1)[98]
B7H1$^{-/-}$	Dr. Lieping Chen	mice lack the coinhibitory molecule B7H1[99]
PPARγ$^{fl/fl}$	Charles River	mice carry two loxP sites flanking exons two and three of the PPARγ gene[100]
CD45.1	Charles River	mice that carry the congenic marker CD45.1

LysM-Cre x PPARγ$^{fl/fl}$	own breeding	mice expressing the Cre-recombinase under the control of the lysozyme M (LysM) promoter[101] crossed to PPARγ$^{fl/fl}$ mice; mice lack PPARγ specifically in myeloid cells (Figure 9a)
2D2	own breeding	TCR transgenic line which produces MHC-II-restricted, MOG_{35-55}-specific $CD4^+$ T cells[102]
Thy1.1 (CD90.1)	Charles River / own breeding	mice that express the congenic marker Thy1.1 (or CD90.1)

3.2 Methods

3.2.1 Cell culture

3.2.1.1 Production of GM-CSF-containing supernatant

Ag8653 fibroblasts were taken up in Ag8653 medium and cultured in 30 ml in 175 cm^2 flasks until confluency at 37°C. The addition of the antibiotic Neomycin (G418; 1 mg/ml) allowed to positively select transgenic modified cells that bear the capacity to produce GM-CSF. After confluency was reestablished, cells were harvested, washed three times with PBS, and $1.5x10^6$ cells, resuspended in 30 ml Ag8653 medium without G148, were transferred to a new 175 cm^2 flask. After three days, the supernatant was collected and centrifuged for 10 min at 553 × g to remove remaining cells. Following another centrifugation step (15 min, 1942 × g) of the supernatant in order to remove debris, the supernatant was collected, sterile filtered (pore size = 0.2 μm), and stored in aliquots at -20°C.

3.2.1.2 Generation of BM-DCs

The hind legs of wild type C57BL/6 mice were dissected and collected in PBS on ice. After removal of skin residues and muscle tissue, bones were disinfected with 70 % Ethanol, and subsequently washed in PBS. Femoral and tibial bones were opened on each side and the bone marrow was flushed out with medium using a syringe attached to a 27 G needle. Following a centrifugation step of 5 min at 486 × g, cells were filtered through a 30 μm cell strainer, and centrifuged again at 486 × g for 10 min. Cells were resuspended in BM-DC culture medium supplemented with freshly added 30 % GM-CSF-containing Ag8653 supernatant. Cells were plated on 3 petri dishes per 2 hind legs in 15 ml per dish and incubated at 37°C. At day 3 or 4, cells were split 1:1 into new petridishes. BM-DCs were used for experiments after seven or eight days of cultivation.

For PIO-treatment, 10 μM PIO was added to the bone marrow cell culture from day 0 of differentiation procedure. When medium was changed, 10 μM PIO was freshly added to the appropriate petridishes.

3.2.1.3 Conditional knockout of PPARγ in BM-DCs

Conditional PPARγ knockout BM-DCs were generated *in vitro* by Cre-mediated site-specific recombination of loxP sites integrated into exon 1 and exon 2 of the PPARγ gene of $PPAR\gamma^{fl/fl}$ mice. First, bone marrow precursor cells were isolated as described in 3.2.1.2 from $PPAR\gamma^{fl/fl}$ or, as control, wildtype C57BL/6 mice. Precursor cells were treated with 3 μM of a membrane-permeable Cre recombinase (HTNCre) for 6 h, washed twice, and cultured as described in 3.2.1.2 for 4 days. On day 3 of the differentiation period, the protocol was repeated and cells were cultured for another 4 days. PIO-treatment was performed by addition of 10 μM PIO during the whole differentiation period.

3.2.1.4 Generation of M-CSF containing supernatant

L929 cells were taken up in L929 medium and cultured in 30 ml in 175 cm^2 flasks for 48 h at 37°C. Then, L929 cells were split and $0.5x10^5$/ ml seeded onto 15 cm^2 dishes. After four days, the supernatant was collected and centrifuged for 10 min at 553 × g to remove remaining cells. Afterwards, the supernatant was sterile filtered (pore size = 0.2 μm), and stored in aliquots à 45 ml at -20°C.

3.2.1.5 Generation of BM-Ms

Generation of BM-Ms was performed as described for BM-DCs (3.2.1.2). To generate BM-Ms, 30 % M-CSF-containing L929 supernatant was freshly added to the culture. At day 3 or 4, the supernatant containing non-adherent cells was sucked off and fresh medium with 30 % M-CSF-containing supernatant was added. BM-Ms were used for experiments after seven days of cultivation.

For PIO-treatment, 10 μM PIO was added to the bone marrow cell culture from day 0 of the differentiation procedure. When medium was changed, 10 μM PIO was freshly added to the appropriate petridishes.

3.2.1.6 Generation of primary microglia

To prepare mixed glial cultures, brains were removed from post-natal day 1–5 C57BL/6 mice. Brains were first stripped of the meninges and cortices and afterwards mechanically dissociated. Cell homogenates were seeded into 75 cm^2 culture flasks in 10 ml primary microglia medium which was changed when it became acidic. After 2 weeks, microglial cells had started to grow on the established stromal cell layer . From this time, microglial cells were harvested by vigorously tapping the flasks and filtering the cell suspension through 40 µm wide gauze to remove stroma cells that had been shaked of. Fresh medium was added and microglia were again harvested, when microglia cells had differentiated again.

For PIO-treatment, 10 µM PIO in 10 ml fresh medium was added to the flasks. After 4 days half the medium was changed and 5 ml of fresh medium containing 10 µM PIO was added. Untreated cells were treated the same way without addition of PIO.

3.2.1.7 Generation of primary neurons

4-well chamber culture dishes were pretreated for 24 h with 0.01 mg/ml poly-l-ornithine and 10 µg/ml laminin. To establish primary neuronal cultures, brains were prepared from C57BL/6 mice embryos (E15-E16) and collected in PBS on ice. Then, hippocampi were isolated and dispersed mechanically. After centrifugation, cells were resuspended, counted, and seeded at a concentration of $1x10^5$ cells/ml in BME-based neuronal medium with 1 ml per well. After 4 d, neurons had become morphologically mature and were cocultured with primary microglial cells as described in 3.2.12.7.

3.2.2 Flow-cytometry

Cells were stained as described in the following sections. For all experiments, data was acquired using a FACSCantoII and results were analysed using FlowJo software.

3.2.2.1 Surface staining

Staining for surface molecules was performed in 96-well round bottom plates with $1x10^5$-$1x10^6$ cells per well. Cells were washed once with FACS buffer, before addition of 50 µl of the appropriate antibody + anti-CD16/32 (to block the FcγR) diluted in FACS-buffer at a previously titrated concentration. Staining was performed for 10 min

at room temperature. Then, cells were washed once with FACS buffer and analysed by flow-cytometry.

For surface analysis of blood cells, erythrocytes were lysed before staining procedure. To this end, blood was collected in PBS containing heparin and centrifuged for 3 min at 3000 rpm in Biofuge Fresco (Heraeus). After the supernatant was discarded, 500 µl ACK lysis buffer was added, and samples were incubated for 10 min at room temperature. After 3 min centrifugation at 3000 rpm in a Biofuge Fresco (Heraeus), cells were resuspended in FACS buffer and stained for surface molecules.

3.2.2.2 Intracellular staining of the mannose receptor (MR)

For intracellular staining of the MR in BM-DCs, cells were surface stained for CD11c (3.2.2.1), fixed in 4 % PFA for 15 min on ice, permeabilised with permeabilisation buffer, and stained with an antibody against the MR diluted in permeabilisation buffer. Staining was performed for 30 min on ice. After washing with permeabilisation buffer, cells were resuspended in FACS buffer, and analysed by flow-cytometry.

3.2.2.3 Intracellular cytokine staining

For intracellular cytokine staining, cells were cultured for 4 h in the presence of 1 µl/ml of both, Monensin and BrefeldinA, and staining was performed using the BD Cytofix/Cytoperm™ Fixation/Permeabilization Solution Kit according to the manufacturer´s protocol. Briefly, after staining of surface molecules, cells were fixed in BD Cytofix/Cytoperm solution for 15 min on ice, followed by two wash steps with BD Perm/Wash buffer. The antibody was added in BD Perm/Wash buffer and staining was performed for 30 min on ice, followed by another two wash steps with BD Perm/Wash buffer. For flow cytometric analysis, cells were resuspended in FACS Buffer.

3.2.2.4 Uptake of soluble OVA – *in vitro*

To detect uptake of soluble OVA, 3 µg/ml soluble Alexa647-labelled OVA was added to BM-DCs. After incubation for 15 min at 37°C, BM-DCs were collected in FACS buffer, stained for surface expression of CD11c (3.2.2.1), washed, and analysed by flow-cytometry.

3.2.3 Detection of reactive oxygen species (ROS)

To determine the production of ROS by BM-Ms or pMg, BM-Ms were prestimulated with 100 ng/ml LPS for 30 min and pMg were prestimulated with 1 μg/ml LPS for 24 h. After the stimulation period, cells were washed three times with 37°C warm PBS and 20 μM H_2DCFDA in 37°C warm PBS was added to the cells. ROS-mediated convergence of H_2DCFA into fluorescent DCF was detected in a fluorescence plate reader at a wavelength of 485 nm (excitation) and 530 nm (emission).

3.2.4 Detection of nitric oxide (NO)

To determine NO production by BM-Ms or pMg, cells were stimulated for 48 h with 100 ng/ml LPS or 1 μg/ml LPS + 5 pg/ml IFN-γ, respectively. Nitrite concentrations were determined in the supernatants with the Griess Reagent Kit for Nitrite Determination. A standard dilution of nitrite standard solution (component C) in deionised H_2O was prepared, starting from 100 μM with dilution steps of 1:1. For analysis, 150 μl of the standard or supernatants were mixed with 130 μl deionised H_2O + 10 μl component A + 10 μl component B. The mixture was incubated for 30 min at room temperature. Afterwards, the concentration of nitrite was measured at a wavelength of 548 nm in a spectophotometric microplate reader.

3.2.5 Quantitative real-time RT-PCR

For quantitative real-time RT-PCR, mRNA was isolated from the upper cervical myelon of EAE-diseased mice (on day 21 of EAE) or from *in vitro* stimulated BM-Ms or pMg using the RNeasy kit from Quiagen according to the manufacturer's protocol. To determine mRNA levels of inflammatory cytokines, chemokines, and iNOS we performed reverse transcription and amplified cDNA. The PCR reaction mixture was prepared with PowerSYBR Green PCR Master Mix or TaqMan Gene Expression Master Mix. For analysis, we used gene-specific primers (IL-1β, IL-12p40, IL-23p19, TNF-α, IFN-γ), QuantiTect Primer Assays (iNOS) from Qiagen, or FAM-labelled TaqMan probes (CCL2, CCL3, CCL5, CCL20, CXCL10, GAPDH). Data was analysed by the ΔC_T method and normalised to GAPDH expression.

3.2.6 Enzyme-linked immunosorbent assay (ELISA)

ELISA microtiter plates were coated with 50 µl per well of the primary capture antibody in ELISA coating buffer and incubated for 1 h at 37°C or overnight at 4°C. After removing unbound antibody by three wash steps with ELISA washing buffer, 100 µl ELISA blocking buffer was added to the wells for 30 min at room temperature, which was removed by another three wash steps. After upside down centrifugation of the plate for 2 min at 550 × g, 50 µl of each sample (supernatants in triplicates) as well as the cytokine standard (1:4 dilution series, 9 steps) was added and plates were incubated for 1 h at 37°C or overnight at 4°C. After the plate was washed three times, 50 µl of the biotinylated detection antibody in blocking buffer was added, and the plate was incubated for 1 h at 37°C or overnight at 4°C. After thorough washing with ELISA washing buffer, 1 µg/ml streptavidin-conjugated peroxidase in PBS was added for 30 min, incubated at 4°C, subsequently washed, and centrifuged upside down for 2 min at 550 × g. 50 µl of TMB substrate was applied to each well and the absorbance was measured at 650 nm in an ELISA plate reader. The enzymatic reaction was stopped by addition of 50 µl 0.18 M H_2SO_4 stopping solution. The absorbance was measured at 450 nm again.

3.2.7 Enzyme-linked immunosorbent spot (ELISpot) assay

ELISpot analysis was performed according to the manufacturer's instructions. To this end, required wells of the IFN-γ or IL-17A microplates were incubated with 200 µl of sterile culture medium for 20 min at room temperature. The culture medium was aspirated and $1x10^4$ cells isolated from the CNS were added in 50 µl to each well. Next, $2x10^4$ DCs which had been loaded with 10 µM MOG or left untreated were added in 50 µl to the appropriate wells. The cells were incubated at 37°C for 24 h. Afterwards the plates were washed by filling each well with ELISpot wash buffer from the R&D Systems Kit using a squirt bottle. After the last wash step, any washing buffer was completely removed by aspiration. Then, 100 µl of the detection antibody was added and the plate was incubated overnight at 4°C. After thorough washing and aspiration of the washing buffer, 100 µl of Strepatavidin-conjugated alkaline phosphatase was added and incubated for 2 h at room temperature. Next, after plates were washed thoroughly,

100 µl BCIP/NBT Chromogen was added to each well and incubated for 1 h at room temperature. Subsequently, wells were rinsed with deionised water to remove residual BCIP/NBT Chromogen. Last, the flexible plastic underdrain was removed from the bottom of the microplate and the bottom of the microplate was wiped, dried completely at room temperature, and spot numbers were counted with an automated ELISpot Reader.

3.2.8 Oral treatment with pioglitazone (PIO)

Seven days before splenic DC isolation or MOG_{35-55} immunisation as well as during EAE, mice were treated with 30 mg/kg body weight PIO dissolved in 0.5 % carboxymethylcellulose (CMC) or the vehicle only by daily oral gavage.

3.2.8.1 OVA uptake *in vivo*

On day 7 of oral PIO-treatment, mice were injected intravenously (i.v.) with 5 µg/g body weight fluorescently-labelled $OVA^{Alexa647}$ in PBS for analysis of MR expression and OVA uptake. After 45 min, splenic DCs were isolated as described in 3.2.10, stained for CD11c (see 3.2.2.1) and the MR (see 3.2.2.2), and analysed by flow-cytometry.

For coculture assays of splenic DCs *ex vivo* with B3Z cells, mice received 100 µg/g body weight purified OVA in PBS i.v. After 45 min, splenic DCs were isolated and coculture assays were set up as described in 3.2.12.5.

3.2.9 Determination of cell numbers

To determine the cell number of a cell suspension, an aliquot was diluted in 0.04% trypan blue to allow discrimination of live and dead cells. 10 µl of this suspension was applied to a Neubauer counting chamber and living cells were counted in all four large squares. The cell count was calculated using the following formula:

$$\text{cell number / ml} = (\text{counted viable cells / 4}) \times \text{dilution} \times 10^4.$$

3.2.10 Isolation of splenic dendritic cells

Spleens were removed and digested by perfusion with 0.4 mg / ml CollagenaseA in PBS. After incubation in a water bath for 15 min at 37°C, spleens were homogenised by gently pressing the tissue through a metal cell strainer, and cell homogenates were resuspended in ice cold MACS buffer. Cells were centrifuged for 5 min at 486 × g and the supernatant was discarded. Cells were resuspended in MACS buffer, filtered through 40 µm gauze, and centrifuged for 5 min at 486 × g. The cell pellet was resuspended in 500 µl of MACS Buffer containing 20 µl of αCD11c micro beads per spleen and the sample was incubated for 15 min at 4°C. Afterwards, 25 ml MACS-buffer was added and cells were centrifuged for 5 min at 486 × g in order to remove unbound magnetic beads. Cells were resuspended in 3 ml MACS buffer and purified by positive selection using the AutoMACS Separation Technology. After the isolation procedure, DCs were washed once, counted, and cell numbers were adjusted to the required concentration.

3.2.11 Isolation of splenic naive $CD4^+$ and $CD8^+$ T cells

For the isolation of naive $CD4^+$ T cells spleens and inguinal as well as mesenteric lymph nodes were homogenised by gently pressing the tissue through a metal cell strainer. After centrifugation for 5 min at 486 × g, cells were resuspended in MACS buffer, filtered through 40 µm wide gauze, and again centrifuged for 5 min at 486 × g. Afterwards, cells were resuspended in 500 µl of MACS Buffer and 25 µl of αCD4 microbeads were added per spleen and lymph nodes. Cells were incubated for 15 min at 4°C and the reaction was stopped by adding a large volume of MACS buffer. Cells were centrifuged for 5 min at 486 × g, resuspended in 3 ml MACS buffer, and purified by positive selection using the AutoMACS Separation Technology.

For isolation of naive $CD8^+$ T cells from OT-I Rag-$1^{-/-}$ mice, spleens and lymph nodes were collected in PBS on ice. After homogenisation of the tissue by gently pressing it through a metal cell strainer, the cell suspension was collected, and centrifuged for 5 min at 486 × g. After resuspension in 10 ml 37°C warm T cell medium, cells were applied to a sterile 10 ml syringe filled with 0.6 g nylon wool, which had been blocked

for 1 h with T cell medium, and were incubated for 1 h at 37°C to allow macrophages and DCs to adhere. Next, T cells were collected by carefully rinsing the nylon wool with 20 ml T cell medium (37°C).

After the isolation procedure, T cells were washed once with T cell medium, counted, and cell numbers were adjusted to the required concentration.

3.2.12 Coculture assays

3.2.12.1 Coculture of BM-DCs with B3Z or OT-I T cells

For determination of cytokine production / CPRG conversion and proliferation assays, BM-DCs or freshly isolated splenic DCs were cocultured with T cells at a ratio of 1:2 (DC : T cell), if not otherwise stated. In most experiments, 0.5 mg/ml purified OVA was added to cocultures. Supernatants were collected after 48 h of coculture and cytokines were detected by ELISA (3.2.6). To determine cytokine production after restimulation, viable $CD8^+$ T cells were harvested on day 5 of coculture by density gradient centrifugation with lymphocyte separation medium, washed twice, and cultured in triplicates for another 24 h in the presence of 10 µg/ml αCD3 antibody coated on a 96-well flatbottom plate. Cytokine production was determined after 24 h by ELISA (3.2.6).

3.2.12.2 Proliferation Assays

To determine proliferation profiles, OT-I T cells were labelled with 2.5 µM CFSE in 5 ml PBS for 10 min at 37°C after isolation as desribed in 3.2.11. The CFSE reaction was stopped by addition of 5 ml FCS for 1 min at room temperature followed by centrifugation for 5 min at 486 × g. Then, cells were resuspended in medium, counted, and cell numbers were adjusted to the required cell concentration. Proliferation was analysed by flow-cytometry after 3 days of coculture.

3.2.12.3 *In vitro* cytotoxicity assay

RMA cells were resuspended and divided into two fractions of which one fraction was loaded with 1 µM of the $H\text{-}2K^b$ peptide S8L for 15 min at 37°C. Subsequently, peptide-loaded cells were labelled with 2.5 µM CFSE whereas the unloaded cell fraction was labelled with 0.25 µM CFSE for 15 min at 37°C. Cells were washed once with cold PBS, resuspended, and mixed in a 1:1 ratio. $5x10^3$ cells, i.e. $2.5x10^3$ S8L-loaded cells,

were seeded into 96-well plates. OT-I T cells, that were isolated from cocultures with PIO-treated or untreated BM-DCs by employing a gradient with lymphocyte-separation medium, were added to the target cells in different target : T cell ratios. After 4 h, cells were analysed by flow-cytometry and the specific cytotoxicity was calculated as follows:

$$\% \text{ OVA-specific cytotoxicity} =$$
$$100 - [100 \times (CFSE^{high} / CFSE^{low})_{sample} / (CFSE^{high} / CFSE^{low})_{control}]$$

$5x10^3$ RMA cells cultured without T cells served as controls.

3.2.12.4 *In vivo* cytotoxicity assay

PIO-treated or vehicle-treated wild-type mice were immunised with $1x10^6$ PIO-treated or untreated OVA-loaded BM-DCs subcutaneously (s.c.). 5 d later, target cells were prepared to assess *in vivo* cytotoxic activity. As target cells, splenocytes were either pulsed with S8L peptide (1 μg/ml, 45 min at 37 °C) and labelled with a high concentration of CFSE (1 μM, 15 min at 37 °C; $CFSE^{high}$ cells) or mock-treated and labelled with a low concentration of CFSE (0.1 μM; $CFSE^{low}$ cells). Cells were washed twice with PBS and equal numbers of cells from each population were injected i.v. (10^7 target cells). Animals were sacrificed after 18 h and the presence of target cells in the draining lymphnodes was determined by flow-cytometry. The specific cytotoxicity was calculated as in 3.2.12.3. Target cells injected into non-immunised mice served as controls.

3.2.12.5 OVA uptake *in vivo* and *ex vivo* coculture of splenic DCs with B3Z cells

45 min after injection of purified OVA (see 3.2.8.1), splenic DCs were isolated as described in 3.2.11 and $0.5x10^5$ DCs were cocultured with $1x10^5$ B3Z cells in 96-well plates for 72 h. Activation of B3Z cells was determined by measuring the conversion of CPRG by absorbance spectrophotometry at 595 nm.

3.2.12.6 Coculture of memory T cells with BM-DCs

For induction of an OVA-specific $CD8^+$ T cell memory response *in vivo*, $CD8^+$ T cells derived from OT-I mice carrying the congenic marker CD90.2 were transferred i.v. into C57BL/6 mice carrying the congenic marker CD90.1. After 24 h, mice were immunised with OVA-expressing adenoviruses (AdOVA, 1.10^7 PFU / mouse) i.v.. After 30 days,

OVA-specific $CD8^+$ T cells were isolated by immuno-magnetic separation using a $CD8^+$ T cell isolation kit according to the manufacturer's instructions followed by further purification using magnetic beads labelled with an antibody directed against CD90.2. Isolated $CD8^+CD90.2^+$ T cells were restimulated *in vitro* by either PIO-treated or untreated OVA-loaded BM-DCs. After 36 h, production of IFNγ was assessed by ELISA (3.2.6).

3.2.12.7 Coculture of primary microglia with primary neurons

pMg that were pretreated with 10 μM PIO for 5 days or left untreated were harvested and stimulated for 48h with 1 μg/ml LPS + 10 ng/ml IFN-γ with or without PIO in primary microglia medium which contained N2-supplement instead of FCS. Microglia were harvested, resuspended in neuronal medium, and $5x10^4$ pMg were added to each well of neuron culture chamber slides containing $2.5x10^4$ neurons (ratio of 1:5 (microglia : neurons)). After 24 h, staining and microscopy was performed as described in 3.2.13.2.

3.2.13 Microscopy

3.2.13.1 Microscopical analysis of S8L presentation by BM-DCs

BM-DCs were treated with 10 μM PIO or left untreated as described in 3.2.1.2. On day 6 of differentiation procedure, 10 mg/ml purified OVA was added to the appropriate cell culture dishes overnight. Then, $4x10^5$ BM-DCs were seeded into 24-well plates and left at 37°C to allow cells to adhere. Next, cells were washed with PBS and incubated with 300 μl blocking solution I to block non-specific binding sites. After incubation for 1 h at room temperature, cells were washed three times with PBS, and stained with the biotinylated antibody 25D1.16 (1:50 in PBS + 1 % normal mouse serum) to detect the OVA-derived peptide SIINFEKL (S8L) bound to $H\text{-}2K^b$ molecules. Following 30 min of incubation at room temperature, cells were washed three times, incubated with Alexa647-conjugated strepatavidin for 15 min at room temperature, and washed three times with PBS. Lastly, 1.2 μg/ml Hoechst 33342 in PBS was added for 5 min at room temperature and cells were washed again. S8L presentation was analysed by microscopy using an Olympus IX81 microscope. Analysis of the mean fluorescence intensity of 25D1.16 staining was performed using the Olympus SCAN^R software.

3.2.13.2 Microscopical analysis of neuron-microglial cocultures

After 24 h of neuron-micrgolial coculture, the supernatant was slowly sucked off, cells were washed carefully two times with PBS, and staining was performed at room temperature. Cells were fixed in 4 % PFA for 15 min, subsequently blocked with blocking solution II for 1 h, and stained with the primary antibodies against β-tubulin 3 (for detection of neurons) and Iba1 (for detection of microglia) added in blocking solution II for 2 h. Afterwards, cells were washed three times with PBS, the secondary antibodies goat-anti-mouse-Cy3 (neurons) and goat-anti-rabbit-Alexa488 were added for 2 h in blocking solution II, and finally, after three wash steps with PBS, cover slides were fixed with Mowiol. Cells were examined under an Olympus IX81. Ten randomly selected areas were scanned and relative neuronal neurite density was calculated by counting all β-tubulin 3 positive neurites that crossed three parallel lines per image. The mean neurite density per area was determined and afterwards the mean neurite density per sample, i.e. per 10 randomly selected areas, was calculated. The relative neuronal neurite density of cocultures with untreated C57BL/6 primary microglia served as control and was set as 1.

3.2.14 Experimental autoimmune encephalomyelitis (EAE)

EAE was induced by s.c. injection of 50 μg MOG_{35-55} peptide emulsified in complete Freund's adjuvant with 8 mg/ml heat-inactivated *Mycobacterium tuberculosis* and two intraperitoneal (i.p.) injections of 100 ng *Bordetella pertussis* toxin on days 0 and 2. Clinical assessment of EAE was performed daily using a scale ranging from 0 to 8: 0, no paralysis; 1, limp tail; 2, ataxia or unilateral hind limb paresis; 3, severe unilateral or weak bilateral hind limb paresis; 4, severe bilateral hind limb paresis; 5, complete bilateral hind limb plegia; 6, complete bilateral hind limb plegia and partial fore limb paresis; 7, severe tetraparesis/plegia; 8, moribund/dead animals.

3.2.15 Isolation of CNS mononuclear cells

For mononuclear cell isolation from the CNS of EAE-diseased mice, mice were anesthesised with Avertin and then perfused with 25 ml of GBSS and heparin. Afterwards the brain was carefully dissected from the skull and the spinal cord was flushed out of the spinal column with GBSS containing heparin employing a 20 G

needle attached to a 10 ml syringe. Brain and spinal cord were dissected, taken up in 10 ml of 0.4 mg / ml CollagenaseA in PBS, and left for 30 min at 37°C for tissue digestion in a rotary shaker. Then, the tissue was homogenised by pressing it through a metal cell strainer and cells were washed once with icecold PBS + 1 % FCS. Subsequently, cells were resuspended in 2.5 ml of 30 % Percoll and a gradient was created by underlayering the cell suspension with 2.5 ml of 37 % Percoll solution which was subsequently underlayered with 2.5 ml of 70 % Percoll solution. The gradient was centrifuged for 30 min at 859 × g with acceleration 7 and break 1. Mononuclear cells were collected from the 30 % : 37 % as well as the 37 % : 70 % interface and washed two times with icecold PBS + 1 % FCS. In case of analysis of myeloid cell surface markers, cells were resuspended in FACS buffer and staining was performed as described in 3.2.2.1. For analysis of T cell cytokine production by intracellular FACS staining (3.2.2.3), cells were resuspended in T cell medium containing 5 ng/ml PMA and 200 ng/ml IONO as well as 1 µl/ml of both, BrefeldinA and Monensin. For ELISPOT analysis of T cells (3.2.7), cells were resuspended in T cell medium.

3.2.16 Histology

For histological staining, the CNS of diseased mice was perfused with 25 ml of GBSS containing heparin and afterwards fixed by perfusion with with 25 ml 4 % PFA. Next, the brain was carefully dissected from the skull and the spinal chord was isolated and stored in 4 % PFA. Immunohistochemistry of the spinal chord was kindly performed by Dr. Ildiko Dunay and Prof. Marco Prinz (Department of Neuropathology, University of Freiburg, Germany) as described[42]. To determine the degree of demyelination, three slices of the spinal chord were stained with luxol fast blue (LFB) and afterwards incubated with Schiff reagent which stains demyelinated areas in pink. To quantify the percentage of demyelinated area, the total area as well as the proportion of demyelinated area per section was analysed using the Cell Analysis Software. To detect axonal damage, sections were stained for amyloid precursor protein (APP) and APP deposits were counted. Immunohistochemical staining of MAC-3 was performed to detect CNS-resident microglia and infiltrating macrophages and CD3 to detect T cells. For quantification, numbers of APP deposits or immune cells were applied to the total

area in mm^2 per section. Three sections per animal were analysed with 5 mice per group.

3.2.17 Ablation of $CCR2^+$ inflammatory monocytes

$CCR2^+$ inflammatory monocytes were depleted during EAE by i.p. injection of 20 µg αCCR2 (MC-21) or Isotype Control (Rat IgG2b). Antibodies were administered every 24 h from days 13 to 17 post EAE-induction. 8 h after the first injection, depletion of inflammatory monocytes, i.e. $CD11b^+Ly\text{-}6C^{hi}Ly\text{-}6G^-$ cells, was monitored in the blood by flow-cytometry (3.2.2.1).

3.2.18 Monocyte differentiation experiments

3.2.18.1 *In vivo* labelling of Ly-$6C^{hi}$ monocytes

EAE was induced in C57BL/6 mice (3.2.14). On day 12 after immunisation, mice were administered 200 µl clodronate liposomes by i.v. injection which results in depletion of blood monocytes or received PBS liposomes as control. 12 h later, i.e. during the time of leukocyte reconstitution, mice received 0.5 µm Flouresbrite FITC-dyed polystyrene beads diluted 1:25 in PBS by i.v. injection. Another 12 h later, CNS mononuclear cells were isolated (3.2.15) and infiltrating $FITC^+$ monocytes were analysed for CD45 expression by flow-cytometry (3.2.2.1).

3.2.18.2 Adoptive transfer of $CD45.2^+$ monocytes

EAE was induced in CD45.1 mice (3.2.14). On day 12, $CD115^+$ monocytes were isolated from the bone marrow of congenic mice for adoptive transfer. To this end, bone marrow cell suspensions from C57BL/6 mice ($CD45.2^+$) were centrifuged at 486 × g for 5 min and afterwards resuspended in 40 µl MACS buffer per $1x10^7$ cells which contained 10 µl/ml αCD16/CD32 to block Fcγ receptors. Cells were incubated for 10 min at room temperature after which 100 ng of biotinylated αCD115 per $1x10^6$ cells was added to the cell suspension and further incubated for 10 min at room temperature. After addition of MACS buffer and centrifugation for 10 min at 486 × g, cells were incubated with 80 µl MACS buffer + 20 µl αbiotin microbeads per $1x10^7$ cells for 15 min at 4°C. Subsequently, cells were washed once with MACS buffer, resuspended, and separated by positive selection using the AutoMACS Separation Technology.

Isolated cells were analysed by flow-cytometry for CD11b and Ly-6C expression (3.2.2.1). Cells were counted and the percentage of $CD11b^+Ly\text{-}6C^+$ cells was applied to the total cell number to calculate the number of isolated $Ly\text{-}6C^+$ monocytes. Finally, $1x10^7$ $Ly\text{-}6C^+$ monocytes in 200 µl PBS were adoptively transferred by i.v. injection into recipient mice. 12 h after monocyte transfer, CNS mononuclear cells were isolated (3.2.15) and transferred $CD45.2^+$ monocytes were analysed for CD45 expression (3.2.2.1).

3.2.19 Statistics

Results are depicted as mean ± standard error of the mean (SEM). Statistical significance was calculated by an unpaired two-tailed Student's t test using Microsoft Excel software. p values of 0.01 to 0.05 were considered significant (*), p values of 0.001 to <0.01 highly significant (**) and p of <0.001 extremely significant (***).

4 Results

4.1 Impact of PPARγ activation in dendritic cells on cross-priming of cytotoxic T cells

Dendritic cells (DCs) are professional antigen-presenting cells (APCs) that are capable of cross-presenting extracellular antigens on MHC-I molecules[15,16] which is a prerequisite for the activation of antigen-specific naive $CD8^+$ T cells. We and others have shown that DC immunogenicity and their capacity to activate $CD4^+$ T cells is regulated by the nuclear transcription factor PPARγ. Activation of PPARγ interferes with inflammation-induced upregulation of costimulatory molecules like CD80, CD86, and CD40 as well as production of proinflammatory cytokines, e.g. IL-6 and IL-12, upon inflammatory stimulation of DCs[78,79]. This "less stimulatory mode" results in $CD4^+$ T cell anergy[79]. However, if PPARγ is also involved in regulation of DC cross-priming capacity and resulting antigen-specific $CD8^+$ T cell responses is not known. Therefore, we investigated if PPARγ activation influences cross-presentation by DCs and subsequent activation of naive $CD8^+$ T cells.

4.1.1 The expression of the MR by DCs is increased after activation of PPARγ

In this study we focused on the influence of PPARγ activation in DCs on mannose receptor (MR)-mediated cross-presentation of the soluble model antigen ovalbumin (OVA). Burgdorf et al. have demonstrated that the MR is essential for cross-presentation of soluble OVA as MR-deficient BM-DCs were not capable of cross-presenting OVA[25,26] and furthermore, that the antiinflammatory nuclear transcription factor PPARγ was expressed primarily by MR^+ DCs compared to MR^- DCs (fold change of 2.74; $p=0.0015$)[103] which is in line with previous observations by Coste et al. that have correlated PPARγ activation to increased levels of MR mRNA in DCs[104].

These reports led us to hypothesise that PPARγ activation in BM-DCs results in enhanced MR expression. Therefore, we differentiated bone marrow precursor cells in the presence of the synthetic PPARγ agonist pioglitazone (PIO) and analysed MR expression on day 7 by flow-cytometry. Indeed, we observed that PIO-treatment

resulted in an increased proportion of MR-expressing BM-DCs when compared to untreated DCs (Figure 1a,b). As PIO potentially could have mediated its effect in a PPARγ-independent fashion, we next investigated whether increased expression levels of the MR were still observed in PIO-treated PPARγ^{KO} BM-DCs. To this end, we generated conditional PPARγ^{KO} BM-DCs *in vitro* by treatment of bone marrow precursor cells derived from PPARγ$^{fl/fl}$ mice with a membrane-permeable Cre-recombinase (HTNCre) which leads to deletion of exon 1 and 2 and thus a non-functional PPARγ gene in 70-80 % of all cells[79,100]. Importantly, PIO-treatment of conditional PPARγ^{KO} DCs did not result in significant upregulation of the MR as observed in HTNCre-treated wildtype BM-DCs (Figure 1c,d). Thus, activation of PPARγ in DCs by PIO-treatment increases the proportion of MR-expressing cells which is mediated by PPARγ-dependent effects of PIO.

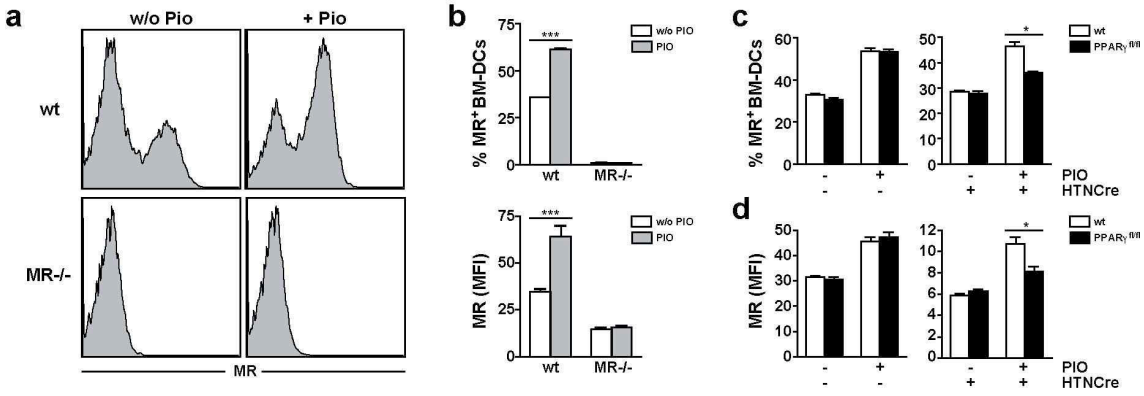

Figure 1 PPARγ activation in BM-DCs results in upregulation of the MR.

(a) Wildtype (wt) or MR-deficient (MR-/-) BM-DCs were treated with 10 μM PIO during the differentiation procedure or were left untreated. On day 7, MR expression was analysed by flow-cytometry. (b) Graphs show the analysis of histograms in (a); i.e. the mean percentage of MR$^+$ BM-DCs (upper panel) ± SEM and the average mean fluorescence intensity (MFI; lower panel) ± SEM. (c+d) Bone marrow precursor cells were isolated from wt or PPARγ$^{fl/fl}$ mice and treated for 6 h with HTNCre on days 0 and 4 of the differentiation procedure. Due to this procedure, PPARγ was ablated in PPARγ$^{fl/fl}$ BM-DCs but not in wt BM-DCs (c+d; –HTNCre: left panel; +HTNCre: right panel). 10 μM PIO was added to the appropriate dishes. On day 7 of differentiation, MR expression was analysed by flow-cytometry. (c) The mean percentage of MR$^+$ BM-DCs ± SEM or (d) the average MFI ± SEM is shown. Experiments were performed at least three times and data of one representative experiment is shown. * $p<0.05$; *** $p<0.001$.

4.1.2 PPARγ-activation in DCs enhances MR-mediated OVA-uptake

We next asked whether the observed PPARγ-mediated upregulation of MR expression leads to enhanced uptake of soluble OVA as the MR mediates uptake of OVA in DCs[25,26]. To this end, we treated BM-DCs with PIO or left cells untreated and incubated these cells with fluorescently-labeled OVA. Flow-cytometrical analysis revealed that PIO-treated BM-DCs took up significantly more OVA when compared to untreated BM-DCs (Figure 2a,b). As MR-deficient BM-DCs did not take up OVA and we did not observe an increase in OVA uptake after PPARγ activation (Figure 2a,b), it can be concluded that increased uptake of OVA after PIO-treatment of wildtype BM-DCs was mediated by enhanced MR expression. To confirm that increased OVA-uptake after PIO-treatment was mediated by PPARγ-dependent effects of PIO, we repeated the experiment in conditional PPARγ^{KO} BM-DCs. We observed that ablation of PPARγ in BM-DCs abrogated the differences that were observed in PIO-treated compared to untreated wildtype BM-DCs and uptake of OVA was not enhanced in PIO-treated PPARγ^{KO} BM-DCs (Figure 2c,d). Thus, these data demonstrate that PPARγ activation after PIO treatment was responsible for the observed increase in MR-mediated OVA uptake.

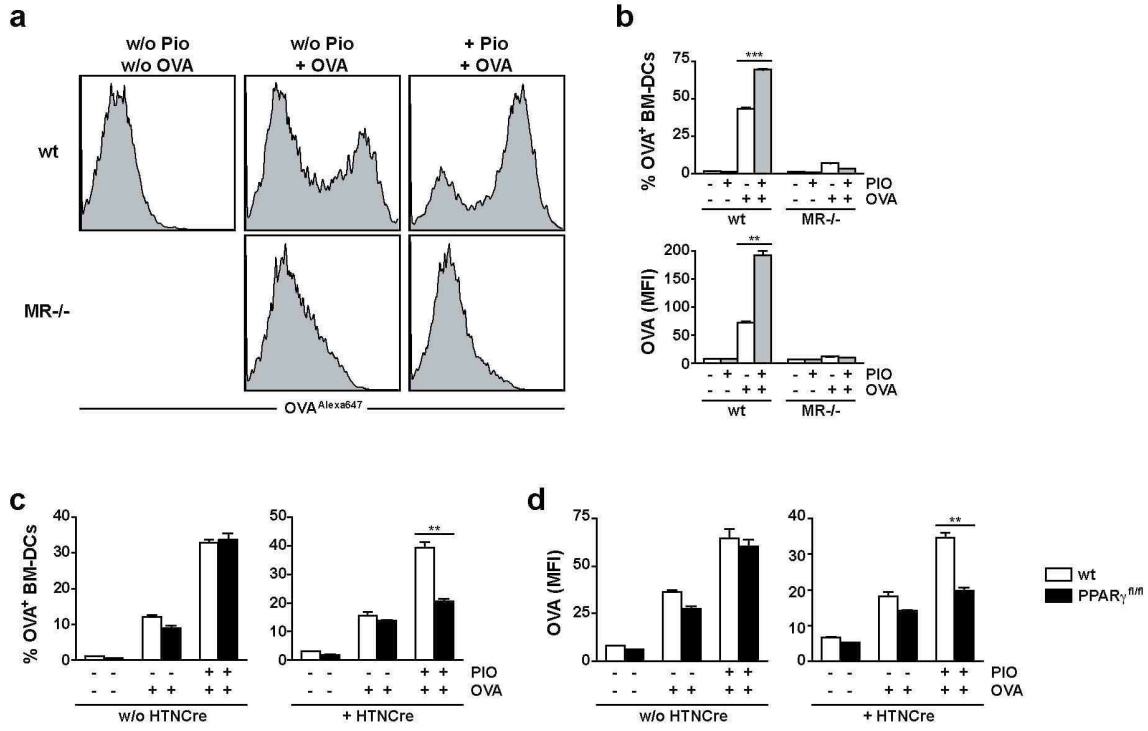

Figure 2 PPARγ-mediated increase of MR expression results in enhanced MR-mediated uptake of OVA.

(a) PIO-treated or untreated wt or MR-/- BM-DCs were incubated with 3 μg/ml AlexaFluor647-labelled OVA at 37°C. After 15 min, OVA uptake was determined by flow-cytometrical analysis. (b) Graphs show the analysis of histograms in (a); i.e. mean percentage of OVA^+ BM-DCs (upper panel) ± SEM and the average MFI (lower panel) ± SEM. (c+d) Bone marrow precursor cells were isolated from wt or $PPAR\gamma^{fl/fl}$ mice and treated for 6 h with HTNCre on days 0 and 4 of the differentiation procedure. During this procedure, PPARγ was ablated in $PPAR\gamma^{fl/fl}$ BM-DCs but not in wt BM-DCs (c+d; –HTNCre: left panel; +HTNCre: right panel). 10 μM PIO was added to the appropriate dishes. On day 7 of differentiation, OVA uptake experiments were performed as in (a) and uptake was analysed by flow-cytometry. (c) The mean percentage of OVA^+ BM-DCs ± SEM or (d) the average MFI ± SEM is shown. Experiments were performed at least three times and data of one representative experiment is shown. * *p<0.01; *** p<0.001.

4.1.3 Increased OVA-uptake after PPARγ activation in DCs results in enhanced OVA cross-presentation

As Burgdorf et al. have shown that soluble OVA, which has been taken up via the MR, is cross-presented on MHC-I molecules[25], we hypothesised that the observed PPARγ-induced increase in MR-mediated uptake of soluble OVA leads to enhanced cross-presentation of OVA by DCs. To this end, we incubated PIO-treated or untreated BM-DCs with purified OVA for 16 h. Then, OVA-loaded BM-DCs were stained with the antibody 25-D1.16 which binds to the OVA-derived epitope SIINFEKL (S8L) when complexed to the MHC-I molecule K^b [25,105-108]. We performed microscopical analysis of OVA-loaded BM-DCs using the Scan^R software to determine the mean fluorescence

intensity (MFI) of 25-D1.16 staining and hence the amount of cross-presented OVA. Importantly, we observed that PIO-treated BM-DCs exhibited significantly enhanced MFI of α25-D1.16-staining compared to untreated DCs (Figure 3a) which demonstrates that cross-presention of OVA was enhanced after PPARγ activation. In a second approach we incubated PIO-treated or untreated DCs with soluble OVA and subsequently cocultured OVA-loaded DCs with the T cell hybridoma B3Z which recognises S8L in the context of MHC-I K^b [109] and does not depend on costimulatory signals for activation[109-111]. Importantly, activated B3Z cells produce β-galactosidase under control of the IL-2 promoter whose activity directly correlates with the amount of cross-presented S8L. As shown in Figure 3b, we observed that coculture with PIO-treated BM-DCs resulted in significant increased activation of B3Z cells confirming that PPARγ-activation in DCs indeed resulted in enhanced levels of cross-presented OVA.

Taken together, PPARγ activation by PIO led to upregulation of the MR in DCs which resulted in enhanced uptake of soluble OVA and in turn cross-presented OVA-derived peptides.

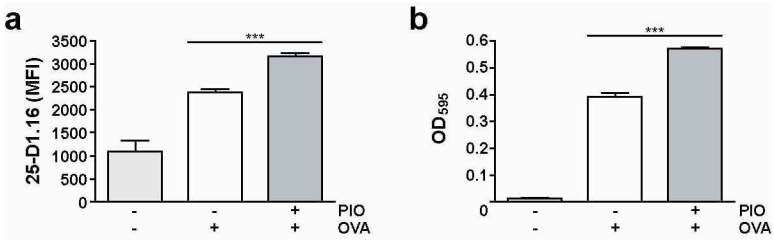

Figure 3 **Increased OVA-uptake after PPARγ activation in DCs results in enhanced OVA cross-presentation.**

(a) Wildtype BM-DCs were treated with 10 μM PIO or left untreated. On day 6 of the differentiation procedure, 10 mg/ml purified OVA was added overnight. For detection of cross-presented OVA, BM-DCs were stained with a biotinylated 25-D1.16 antibody and Alexa647-labelled Streptavidin. The MFI of 25-1.16 staining was analysed using the SCAN^R software from Olympus. The graph shows the average MFI ± SEM. (b) PIO-treated or untreated BM-DCs were cocultured with B3Z cells at a ratio of 1:2 (BM-DC:B3Z) in the presence or absence of 0.5 mg/ml purified OVA. After 24 h, CPRG solution was added to the cells and activation of B3Z cells was determined by spectophotometric analysis of CPRG-conversion at 595 nm. The graph shows the mean optical density at 595 nm (OD_{595}) ± SEM. (Experiment performed by Luisa Klotz). All experiments were performed at least 3 times. Data of one representative experiment are shown. Within one experiment, n ≥ 3. *** $p<0.001$.

4.1.4 PPARγ-activation in DCs results in impaired antigen-specific CD8$^+$ T cell activation

As PIO-mediated activation of PPARγ in DCs resulted in enhanced levels of MR-mediated uptake and increased levels of cross-presented OVA-peptides, we next asked whether also cross-priming of naive OVA-specific CD8$^+$ T cells by PIO-treated BM-DCs is altered. Therefore we made use of T cell receptor transgenic OT-I mice which express an OVA-specific T cell receptor that recognises the S8L epitope bound to MHC-I K^b. In contrast to B3Z cells, naive CD8$^+$ OT-I T cells depend on constimulation and cytokines for full activation[112]. To investigate whether PPARγ activation affects priming of naive T cells, we set up coculture assays of PIO-treated or untreated BM-DCs with naive OT-I T cells in the presence of 0.5 mg/ml purified OVA. After 48 h, we analysed the T cell activation status and determined IFN-γ secretion in the supernatant by ELISA and analysed the CFSE dilution profile by flow-cytometry to determine proliferation. As shown in Figure 4a and Figure 4b, PIO-treated DCs were strongly impaired in their capability to efficiently cross-prime naive CD8$^+$ T cells as T cells primed by PIO-treated BM-DCs produced significantly less IFN-γ through a range of DC:T cell ratios (Figure 4a) and exhibited impaired proliferation (Figure 4b). As these results suggested that naive OT-I T cells were not appropriately activated, we next performed an *in vitro* cytotoxicity assay which allows to analyse the cytotoxicity of CD8$^+$ T cells and hence, whether T cells had acquired effector functions during priming. To this end, OT-I T cells were isolated after 5 days of priming by PIO-treated or untreated BM-DCs using density gradient centrifugation and subsequently incubated with CFSE-labelled, S8L-loaded target cells. Lysis of target cells and hence, the capability of OT-I T cells to perform effector functions, was analysed after 4 h by flow cytometry. Importantly, OT-I T cells primed by PIO-treated BM-DCs exhibited significantly reduced cytotoxic capacity compared to OT-I T cells activated by untreated DCs (Figure 4c) which demonstrates that, although PPARγ activation results in enhanced cross-presentation of OVA, naive T cell priminig is impaired.

We wondered whether this impairment in activation of OVA-specific T cells can also be observed during reactivation of OVA-specific CD8$^+$ memory T cells. To this end, we adoptively transferred naive CD45.2$^+$ OT-I T cells into CD45.1$^+$ recipient mice which were infected one day later with an OVA-expressing adenovirus to generate memory

CD8$^+$ T cells. 30 days post infection, we isolated CD45.2$^+$ cells, i.e. OVA-specific memory CD8$^+$ T cells, cocultured them *ex vivo* with OVA-loaded, PIO-treated or untreated BM-DCs and determined IFN-γ production by ELISA. Importantly, PPARγ activation in BM-DCs did not influence their reactivation capacity as memory T cells were equally well reactivated by PIO-treated or untreated DCs and produced similar amounts of IFN-γ (Figure 4d).

Taken together, PPARγ activation in DCs impairs activation of naive CD8$^+$ T cells and subsequent differentiation into effector T cells. In contrast, reactivation of established CD8$^+$ T cell responses remains unaffected.

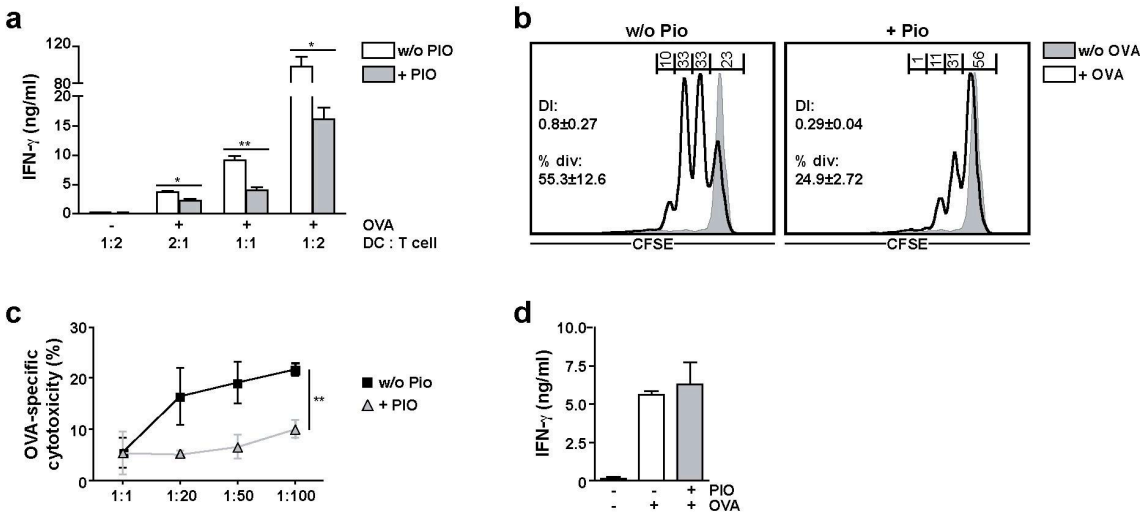

Figure 4 PPARγ-activation in DCs results in impaired antigen-specific CD8$^+$ T cell activation.

(a) Wildtype BM-DCs were treated with 10 μM PIO or left untreated and subsequently cocultured with naive OVA-specific CD8$^+$ T cells derived from OT-I mice in the presence of 0.5 mg/ml OVA at the indicated DC:T cell ratios. After 48 h, the concentration of IFN-γ in the supernatant was determined by ELISA. The mean concentration of IFN-γ ± SEM is depicted. (Experiment performed by Sven Burgdorf). (b) PIO-treated or untreated BM-DCs were cocultured with CFSE-labelled OT-I T cells as described in (a) at a ratio of 1:2 (DC:OT-I). After 72 h, flow-cytometrical analysis of CFSE-dilution was performed. Within histograms, the mean division index (DI) ± SEM and the percentage of divided cells (% div) ± SEM is shown on the left side and the average percentage of cells per cycle is shown above the graph. (c) OT-I T cells were isolated after 5 d priming by PIO-treated or untreated BM-DCs and incubated at the indicated target cell:T cell ratios with OVA-peptide-loaded CFSE-labelled target cells. 4 h later, the OVA-specific cytotoxicity was analysed by flow-cytometry. The mean OVA-specific cytotoxicity ± SEM is shown. (d) CD90.2$^+$ OT-I T cells were adoptively transferred into congenic CD90.1 mice 24 h before infection with an OVA-expressing Adenovirus. After 30 d, CD90.2$^+$ memory T cells were isolated by immunomagnetic separation and *ex vivo* restimulated by PIO-treated or untreated, OVA-loaded BM-DCs. 18 h later, reactivation of memory T cells was determined by detection of IFN-γ in the supernatant by ELISA. The graph shows the mean concentration of IFN-γ ± SEM. All experiments were performed at least 2 times. Data of one representative experiment are shown. Within one experiment, n ≥ 3. * $p<0.05$; ** $p<0.01$.

4.1.5 Enhanced B7H1 expression after activation of PPARγ in DCs restricts priminig of naive CD8$^+$ T cells

PPARγ activation in DCs interferes with upregulation of costimulatory molecules and cytokine production upon inflammatory stimulation[78,79]. Therefore we next asked whether impaired priming of naive OVA-specific OT-I T cells by PIO-treated, naive BM-DCs was the result of a change in expression of coinhibitory and costimulatory molecules and compared expression on PIO-treated or untreated BM-DCs by flow-cytometrical analysis. We observed a significantly enhanced expression of the coinhibitory molecule B7H1 on PIO-treated BM-DCs (Figure 5a). Furthermore, when we incubated PIO-treated or untreated BM-DCs with fluorescently-labelled OVA, we observed that OVA uptake and hence MR expression correlated with B7H1 expression and that the proportion of B7H1$^+$OVA$^+$ BM-DCs was increased among PIO-treated compared to untreated BM-DCs (Figure 5b). Interestingly, the expression of costimulatory molecules, i.e. CD40, CD80, CD86, and ICOSL, was not significantly altered due to PIO-treatment (Figure 5c) which strongly suggests that a change in conhibition but not costimulation is the reason for impaired priming of naive CD8$^+$ T cells by PIO-treated DCs. However, as the coinhibitory molecule B7DC was only marginally expressed on immature BM-DCs and not altered in response to PIO-treatment (Figure 5d) our data strongly indicate that B7H1 is the main mediator of PPARγ-induced impairment of naive CD8$^+$ T cell priming.

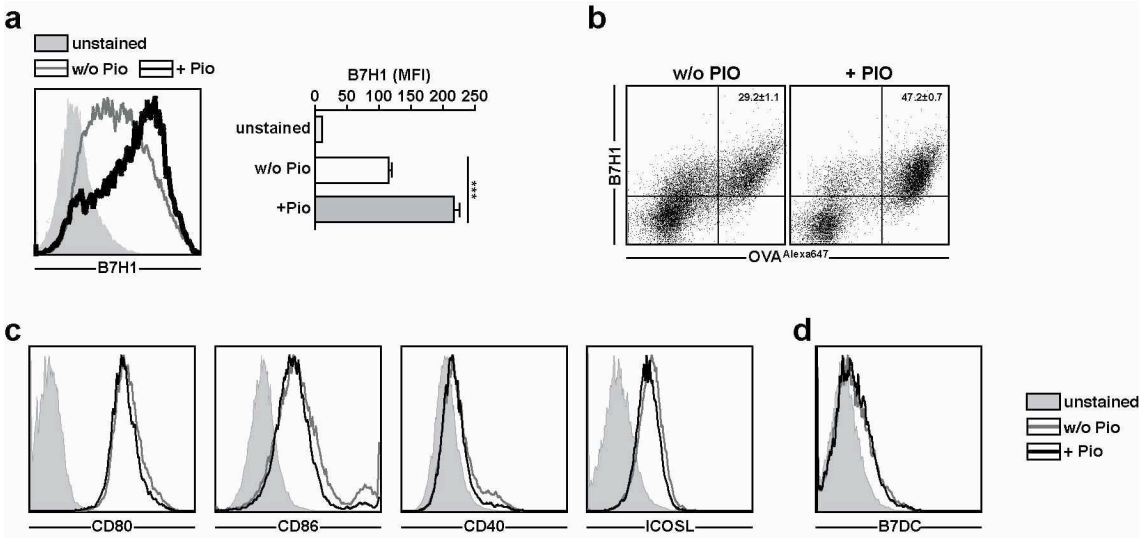

Figure 5 **PPARγ activation leads to enhanced expression of B7H1 but not to changes in other costimulatory and coinhibitory molecules.**

(a) BM-DCs were treated with 10 μM PIO or left untreated, stained for B7H1, and analysed by flow-cytometry. The accompanying graph depicts the average MFI of B7H1 expression ± SEM. (b) PIO-treated or untreated BM-DCs were incubated with 3 μM Alexa647-labelled OVA for 15 min at 37°C. Subsequently, cells were stained for B7H1, and analysed by flow-cytometry. Numbers in dotplots represent the mean percentage of $B7H1^+OVA^+$ BM-DCs ± SEM. (c,d) PIO-treated or untreated BM-DCs were stained for expression of (c) costimulatory molecules CD80, CD86, CD40, and ICOSL and (d) the coinhibitory molecule B7DC and analysed by flow-cytometry. All experiments were performed at least 2 times. Data of one representative experiment are shown. Within one experiment, $n \geq 3$. *** $p<0.001$.

We next investigated whether the observed upregulation of B7H1 was responsible for PIO-induced impairment of naive $CD8^+$ T cell activation. To this end, we treated B7H1-deficient BM-DCs with PIO or left cells untreated which were then cocultred with OT-I T cells. To determine T cell activation we measured IFN-γ production in the supernatant by ELISA and analysed CFSE dilution profiles by flow-cytometry. Importantly, T cells primed by PIO-treated B7H1-deficient BM-DCs produced significantly higher amounts of IFN-γ (Figure 6a) and exhibited strongly increased proliferation (Figure 6b). Hence, as PIO-treatment in the absence of B7H1 resulted in increased T cell priming *in vitro*, these data strongly suggest that the impaired T cell priming capacity of PIO-treated wildtype BM-DCs was mediated by upregulation of B7H1.

As coinhibitory signalling of B7H1 expressed by APCs is mediated by interaction with PD-1 expressed on the T cell surface[28] we next hypothesised that the interference with B7H1 – PD-1 interaction during coculture experiments will restore the capacity of PIO-treated wildtype BM-DCs to activate naive $CD8^+$ T cells. To this end, we first confirmed PD-1 expression on freshly isolated OT-I T cells by flow-cytometry (Figure 6c). Then, we set up coculture assays of PIO-treated or untreated wildtype BM-DCs with naive OT-I T cells and specifically blocked the interaction of B7H1 and PD-1 by adding a PD-1-specific antibody[92] (right graph) or the appropriate isotype control (left graph). Importantly, we observed that blocking the interaction of PD-1 and B7H1 abrogated the impairment of PIO-treated DCs to cross-prime naive $CD8^+$ T cells as T cells primed by PIO-treated DCs produced slightly enhanced levels of IFN-γ when compared to T cells primed by untreated DCs (Figure 6d).

To summarise, these data demonstrate that impaired cross-priming capability of BM-DCs after PPARγ activation is mediated by upregulation of B7H1 on APCs and its interaction with PD-1 expressed on the T cell surface.

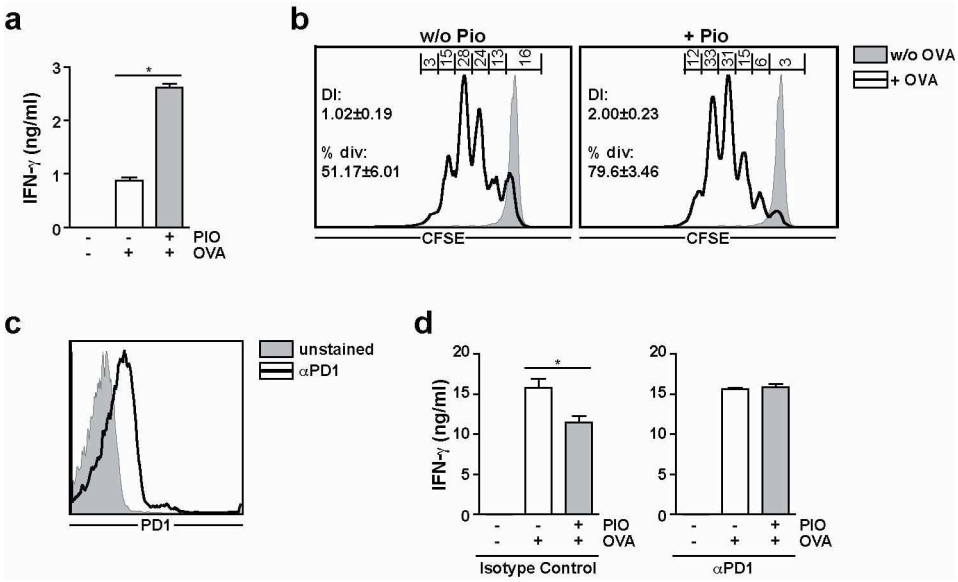

Figure 6 **Upregulation of B7H1 in PPARγ-activated BM-DCs restricts cross-priming of naive OT-I T cells.**

(a) BM-DCs were generated from B7H1-deficient mice and treated with 10 μM PIO or left untreated. BM-DCs were cocultured with OVA-specific OT-I T cells at a ratio of 1:2 (BM-DCs:OT-I) in the presence or absence of 0.5 mg/ml purified OVA and T cell activation was determined by quantification of IFN-γ in the supernatant by ELISA. The average IFN-γ concentration ± SEM is shown. (b) PIO-treated or untreated B7H1-deficient BM-DCs were cocultured with CFSE-labelled OT-I T cells to determine T cell proliferation. After 48 h, the CFSE dilution profile was analysed by flow-cytometry. Numbers on the left side in histograms display the mean division index (DI) ± SEM and average percentage of divided cells (% div) ± SEM. Numbers above the histogram show the mean percentage of cells within one cycle. (c) OT-I T cells were isolated from spleen and lymph nodes of OT-I mice, stained for PD-1, and analysed by flow-cytometry. (d) PIO-treated or untreated wldtype BM-DCs were cocultured with OT-I T cells at a ratio of 1:2 (BM-DCs:OT-I) in the presence of 20 μg/ml PD-1 blocking antibody or isotype control. After 18 h, T cell activation was determined by detection of IFN-γ in the supernatant by ELISA. The mean concentration of IFN-γ ± SEM is depicted. All experiments were performed at least 2 times and data of one representative experiment is shown. * $p<0.05$.

4.1.6 Activation of PPARγ in splenic DCs impairs cross-priming of naive CD8$^+$ T cells *in vivo* by upregulation of B7H1

Next, we asked the question whether the observed effect of PPARγ activation on cross-presentation by BM-DCs *in vitro* is also observed after PPARγ activation in DCs *in vivo*. Therefore we administered 30 mg/kg bodyweight PIO or the vehicle only to C57BL/6 mice by daily oral gavage for 7 days. First we investigated whether PIO-treatment changes MR-expression and MR-mediated OVA-uptake in splenic DCs. To this end, PIO-treated or untreated mice were injected with 5 μg/g bodyweight fluorescently-labelled OVA, splenic CD11c$^+$ DCs were isolated 45 min later, and DCs were analysed with regard to OVA-uptake as well as MR-expression by flow-cytometry. We observed that also *in vivo*, PIO-treatment increased the proportion of

MR-expressing DCs and enhanced OVA-uptake (Figure 7a) thus, confirming our *in vitro* findings in PIO-treated BM-DCs.

Next, we hypothesised that enhanced uptake of OVA following PIO-treatment *in vivo* in turn results in increased cross-presentation of OVA. To this end, PIO-treated or untreated wildtype mice were injected with 100 μg/g bodyweight purified OVA. 45 min later, splenic DCs were isolated, cocultured with B3Z cells, and activation of B3Z cells was determined by spectophotometric analysis of CPRG-conversion. Importantly, PIO-treated splenic DCs not only exhibited increased MR-mediated OVA-uptake but furthermore, activated B3Z cells more efficiently than untreated DCs (Figure 7b). Thus, these observations demonstrate that also *in vivo*, PPARγ activation in DCs results in increased cross-presentation of OVA.

As our *in vitro* findings showed that PIO-treated BM-DCs were impaired in their capacity to prime naive OT-I T cells we next wanted to investigate whether *in vivo* PIO-treatment changes the cross-priming ability of splenic DCs. To this end, we isolated splenic DCs from PIO-treated or untreated wildtype mice and cocultured these *ex vivo* with naive OT-I T cells in the presence of 0.5 mg/ml purified OVA. We determined T cell activation by measuring the amount of IL-2 and IFN-γ in the supernatant by ELISA. In line with our observations in cocultures of BM-DCs and OT-I T cells, we observed that T cells primed by PIO-treated splenic DCs produced significantly reduced amounts of IL-2 and IFN-γ hence suggesting that T cells were not properly activated (Figure 7c; Priming). Importantly, this difference in cytokine production was still observed when we restimulated equal numbers of OT-I T cells with αCD3 for 24 h following isolation from cocultures after 5 days (Figure 7c; Restimulation). These data strongly suggested that naive $CD8^+$ T cells primed by PIO-treated splenic DCs did not undergo functional differentiation into effector cells. This led us to investigate the cytotoxic activity of $CD8^+$ T cells *in vivo* and performed an *in vivo* cytotoxicity assay[113]. To this end, we injected PIO-treated, OVA-loaded BM-DCs s.c. into PIO-treated mice or untreated, OVA-loaded BM-DCs into vehicle-treated mice. 5 days later, we injected $1x10^7$ fluorochrome-labelled target cells i.v. that were loaded with the OVA-derived peptide S8L in order to determine antigen-specific cytotoxicity. Analysis of the specific elimination of S8L-loaded target cells in the draining lymph nodes revealed that in PIO-treated mice, S8L-loaded target cells were not lysed whereas OVA-specific cytotoxicity

was detected in vehicle-treated animals (Figure 7d). Taken together, these data demonstrate that *in vivo* activation of PPARγ in DCs strongly impaired $CD8^+$ T cell activation and their differentiation into effector T cells.

In vitro we showed that PPARγ activation in BM-DCs resulted in enhanced B7H1 expression which was responsible for the impairment of DCs to efficiently cross-prime cytotoxic T cells. Therefore, we next asked whether also *in vivo* B7H1 upregulation after PIO-treatment mediates impairment of naive $CD8^+$ T cell priming. To this end, we treated B7H1-deficient mice with PIO or the vehicle only, isolated splenic DCs on day 7 of PIO-treatment, and cocultured them with OT-I T cells in the presence of OVA. Importantly, OT-I T cells were fully activated by PIO-treated B7H1-deficient DCs and produced similar amounts of IL-2 and IFN-γ during priming as well as after restimulation when compared to T cells primed by vehicle-treated $B7H1^{-/-}$ DCs (Figure 7e; Priming and Restimulation). Importantly, these data suggest that also *in vivo*, PIO-induced changes in the cross-priming capability of DCs were mediated by upregulation of B7H1.

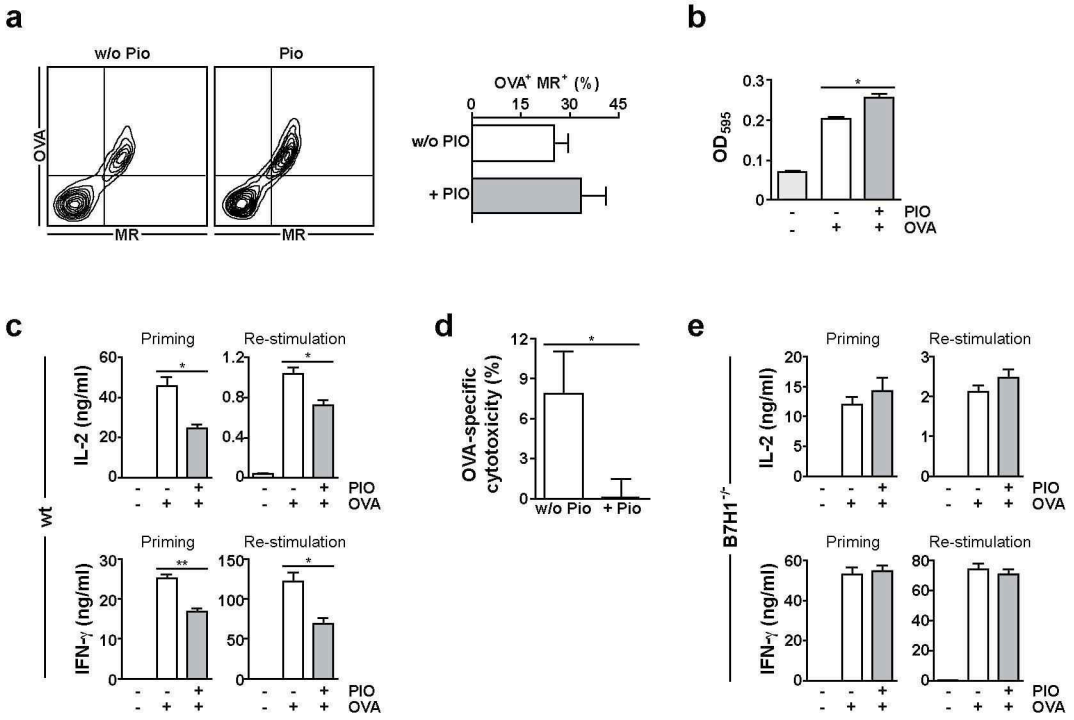

Figure 7 **Activation of PPARγ in splenic DCs impairs cross-priming of naive $CD8^+$ T cells *in vivo* by upregulation of B7H1.**

(a+b) C57BL/6 mice were treated with 30 mg/kg PIO or the vehicle only by daily oral gavage. On day 7 of PIO-treatment, mice received (a) 5 μg/g body weight Alexa647-labelled OVA or (b) 100 μg/g body weight purified OVA by i.v. injection. 45 min later, splenic $CD11c^+$ DCs were isolated by immunomagnetic separation. (a) DCs were analysed for OVA uptake and MR expression by flow-cytometry. The graph shows the average percentage of MR^+OVA^+ splenic DCs ± SEM. (b) DCs were cocultured with B3Z cells at a ratio of 1:2 (DCs:B3Z). Activation of B3Z cells was determined by spectophotometric analysis of CPRG conversion at 595 nm 24 h later. The mean optical density at 595 nm (OD_{595}) ± SEM is depicted. (c) On day 7 of PIO-treatement, splenic $CD11c^+$ DCs were cocultured with OT-I T cells at a ratio of 1:2 (DC:OT-I) in the presence of 0.5 mg/ml OVA. After 48 h, the amount of IL-2 and IFN-γ was analysed in the supernatant by ELISA to determine T cell activation (Priming). On day 5 of coculture, T cells were isolated by density gradient centrifugation and restimulated in the presence of 4 μg/ml platebound αCD3 for 24 h after which the concentration of IL-2 and IFN-γ was determined in the supernatant by ELISA (Restimulation). Graphs depict the mean concentration of each cytokine ± SEM. (Experiment performed by Luisa Klotz). (d) On day 7 of PIO-treatment, mice received $1x10^6$ OVA-loaded, PIO-treated BM-DCs whereas vehicle-treated mice received $1x10^6$ OVA-loaded, untreated BM-DCs by subcutaneous injection. After 5 d, the antigen-specific cytotoxicity was determined *in vivo* by transfer of $1x10^7$ S8L-loaded, $CFSE^{hi}$-labelled and analysis of specific elimination of S8L-loaded cells by flow-cytometry in the draining lymph nodes. Data is depicted as mean percentage of OVA-specific cytotoxicity ± SEM. (e) B7H1-deficient mice were treated with 30 mg/kg PIO or with the vehicle only by daily oral gavage for 7 d. $CD11c^+$ splenic DCs were cocultured with OT-I T cells as described in (c). The amount of IL-2 and IFN-γ in the supernatant was analysed by ELISA during priming and after restimulation. All experiments were performed at least 2 times. Data of one representative experiment are shown. Within one experiment, $n \geq 3$. * $p<0.05$; ** $p<0.01$.

4.1.7 Summary of chapter 6.1

In the first part of this thesis we investigated whether activation of PPARγ in DCs influences cross-priming of naive $CD8^+$ T cells. We demonstrated that treatment with the synthetic PPARγ agonist PIO resulted in increased expression of the MR *in vitro* and *in vivo* which strongly enhanced uptake of the soluble model antigen OVA and subsequent cross-presentation of OVA-derived peptides. However, despite increased levels of cross-presented antigen, naive $CD8^+$ T cells were not properly activated and did not mature into cytotoxic effector cells. We revealed that PPARγ activation resulted in significant enhanced expression of the coinhibitory molecule B7H1 and that its interaction with the ligand PD-1 on T cells was responsible for the observed impairment of PIO-treated DCs to activate naive $CD8^+$ T cells. To summarise, these findings demonstrate a new mechanism of DC-mediated tolerance induction in $CD8^+$ T cells which potentially plays a role in inhibiting the activation of autoreactive $CD8^+$ T cells.

4.2 PPARγ in myeloid cells plays an important role in limiting CNS inflammation during the effector phase of EAE

Although autoreactive T cells are important for the initiation of EAE, the effector mechanisms leading to demyelination and inflammation within the CNS are likely to be provided by other cell types[60]. Indeed, several studies have highlighted the importance of myeloid cells, including CNS-resident microglia and infiltrating inflammatory monocytes and macrophages, for the perpetuation of disease. Heppner et al. showed that microglial paralysis results in delayed onset of disease and repression of clinical signs[62]. Mildner et al. demonstrated that inflammatory monocytes, which are recruited during autoimmune inflammation to the CNS, play an important role during the effector phase of disease and ablation of $CCR2^+$ inflammatory monocytes results in amelioration of disease[63]. However, the main effector mechanisms contributing to CNS-inflammation and disease pathology are mediated by other cell types especially myeloid cells, i.e. monocytes, macrophages, and microglia[62,63]. As PPARγ has been shown to be a regulator of myeloid cell immunogenicity *in vitro*[73,80,114], we hypothesised that during EAE, PPARγ in myeloid cells interferes with innate immune cell-mediated autoimmune inflammation in the CNS.

4.2.1 PIO-treatment ameliorates EAE

Treatment with the pharmacological PPARγ agonist pioglitazone (PIO) ameliorates the disease course in several mouse models of EAE[90]. We first thought to confirm these data and induced EAE in C57BL/6 mice by immunisation with MOG_{35-55} emulsified in complete Freund's adjuvant and concomitantly treated mice with PIO or the vehicle only (CMC) by daily oral gavage. After immunisation, mice were clinically monitored which revealed that PIO-treatment resulted in significant amelioration of disease during the entire observation period, i.e. during the priming as well as the effector phase (Figure 8a).

We next asked the question whether PIO-treatment affects the inflammatory milieu within the CNS. To this end, we isolated the mRNA from the upper cervical myelon of immunised PIO- or vehicle-treated mice during the effector phase, i.e. day 21 after induction of EAE, when myeloid cells play an important role for disease pathology[63],

and analysed the expression levels of proinflammatory mediators, such as proinflammatory cytokines, inducible nitric oxide synthase (iNOS), and chemokines by quantitative real-time RT-PCR. As shown in Figure 8b, we observed significantly reduced expression levels of TNF-α, IL-12, and IL-23 in the CNS of PIO-treated mice compared to vehicle-treated animals and also expression levels of IL-1β and IFN-γ were decreased in the CNS of PIO-treated mice (Figure 8b). Moreover, expression levels of iNOS, the enzyme responsible for production of nitric oxide (NO), were reduced in the CNS of PIO- compared to vehicle-treated animals (Figure 8c). In addition, PIO-treatment resulted in significantly diminished levels of CCL2, CCL3, and CXCL10 (Figure 8d), chemokines which recruit macrophages and monocytes as well as activated T cells to the inflamed CNS, when compared to vehicle-treated animals. The T cell-specific cytokines CCL5 and CCL20 were also reduced in the CNS of PIO-treated animals, however differences did not reach statistical significance (Figure 8d).

To further characterise the ameliorative effect of PIO-treatment, we next investigated whether changes in the inflammatory milieu resulted in histopathological differences between PIO-treated and vehicle-treated mice. To this end, we isolated the CNS at a late stage of EAE, i.e. on day 35 after EAE induction, and performed immunohistological analysis of the spinal cord. We observed that the CNS of PIO-treated animals was characterised by significantly reduced demyelination and axonal damage (Figure 8e) as well as reduced numbers of $Mac3^+$ cells, i.e. macrophages and microglia, and $CD3^+$ T cells (Figure 8f) when compared to vehicle-treated animals.

Taken together, PPARγ activation *in vivo* ameliorated clinical signs of EAE which is characterised by reduced inflammatory responses within the CNS and improved CNS pathology, i.e. diminished demyelination and axonal damage as well as decreased numbers of infiltrating cells.

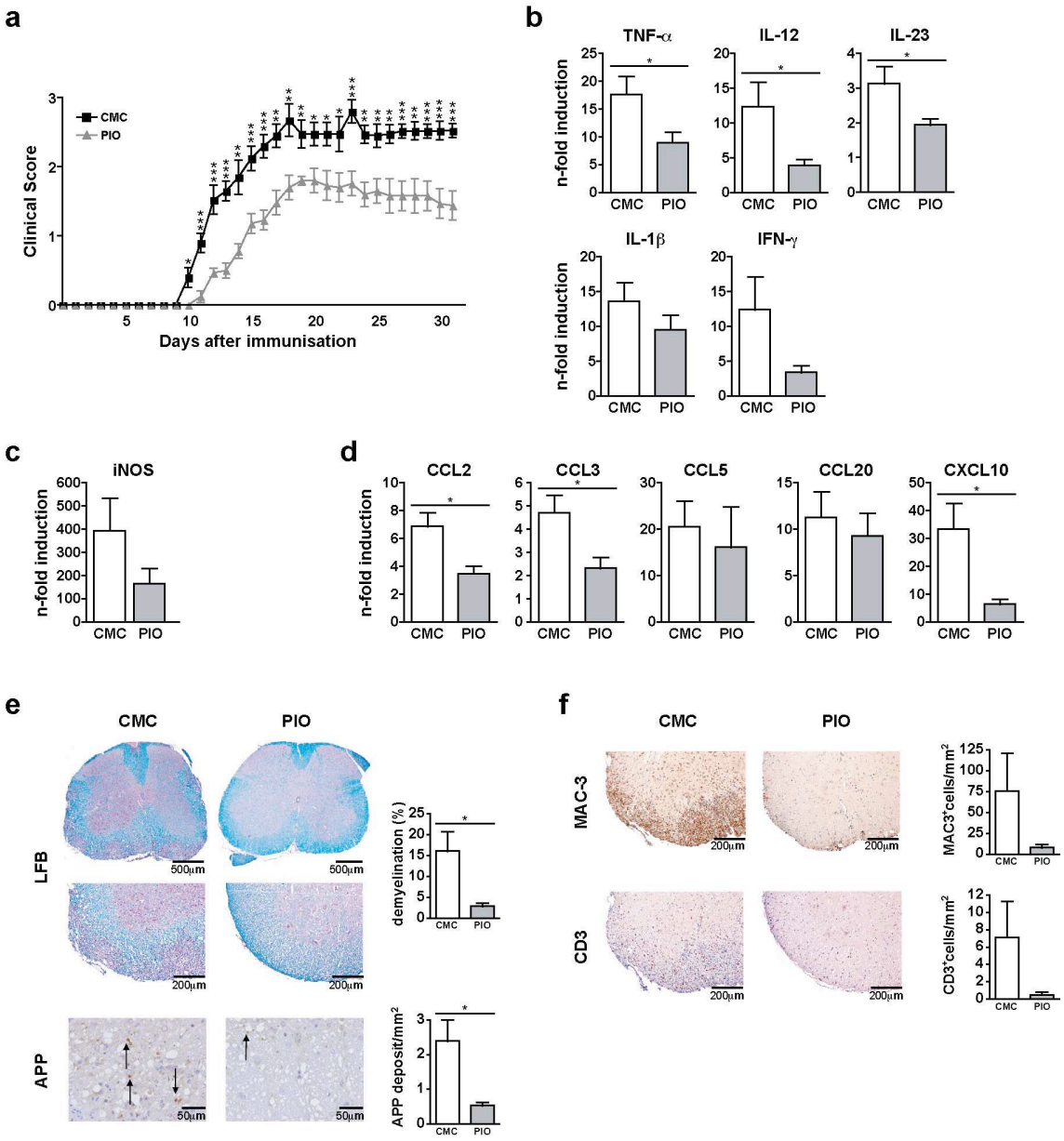

Figure 8 **PIO-treatment ameliorates clinical signs of EAE, reduces inflammatory responses within the CNS, and improves CNS pathology.**

(a) C57BL/6 mice were administered 30 mg/kg body weight PIO in 0.5 % carboxymethylcellulose (CMC) or the vehicle only (CMC) by daily oral gavage. MOG_{35-55}-EAE was induced on day 7 of PIO-treatment and mice were clinically monitored. The mean clinical score ± SEM of one representative experiment out of four experiments is depicted. (b-d) mRNA expression of (b) inflammatory cytokines, (c) iNOS, and (d) chemokines in the CNS of diseased PIO- or vehicle-treated C57BL/6 mice was determined by quantitative real-time RT-PCR on day 21 of EAE (n=10 per group). Data were normalised to endogenous GAPDH expression and are expressed as n-fold induction compared to healthy C57BL/6 mice. Data are expressed as mean expression ± SEM. (e,f) Histopathological analysis of the spinal cord of PIO-treated or vehicle-treated (CMC) mice on day 35 of EAE. (e) shows demyelination (luxol fast blue (LFB)) and axonal damage (amyloid precursor protein (APP)) (n=5 per group); (f) depicts cell infiltrates (MAC-3 for macrophages/microglia; CD3 for T cells) (n=5). * $p<0.05$.

4.2.2 PPARγ is an important regulator of myeloid cells during the effector phase of EAE

We hypothesised that the observed PIO-mediated amelioration of EAE is, at least in parts, due to activation of PPARγ in myeloid cells. However, as *in vivo* PIO-treatment targets all PPARγ-expressing cells we next wanted to confirm that PPARγ in myeloid cells is important for control of EAE.

To answer this question we crossed mice that express the Cre recombinase under the Lysozyme M (LysM) promoter with mice that carry loxP sites within the PPARγ gene ($PPAR\gamma^{fl/fl}$) resulting in the generation of conditional myeloid cell-specific PPARγ knockout mice (LysM-$PPAR\gamma^{KO}$). To confirm a myeloid cell-specific PPARγ knockout in these mice, we analysed mRNA of different immune cell populations by RT-PCR which demonstrated that myeloid cells specifically lacked PPARγ as splenic $CD11b^{+}$ cells including splenic macrophages, peritoneal macrophages, and neutrophilic granulocytes expressed the truncated, non-functional 300 bp cDNA fragment of PPARγ whereas most DCs as well as T and B cells expressed the wildtype full-length 700 bp fragment of PPARγ cDNA (Figure 9a). To analyse the role of PPARγ in myeloid cells during EAE, we immunised LysM-$PPAR\gamma^{KO}$ mice or their wildtype littermates with MOG_{35-55} and monitored the course of disease. We observed that, in comparison to their WT littermates, the disease course in LysM-$PPAR\gamma^{KO}$ mice was significantly aggravated during the effector phase whereas the T cell-mediated induction phase was not altered (Figure 9b). This demonstrates that PPARγ in myeloid cells plays a crucial role in limiting the CNS-pathogenic potential of myeloid cells during the effector phase of EAE.

Mildner et al. have demonstrated that inflammatory monocytes, characterised by expression of CCR2 and high levels of Ly-6C, are crucial for the effector phase of EAE[63]. As in LysM-Cre mice also monocytes are targeted by Cre-mediated recombination[101] and LysM-$PPAR\gamma^{KO}$ mice exhibited an aggravated disease course during the effector phase of EAE, we hypothesised that the knockout of PPARγ in inflammatory monocytes is at least partially responsible for the observed differences between wildtype and LysM-$PPAR\gamma^{KO}$ mice. To assess the role of PPARγ in inflammatory monocytes, we selectively depleted $CCR2^{+}Ly\text{-}6C^{hi}$ monocytes in the

circulation during EAE by injection of the αCCR2 antibody MC-21[63,115,116]. Again, we immunised LysM-PPARγ^{KO} mice or their wildtype littermates and clinically monitored the disease. We selectively depleted CCR2^{+}Ly-6C^{hi} inflammatory monocytes during the effector phase by repetitive injection of αCCR2 every 24 h between days 13 and 17 of EAE. Successful depletion of Ly-6C^{hi} monocytes was confirmed 8 h after the first αCCR2-injection (Figure 9c). We observed that depletion of inflammatory monocytes resulted in amelioration of disease in both, LysM-PPARγ^{KO} mice and their wildtype littermates, and moreover, that the observed differences in disease severity between knockout and wildtype animals were completely abolished (Figure 9d).

In summary, these data demonstrate that PPARγ plays an important role in limiting myeloid cell-mediated pathology during the effector phase of EAE. Importantly, we identified Ly-6C^{hi} inflammatory monocytes as the central myeloid cell population regulated by PPARγ during EAE, as depletion of this population by αCCR2-treatment resulted not only in disease amelioration but abolished the observed differences in disease severity between LysM-PPARγ^{KO} mice and their wildtype littermates.

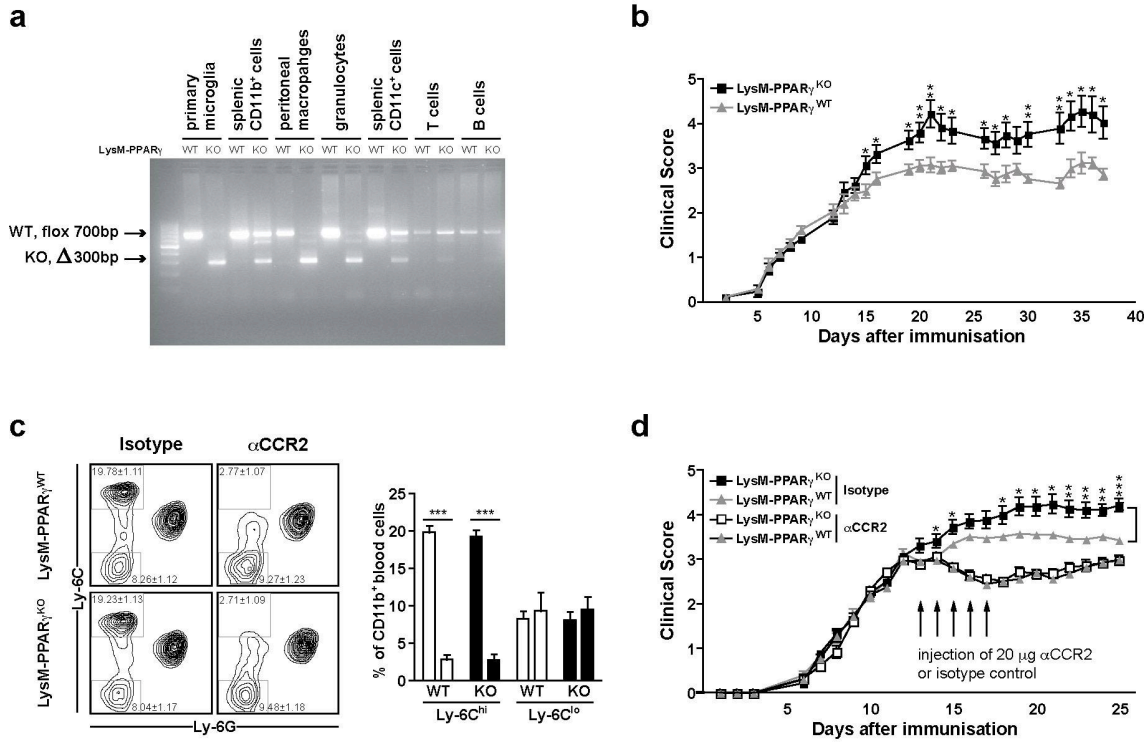

Figure 9 **PPARγ in myeloid cells is important for control of the effector phase of EAE. (Experiments performed in collaboration with Juliane Floßdorf)**

(a) PPARγ was specifically ablated in cells of myeloid origin when PPARγ$^{fl/fl}$ mice were crossed to LysM-Cre transgenic mice as shown by RT-PCR analysis of mRNA derived from primary microglia, splenic CD11b^{+} cells, peritoneal macrophages, and neutrophilic granulocytes, as well as splenic CD11c^{+} cells, T cells, and B cells. Cre-mediated recombination resulted in the expression of a truncated, non-functional 300 bp cDNA fragment of PPARγ, when compared to wildtype full-length 700 bp fragment of PPARγ cDNA. (b) MOG_{35-55}-EAE was induced by active immunisation of LysM-PPARγ^{WT} (n=12) or LysM-PPARγ^{KO} (n=13) mice, and mice were clinically monitored. The mean clinical score ± SEM of two representative out of five independent experiments is shown. (c+d) EAE was induced by active immunisation of LysM-PPARγ^{WT} or LysM-PPARγ^{KO} mice. At the beginning of the effector phase i.e. from d13, mice received 5 injections (every 24 h; arrows) of 20 µg of αCCR2 antibody (MC-21; n=20 per group) or isotype control (RatIgG2b; n=15 per group). (c) Depletion of monocytes was monitored 8 h after the first injection in the blood. Live CD11b^{+} cells were gated and contourplots depict Ly-6C and Ly-6G expression. Upper numbers within the contourplots indicate the percentage of CCR2-expressing Ly-6C^{hi}Ly-6G^{-} monocytes ± SEM (upper gate); lower numbers depict the percentage of Ly-6C^{lo}Ly-6G^{-} monocytes ± SEM (lower gate). Graph depicts the mean percentage of Ly-6C^{hi} or Ly-6C^{lo} monocytes ± SEM in the blood of αCCR2- or Isotype control-treated LysM-PPARγ^{KO} or LysM-PPARγ^{WT} mice. (d) Clinical score of immunised, αCCR2- or isotype control-treated mice. Arrows indicate days of injection. The mean clinical score ± SEM of two independent experiments is shown. * $p<0.05$; ** $p<0.01$; ***$p<0.001$.

4.2.3 Inflammatory monocytes migrate to the inflamed CNS and differentiate into macrophages and activated microglia

The observation that ablation of CCR2^{+} monocytes completely abolished the difference in disease course of LysM-PPARγ^{KO} mice and their wildtype littermates was surprising, as knockout microglia residing behind the BBB were not targeted by this antibody. Although this indicates that the lack of PPARγ in microglia does not strongly contribute to the observed differences in the course of EAE between LysM-PPARγ^{KO} and LysM-PPARγ^{WT} mice, we investigated a second explanation. We hypothesised that during EAE, infiltrating inflammatory monocytes differentiate not only into macrophages but also acquire a microglial phenotype thereby contributing to microglia-mediated neurotoxicty.

To analyse whether inflammatory monocytes differentiate into microglia during EAE, we labelled circulating Ly-6C^{hi} inflammatory monocytes *in vivo* on day 12 after EAE induction and analysed their phenotype after infiltration of the CNS. Labelling of Ly-6C^{hi} monocytes was performed as described before[64,117,118]. After injection of clodronate liposomes, which leads to elimination of blood monocytes[119], mice received FITC-labelled polystyrene beads during the time of leukocyte reconstitution, i.e. 12 h later. This resulted in labelling of circulating Ly-6C^{hi} monocytes (Figure 10a) whereas mainly Ly-6C^{lo} monocytes had taken up the administered FITC-beads in control mice

treated with PBS liposomes (Figure 10a). 12 h after bead injection, mononuclear cells were isolated from the CNS and FITC-labelled infiltrating monocytes were analysed for CD45 expression which is an established marker to discriminate between macrophages ($CD45^{hi}$) and microglia, which express CD45 at low levels in a resting state and at intermediate levels, when they are activated[118,120]. To analyse the phenotype of infiltrating monocytes, we first identified macrophages and microglia by gating on live $CD11b^+$ and Ly-$6G^-$ cells (Figure 10b). Within the population of macrophages and microglia we identified a distinct population of $FITC^+$ cells derived from FITC-labelled inflammatory monocytes (Figure 10c). Further analysis of CD45 expression revealed that the majority of $FITC^+$ cells were macrophages as characterised by high expression levels of CD45 (Figure 10d,e; red population). However, a small but distinct population displayed a microglial phenotype characterised by intermediate expression of CD45 (Figure 10d,e; blue population).

In a corresponding experiment we transferred bone marrow-derived $CD115^+CD45.2^+$ monocytes into EAE-diseased mice carrying the congenic marker CD45.1 on day 12 of EAE. 12 h after monocyte transfer, we analysed CNS infiltrating $CD45.2^+$ monocytes with regard to CD45 expression. Again, we could demonstrate that within the population of transferred $CD45.2^+$ monocytes a distinct subpopulation expressed CD45 at intermediate levels suggesting that they had acquired the phenotype of activated microglial cells after entry into the inflamed CNS (Figure 10f).

Taken together, these data reveal that inflammatory monocytes invading the CNS during ongoing autoimmunity acquire different phenotypes. Besides differentiation into macrophages, monocytes can also acquire a microglial phenotype characterised by intermediate expression of CD45. Importantly, these findings strongly suggest that inflammatory monocytes thereby also contribute to local microglial inflammatory responses and in consequence microglia-mediated disease pathology.

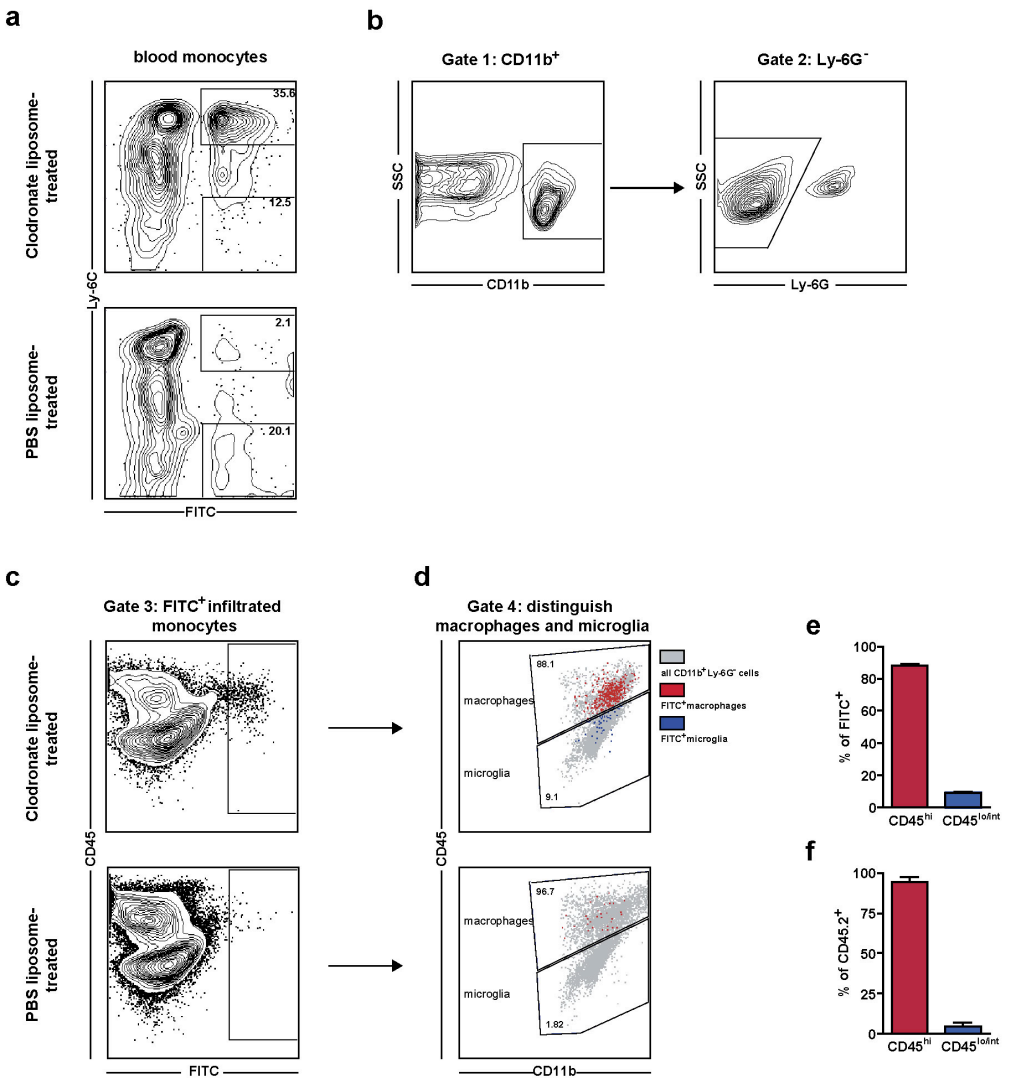

Figure 10 **During EAE, inflammatory monocytes infiltrate the inflamed CNS and differentiate into macrophages and microglia.**

(a-e) MOG_{35-55} EAE was induced in C57BL/6 mice. On day 12 of EAE, mice were treated with clodronate- or PBS-lipsomes and 12 h later FITC-labelled 0.5 µm microsphere beads were administered i.v. (a) Another 12 h later, FITC-labelling of circulating $CD11b^+Ly\text{-}6G^-$ monocytes was monitored by flow-cytometry. Contourplots depict Ly-6C expression and FITC-labelling. Upper numbers show the mean percentage of $FITC^+$ cells within the population of $Ly\text{-}6C^{hi}$ monocytes; lower numbers show the mean percentage of $FITC^+$ cells within the population of $Ly\text{-}6C^{lo}$ monocytes. (b) Gating strategy to identify the population of $CD11b^+Ly\text{-}6G^-$ macrophages and microglia. (c) Identification of infiltrating monocytes by FITC expression. (d) CD45 expression of $FITC^+$ cells. Numbers indicate the mean percentage of macrophage-like (red; $CD45^{hi}$) or microglia-like (blue; $CD45^{lo/int}$) cells among all $FITC^+$ cells. (e) Graph depicts the mean percentage ± SEM of $CD45^{hi}$ or $CD45^{int/lo}$ cells within the population of $FITC^+$ cells derived from clodronate-liposome-treated mice (n=5). (f) $1x10^7$ $CD115^+CD45.2^+$ monocytes were immunomagnetically separated and adoptively transferred into EAE-diseased mice carrying the congenic marker CD45.1. 12 h after injection of monocytes, transferred monocytes isolated from the CNS were analysed by flow-cytometry for CD45 expression. The graph depicts the mean percentage ± SEM of $CD45^{hi}$ or $CD45^{int/lo}$ cells within the population of $CD45.2^+$ transferred monocytes (n=5).

4.2.4 PPARγ impairs neurotoxic responses by myeloid cells

We next wanted to characterise which inflammatory responses are regulated by PPARγ in myeloid cells with particular interest on factors that mediate neurotoxicity. To this end, we treated bone marrow-derived macrophages (BM-Ms) or primary microglia (pMg) with PIO, stimulated the cells with LPS ± IFN-γ, and analysed iNOS expression as well as production of nitric oxide (NO), reactive oxygen species (ROS), and proinflammatory cytokines.

Stimulation of PIO-treated or untreated BM-Ms and pMg, with LPS and IFN-γ for 6 h and subsequent analysis by quantitative real-time RT-PCR revealed that PPARγ activation by PIO-treatment suppressed inflammation-induced upregulation of iNOS expression (Figure 11a). Concomitantly, PIO-treated macrophages and microglia produced significantly reduced amounts of NO in response to LPS and IFN-γ compared to untreated controls (Figure 11b). Importantly, also inflammation-induced production of ROS and TNF-α, both of which are strongly involved in immune-mediated demyelination in the CNS[60], were significantly reduced in PIO-treated compared to untreated macrophages and microglia (Figure 11d). In line with these findings, we also observed that inflammation-induced production of IL-6 and IL-12 was significantly decreased in PIO-treated BM-Ms and pMg compared to untreated macrophages and microglia (Figure 11e,f).

Taken together, these data reveal a potential neuroprotective role for PPARγ in myeloid cells as activation of PPARγ in macrophages and microglia interfered with inflammation-induced production of molecules that mediate neurotoxicity (NO, ROS, and TNF-α) or contribute to inflammatory processes, such as IL-6 and IL-12. These data suggest that PPARγ in myeloid cells is a regulator of innate immune responses within the CNS during ongoing autoimmune inflammation and that activation of PPARγ in myeloid cells limits demyelination and axonal damage (Figure 8e).

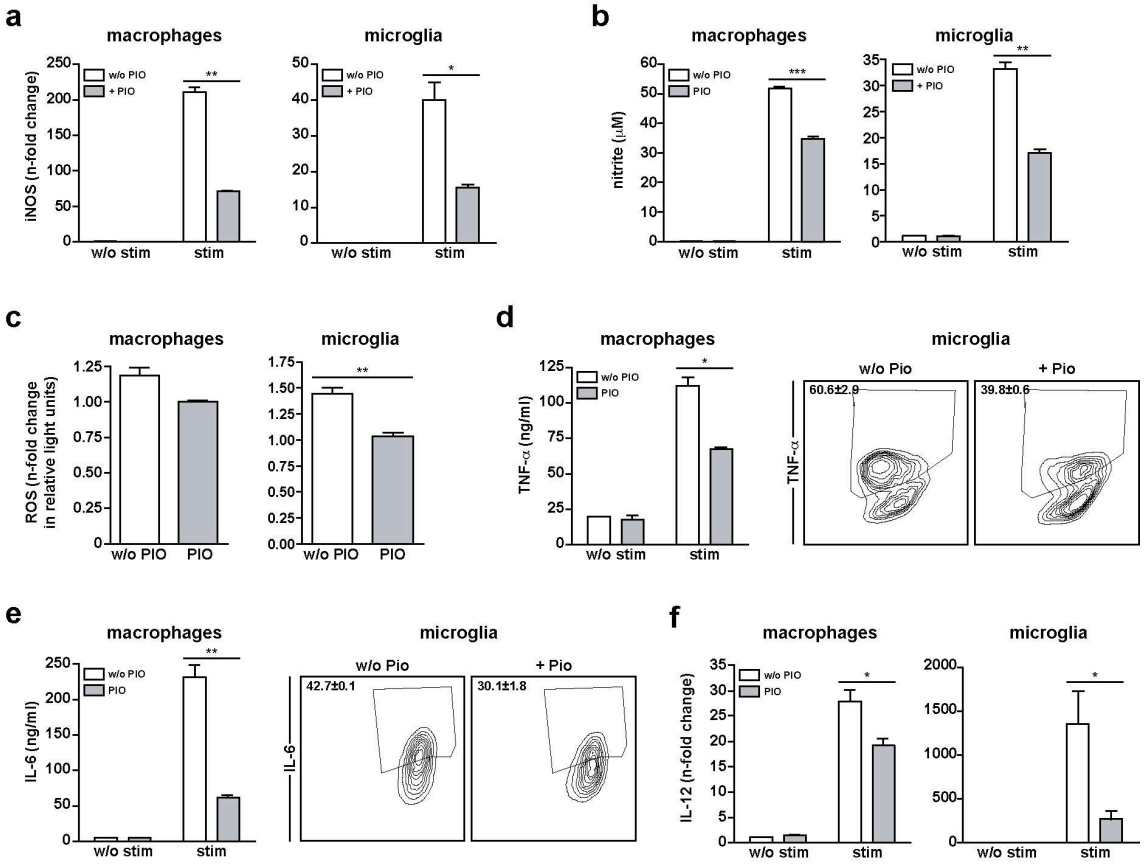

Figure 11 PPARγ regulates neurotoxic responses by macrophages and microglia.

For all experiments, bone marrow-derived macrophages (BM-Ms) or primary microglia (pMg) were pretreated with 10 μM PIO for 7 days. (a) PIO-treated or untreated BM-Ms or pMg were stimulated for 6 h with 1 μg/ml LPS + 5 pg/ml IFN-γ (stim) and iNOS expression levels were determined by quantitative real-time RT-PCR. Data were normalised to endogenous GAPDH expression and are expressed as n-fold induction compared to unstimulated BM-Ms or pMg (w/o stim). (b) NO production by PIO-treated or untreated BM-Ms or pMg was measured after 48 h stimulation with 100 ng/ml LPS and 1 μg/ml LPS, respectively, + 10 ng/ml IFN-γ by indirect measurement of nitrite levels by Griess Assay. (c) To determine the production of reactive oxygen species (ROS), PIO-treated or untreated BM-Ms were stimulated for 30 min with 100 ng/ml LPS. PIO-treated or untreated pMg were stimulated for 24 h with 1 μg/ml LPS. After stimulation, 20 μM H_2DCFDA in PBS was added and production of ROS was detected at 485 nm excitation and 530 nm detection. The induction of ROS is expressed as fold change in relative light units compared to the unstimulated control. (d,e) PIO-treated or untreated BM-Ms were stimulated with 100 ng/ml LPS. Production of (d) TNF-α and (e) IL-6 was determined in the supernatant by ELISA after 24 h and 48 h, respectively. (d,e) PIO-treated or untreated pMg were stimulated for 4 h with 1 μg/ml LPS + 5 pg/ml IFN-γ. Cells were intracellularly stained for (d) TNF-α or (e) IL-6 and analysed by flow cytometry. Numbers depict the average percentage of cytokine$^+$ pMg ± SEM. (f) Expression of IL-12 in PIO-treated or untreated BM-Ms and pMg was determined as in (a). Shown is the mean ± SEM. Data of one representative of at least two independent experiments are shown, within one experiment $n \geq 3$. * $p<0.05$; ** $p<0.01$; ***$p<0.001$.

4.2.5 PPARγ activation in myeloid cells suppresses neurotoxicity

As PPARγ activation resulted in reduced production of neurotoxic mediators by myeloid cells (Figure 11), we next asked whether PPARγ activation in microglial cells indeed mediates neuroprotective effects. To this end, we stimulated PIO-treated or untreated pMg with LPS and IFN-γ ± PIO for 48 h. Activated microglia were cocultured with primary neurons for 24 h and the relative neurite density was analysed by microscopy in order to determine the degree of microglia-mediated neuronal damage. We observed that neurons cocultured with stimulated microglia exhibited significant reduced neurite density (0.64 ± 0.07; Figure 12a,b) when compared to neurons from cocultures with unstimulated pMg (Figure 12a,b). In contrast, coculture with PIO-treated, stimulated microglia only resulted in a small and non-significant reduction of neurite density (0.86 ± 0.07) compared to unstimulated microglia (Figure 12a,b). Importantly, neurite density was significantly higher in cocultures with stimulated PIO-treated microglia compared to untreated, stimulated microglia (Figure 12a,b).

These data demonstrate that PPARγ activation in microglial cells interfered with production of neurotoxic factors in response to inflammatory stimulation, which indeed resulted in neuroprotection under inflammatory conditions.

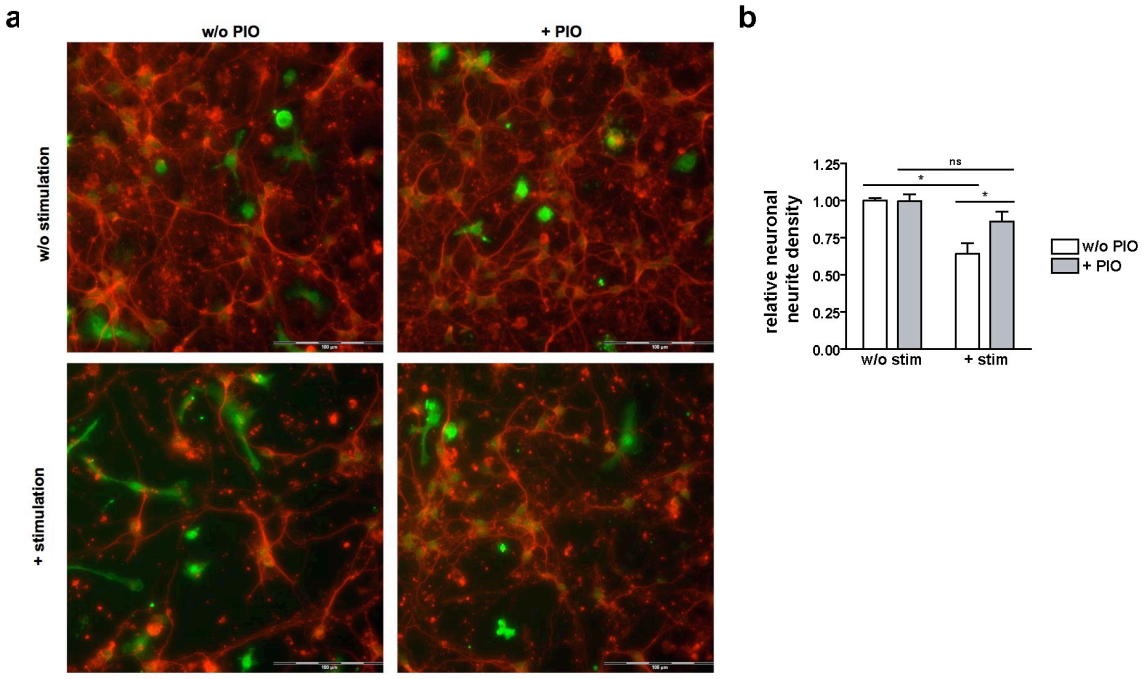

Figure 12 PPARγ interferes with microglial neurotoxic responses.

PIO-treated or untreated primary microglia (pMg) were stimulated with 1 μg/ml LPS + 10 ng/ml IFN-γ for 48 h or were left untreated. $5x10^4$ pMg were cocultured with $2.5x10^5$ primary neurons for 24 h. (a) Neurons and microglia were fixed and double-immunostained with antibodies against tubulin-3 (detects neurons; red signal) and Iba-1 (detects microglia; green signal). Scale bars: 100 μm. (b) Statistical analysis of neurite density depicted as mean neurite density ± SEM compared to unstimulated control (w/o PIO). Data of one representative experiment out of three independent experiments are shown. * $p<0.05$.

4.2.6 During EAE, PIO-treatment reduces the immunogenic potential of CNS myeloid cells

So far, we showed that during EAE the ameliorative effect of PPARγ activation *in vivo* is characterised by reduced demyelination and axonal damage and showed that PPARγ regulates neurotoxicity of macrophages and microglia *in vitro*. Next, we further investigated the impact of PPARγ activation on the immunogenicity of CNS macrophages and microglia *in vivo*. To this end, we isolated macrophages and microglia from the CNS of PIO- or vehicle-treated EAE-diseased mice during the effector phase, i.e. day 21 after immunisation, and analysed the expression of MHC-II and CD40 on these cells which play an important role in the reactivation of autoreactive T cells[51,58,59]. Becher et al. demonstrated that especially the presence of CD40 is important for the induction and perpetuation of EAE[58].

Macrophages and microglia, which are both $CD11b^+$, are characterised by distinct expression of CD45 (Figure 10) and Ly-6C: macrophages are $CD45^{hi}Ly\text{-}6C^+$ whereas microglia are $CD45^{int/lo}Ly\text{-}6C^{lo}$ (Figure 13a). We observed that in PIO-treated animals MHC-II expression was significantly reduced on both, macrophages and microglia, when compared to CNS macrophages and microglia from vehicle-treated mice (Figure 13b). Whereas 25 % of macrophages derived from vehicle-treated mice expressed MHC-II, only 11.75 % of PIO-treated macrophages were $MHC\text{-}II^+$ (Figure 13b) and this was also reflected in the mean fluorescence intensity (MFI) which was significantly reduced by 66 % on PIO-treated macrophages and by 60 % on PIO-treated microglia (Figure 13b). Furthermore, the percentage of CD40-expressing CNS macrophages was reduced from 13.25 % in the CNS of vehicle-treated mice to 7.06 % in PIO-treated animals (Figure 13c) and the MFI of CD40 expression was reduced by 52 % on PIO-treated macrophages (Figure 13c). However, CD40 was not expressed on microglia isolated from EAE-diseased mice and hence, no difference between PIO- and vehicle-treated mice could be observed (Figure 13c). To confirm that this effect was

mediated by PPARγ-dependent actions of PIO, we treated LysM-PPARγ^{KO} mice with PIO or vehicle only and analysed CNS macrophages for MHC-II and CD40 expression by flow cytometry. Importantly, we did not observe a reduction in expression of MHC-II or CD40 on PIO-treated LysM-PPARγ^{KO} macrophages indicating that the suppression of macrophage activation in wildtype mice during EAE by oral treatment with PIO was indeed mediated by *in vivo* activation of PPARγ in myeloid cells (Figure 13d).

Taken together, PPARγ activation regulates the immunogenicity of macrophages and microglia also *in vivo*, which is demonstrated by reduced upregulation of MHC-II and CD40 on CNS myeloid cells in response to the inflammatory milieu in the CNS of EAE-diseased PIO-treated mice.

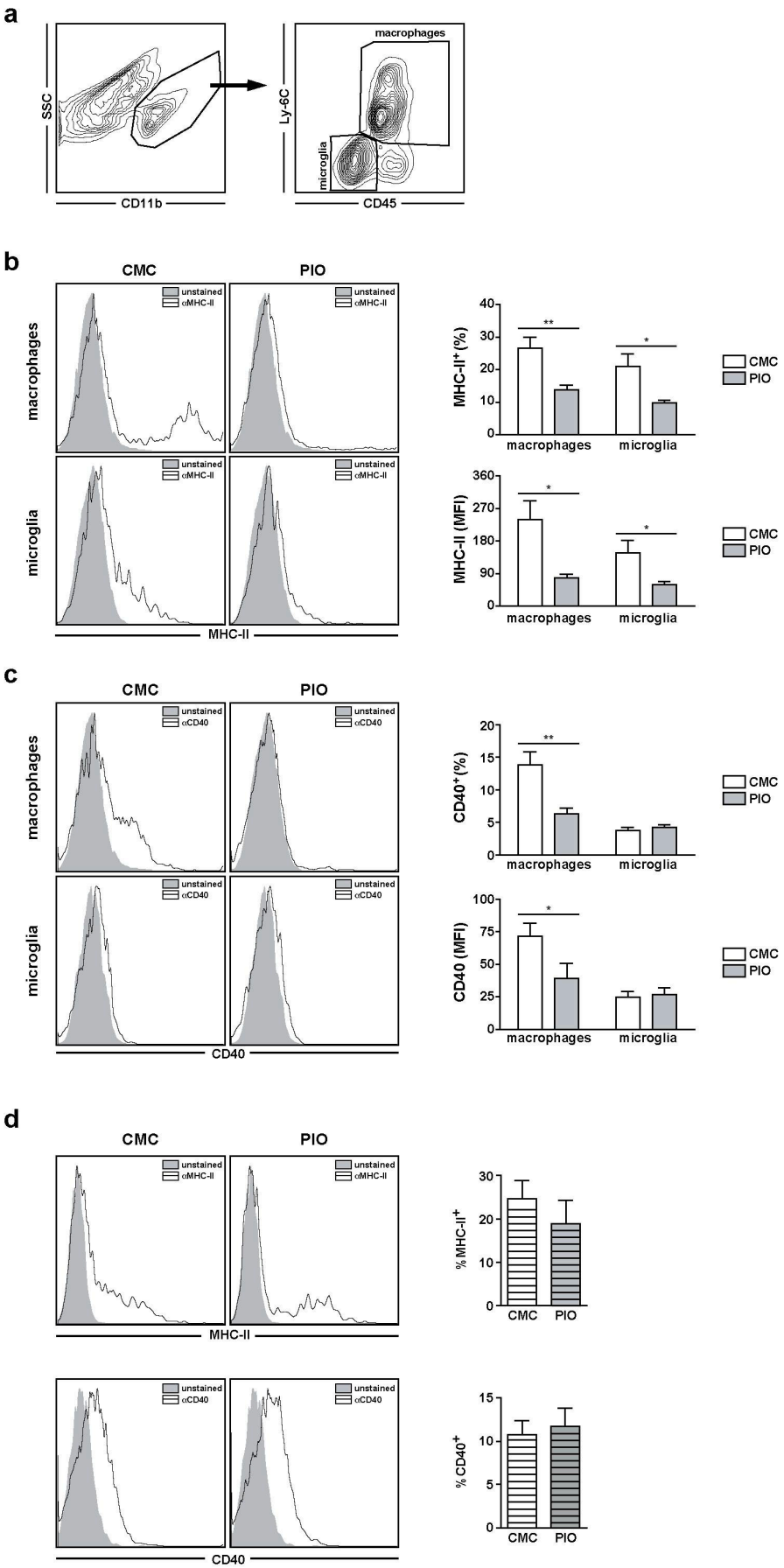
a
SSC
CD11b
Ly-6C
CD45
macrophages
microglia
b
CMC
PIO
unstained
αMHC-II
macrophages
microglia
MHC-II
MHC-II+ (%)
MHC-II (MFI)
CMC
PIO
c
CD40
CD40+ (%)
CD40 (MFI)
d
% MHC-II+
% CD40+

Figure 13 PIO-treatment regulates the immunogenicity of CNS macrophages and microglia. (a-c) C57BL/6 mice or (d) LysM-PPARγ^{KO} mice were administered 30 mg/kg body weight PIO in 0.5 % CMC or the vehicle only by daily oral gavage. MOG_{35-55}-EAE was induced on day 7 of PIO-treatment. Macrophages and microglia were isolated from the CNS of PIO- or vehicle-treated mice during the effector phase of EAE (day 21) and subsequently analysed by flow-cytometry. (a) Discrimination of CNS macrophages ($CD11b^+CD45^{hi}Ly\text{-}6C^+$) and microglia ($CD11b^+CD45^{lo}Ly\text{-}6C^{lo}$). (b) Macrophages and microglia isolated from C57BL/6 mice were stained for (b) MHC-II (n=10) and (c) CD40 (n=9) expression (unstained control (tinted) and specific antibody (line)). Accompanying graphs depict the mean percentage ± SEM or the average mean fluorescence intensity (MFI) ± SEM. (d) Macrophages from LysM-PPARγ^{KO} were stained for MHC-II and CD40. Graphs depict the mean percentage of MHC-II- and CD40-expressing cells ± SEM (n=5 per group). * $p<0.05$; ** $p<0.01$.

4.2.7 Reduced activation of CNS myeloid cells results in diminished T cell responses in the CNS

So far we could show that *in vivo* PIO-treatment leads to diminished expression levels of cytokines important for reactivation of T_H17 cells, such as IL-23 (Figure 8b), and T_H1 cells, such as IL-12 (Figure 8b), in the CNS of diseased mice and importantly, that PPARγ activation in myeloid cells results in reduced expression of MHC-II and CD40 by CNS macrophages and microglia (Figure 13b,c). As these data suggest that *in vivo* PIO-treatment creates a milieu within the CNS that interferes with local reactivation of encephalitogenic T cells we next characterised the $CD4^+$ T cell responses within the CNS.

To this end, we isolated T cells from the CNS of diseased PIO- or vehicle-treated mice during the effector phase of EAE and analysed the cytokine production after *ex vivo* restimulation with PMA/ionomycin by flow-cytometry. In addition, we determined the frequency of antigen-specific IL-17A-producing T_H17 cells or IFN-γ-producing T_H1 cells after restimulation with MOG_{35-55}-loaded DCs by ELISpot analysis.

We observed that $CD4^+$ T cells isolated from the CNS of PIO-treated mice produced significantly less IL-17A after restimulation compared to $CD4^+$ T cells isolated from the CNS of vehicle-treated animals (Figure 14a). Furthermore, $CD4^+$ T cells produced reduced amounts of IFN-γ (Figure 14c), although this difference did not reach statistical significance.

ELISpot analysis confirmed these findings and showed that the frequency of MOG-specific IL-17A-producing $CD4^+$ T cells was significantly reduced in PIO-treated animals with 154 ± 53.4 $IL\text{-}17A^+$ spots per $3x10^4$ $CD4^+$ T cells compared to 503 ± 46.2 $IL\text{-}17A^+$ spots in vehicle-treated mice (Figure 14b). Moreover, the frequency of IFN-γ-

producing $CD4^+$ T cells was reduced. Whereas in vehicle-treated animals 519 ± 83.8 IFN-γ^+ spots per $3x10^4$ $CD4^+$ T cells were observed, in PIO-treated animals only 400 ± 97.3 IFN-γ^+ spots were detected (Figure 14d).

To summarise, PIO-mediated amelioration of the CNS inflammatory milieu, i.e. reduced expression levels of IL-12 and IL-23 as well as diminished surface expression of MHC-II and CD40 on CNS myeloid cells during the effector phase of EAE indeed resulted in reduced T cell responses within the CNS as the frequency and numbers of antigen-specific IL-17A- and IFN-γ-producing T cells were found to be reduced. However, the effect was more pronounced on T_H17 cells.

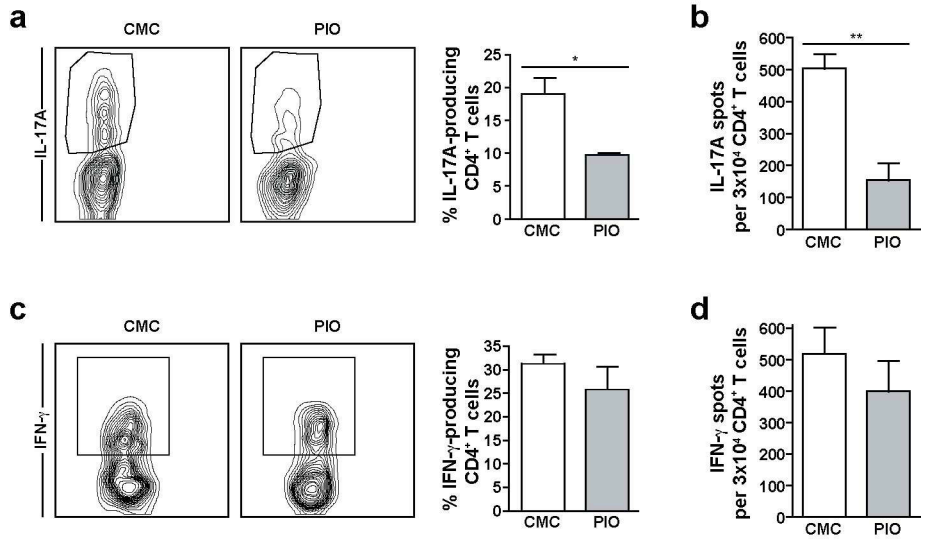

Figure 14 PIO-treatment results in reduced T cell activity during EAE within the CNS.

C57BL/6 mice were administered 30 mg/kg body weight PIO in 0.5 % CMC or the vehicle only (CMC) by daily oral gavage. MOG_{35-55}-EAE was induced and T cells were isolated from the CNS on day 21 of EAE. (a,c) $CD4^+$ T cells were restimulated for 4 h with PMA/ionomycin prior to intracellular cytokine staining for IL-17A or IFN-γ and flow cytometric analysis. Gates in contourplots were set on cytokine$^+$ $CD4^+$ T cells. Graphs depict the mean percentage of cytokine-expressing $CD4^+$ T cells ± SEM (n=5). (b,d) Isolated $CD4^+$ T cells were restimulated with MOG_{35-55}-loaded DCs and numbers of IL-17A and IFN-γ producing cells per $3x10^4$ $CD4^+$ T cells was determined by ELISpot-analysis. Graphs depict the mean number of cytokine-expressing $CD4^+$ T cells per $3x10^4$ $CD4^+$ T cells ± SEM (n=6 per group; ELISpot analysis was performed by Luisa Klotz). One representative experiment out of two independent experiments is shown. * $p<0.05$; ** $p<0.01$.

4.2.8 PPARγ inhibits T cell-mediated licensing of macrophages

During EAE, the interaction of encephalitogenic T cells with CNS APCs, i.e. macrophages and microglia, does not only lead to reactivation of autoreactive T cells but also results in reciprocal activation of macrophages and microglia by encephalitogenic T cells, a process referred to as licensing, that leads to further aggravation of disease[57-60]. We hypothesised that activation of PPARγ in myeloid cells interferes with T cell-mediated licensing of these cells, which would strongly contribute to amelioration of myeloid cell-mediated CNS autimmunity by PPARγ.

To experimentally address whether PPARγ influences T cell-mediated licensing of macrophages, we pretreated BM-Ms with PIO, cocultured them with preactivated MOG_{35-55}-specific T cells in the presence of the specific antigen MOG_{35-55}, and analysed production of NO, TNF-α, and IL-6, as well as CD40 expression and CCL2 production after 24 h or 48 h of coculture.

We observed that upon coculture with activated T cells, macrophages were activated and produced high amounts of the neurotoxic mediators NO and TNF-α, as well as the proinflammatory cytokine IL-6 (Figure 15a-c). Moreover, macrophages exhibited increased expression of CD40 (Figure 15d) and produced high levels of CCL2 (Figure 15e). Importantly, PPARγ activation in macrophages significantly interfered with T cell-mediated licensing, as PIO-treated BM-Ms produced less NO, TNF-α, and IL-6 (Figure 15a-c), exhibited decreased expression of CD40 (Figure 15d), and secreted significantly reduced amounts of CCL2 (Figure 15e).

In conclusion, these findings demonstrate that PPARγ in macrophages interfered with T cell-mediated licensing which resulted in suppressed production of neurotoxic factors and proinflammatory cytokines, decreased upregulation of CD40, and reduced levels of CCL2. These data strongly suggest that during EAE, interference of PPARγ with T cell-mediated licensing ameliorates myeloid-cell-mediated pathology in several ways as this suppresses neurotoxic innate immune responses, T cell reactivation potential, and further recruitment of inflammatory monocytes.

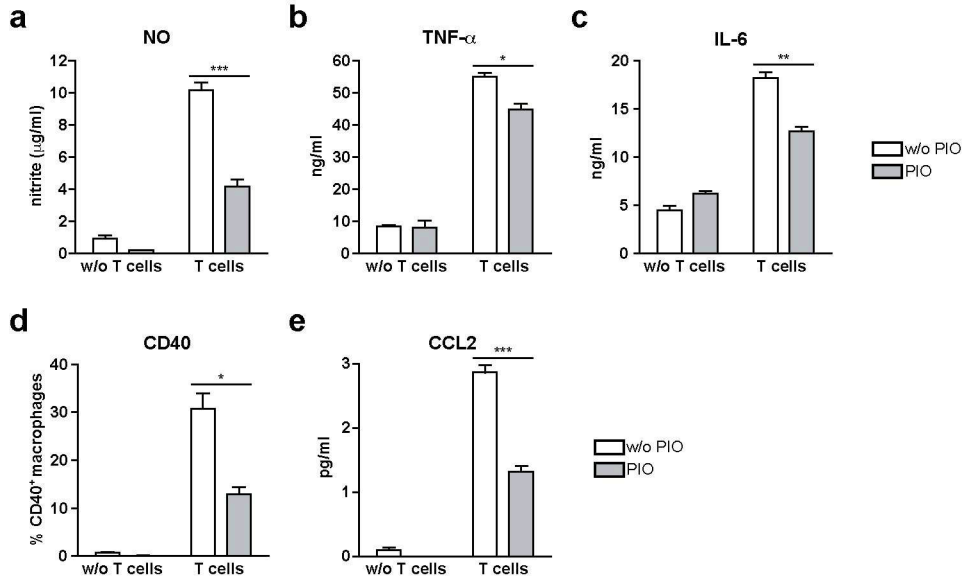

Figure 15 PPARγ controls T cell-mediated licensing of macrophages.

BM-Ms were pretreated with 10 µM PIO for 7 days or left untreated (w/o PIO), and cocultured with αCD3- and αCD28-activated MOG_{35-55}-specific 2D2 $CD4^+$ T cells in the presence of 20 µg/ml MOG_{35-55} at a ratio of (a-d) 10:1 or (e) 1:1 (T cells:BM-Ms). (a) NO production was determined by detecting nitrite levels in the supernatant by Griess Assay after 48 h. (b,c) The concentration of (b) TNFα and (c) IL-6 in the supernatant was quantified by ELISA after 24 h and 48 h of coculture, respectively. (d) CD40 expression by $CD11b^+$ BM-Ms was monitored by flow-cytometry after 24 h of coculture. (e) CCL2 production was determined in the supernatant by ELISA. Shown is one representative experiment out of at least two independent experiments. Graphs depict mean results ± SEM. * $p<0.05$; ** $p<0.01$; ***$p<0.001$.

4.2.9 Summary of chapter 6.2

In the present study, we showed that PPARγ activation *in vivo* resulted in amelioration of EAE during the T cell-mediated induction phase and the effector phase. Further analysis revealed that amelioration was characterised by a strong reduction in levels of inflammatory mediators in the CNS as well as diminished demyelination and axonal damage. We demonstrated that PPARγ in myeloid cells, including CNS-resident microglia and infiltrating macrophages, limited inflammatory responses of myeloid cells during the effector phase of EAE. Importantly, we identified inflammatory monocytes as the key myeloid cell population regulated by PPARγ and could show that monocytes acquire also a microglia-like phenotype during EAE. *In vitro*, activation of PPARγ suppressed innate immune responses involved in neurotoxicity which limited inflammation-induced neurotoxicity mediated by microglial cells. Furthermore, *in vivo* PIO-treatment resulted in reduced expression of MHC-II and CD40 on CNS macrophages and microglia and in line with this we observed that local T cell responses within the CNS of PIO-treated animals were reduced. Importantly, we showed that

PPARγ increased the threshold of myeloid cells towards reciprocal activation of myeloid cells by activated T cells leading to dampened innate immune responses of myeloid cells after T cell-mediated activation, like the production of NO and TNF-α which critically contribute to CNS pathology.

Taken together, PPARγ is a central regulator of monocyte-mediated CNS pathology during autoimmune inflammation which interferes with perpetuation of disease in several ways. On the one hand, it modulates local T cell responses by reducing expression of surface molecules on CNS myeloid cells as well as cytokines necessary for local reactivation of encephalitogenic T cells. On the other hand, PPARγ in myeloid cells suppresses reciprocal activation of myeloid cells by activated T cells which results in neuroprotection through strongly reduced production of neurotoxic factors. Both scenarios result in ameliorated CNS inflammation thus making PPARγ in myeloid cells an attractive target for treatment regimes against CNS autoimmunity.

5 Discussion

5.1 Activation of PPARγ in DCs impairs cross-priming of naive CD8$^+$ T cells by upregulation of B7H1

In the first part of this thesis, we characterised the impact of PPARγ activation in DCs on cross-presentation of soluble antigen and subsequent cross-priming of naive CD8$^+$ T cells. Treatment with the synthetic PPARγ agonist PIO resulted in upregulation of MR expression which in turn led to enhanced MR-mediated uptake of the soluble model antigen OVA and, furthermore, increased amounts of cross-presented OVA *in vitro* and *in vivo*. Importantly, after PPARγ-activation, DCs significantly upregulated the coinhibitory molecule B7H1 which impaired activation of naive CD8$^+$ T cells and resulted in strongly reduced CD8$^+$ T cell effector functions.

Burgdorf et al. demonstrated that MR-expressing DCs represent the subpopulation of DCs that is capable of cross-presenting soluble OVA[25,26] and furthermore, that PPARγ is preferentially expressed by MR$^+$ BM-DCs[103]. Although these data indicate that PPARγ might be involved in the general induction of MR expression in DCs, we showed in this study that PPARγ is not essential for MR baseline expression as PPARγ^{KO} and wildtype BM-DCs expressed the MR at comparable levels (Figure 1c+d). However, we demonstrated that PPARγ in DCs plays an important role in induction of additional MR expression as PIO-mediated activation of PPARγ resulted in significant upregulation of the MR. Although the molecular mechanism of PPARγ-mediated induction of MR expression has not been investigated in this study, it is tempting to speculate that PPARγ-mediated MR upregulation resulted from direct induction of gene transcription after binding to a PPAR response element as two putative PPAR response elements have been identified in the promotor region of the *mannose receptor* gene[104].

Importantly, by employing conditional PPARγ^{KO} BM-DCs we could demonstrate that the observed increase in MR expression and MR-mediated OVA-uptake in DCs was mediated by PPARγ-dependent effects of PIO. However, we still observed a slight increase in MR expression and OVA uptake in response to PIO-treatment in PPARγ^{KO} BM-DCs although both was significantly decreased when compared to PIO-treated

wildtype BM-DCs: 66.7 % for MR expression (Figure 1c,d) and 79.2 % for OVA uptake (Figure 2c,d). As PPARγ^{KO} BM-DCs were generated by Cre-mediated recombination which has been shown to efficiently ablate PPARγ in 70-80 % of the Cre-treated cells[121], we hypothsise that the remaining PIO-effect is most probably due to incomplete PPARγ ablation.

Several studies have identified that CD8α$^+$ splenic DCs are the main cross-presenting DCs *in vivo*[122] and Burgdorf et al. have shown that the MR is expressed by a subpopulation of CD8α$^+$ splenic DCs but not by CD8a$^-$ DCs. MR-expression in CD8α$^+$ splenic DCs was important for transfer of OVA towards cross-presentation after endocytosis[25]. In the study presented here, we extend these findings by showing that PPARγ activation *in vivo* resulted in an increased proportion of MR-expressing splenic DCs (Figure 7a). Although our studies could have suggested that PPARγ also changed the proportion of CD8α$^+$ DCs in the spleen, we did not detect any changes in CD8α expression by splenic DCs after PIO-treatment in preliminary experiments. Therefore we hypothesise that PIO-treatment solely changed the proportion of MR$^+$ splenic DCs within the population of CD8α$^+$ DCs.

PPARγ-activation in BM-DCs *in vitro* and splenic DCs *in vivo* resulted in increased cross-presentation of OVA as demonstrated by increased activation of the costimulation-independent T cell hybridoma B3Z (Figure 3b and Figure 7b). However, despite enhanced cross-presentation we observed that naive, OVA-specific CD8$^+$ T cells exhibited reduced activation and impaired effector functions (Figure 4a,c and Figure 7c,d). In a previous study, Klotz et al. have shown that PPARγ inhibits inflammation-induced upregulation of costimulatory molecules such as CD40, CD80, and CD86 as well as production of the proinflammatory cytokine IL-12 which resulted in CD4$^+$ T cell anergy[79]. However, although our data suggested that missing costimulation might also be the explanation for impaired activation of naive CD8$^+$ T cells by PIO-treated DCs, we show here that in immature DCs PPARγ activation did not significantly alter the expression of costimulatory molecules. Instead PIO-treatment significantly enhanced coinhibitory signals, i.e. the expression of B7H1, which mediates T cell inactivation by signaling via PD-1 expressed by T cells[28]. Importantly, we identified PIO-mediated upregulation of B7H1 in DCs as the key mediator of impaired CD8$^+$ T cell priming after

PPARγ activation as naive $CD8^+$ T cells were properly activated when PIO-treated DCs were deficient in B7H1 or coculture experiments were performed in the presence of a PD-1 blocking antibody. The here presented study reveals a very effective mechanism of antigen-specific $CD8^+$ T cell inactivation which is mediated by strongly enhanced cross-presentation of antigen and simultaneous increase in coinhibitory signaling, namely via B7H1, after activation of PPARγ.

Under physiological conditions this mechanism of tolerance induction might be induced by endogenous PPARγ ligands which include unsaturated fatty acids like linoleic acid metabolites generated by the enzyme 12/15 lipoxygenase or 15-deoxy-$\triangle^{12,14}$-prostaglandin J_2[70]. Interestingly, $PPAR\gamma^{KO}$ BM-DCs exhibit a strongly increased capacity to prime naive $CD4^+$ T cells when compared to $PPAR\gamma^{WT}$ BM-DCs[79] which indicates that endogenous PPARγ ligands could be involved in limiting DC-mediated T cell activation. This could potentially restrict excessive T cell activation and influence the outcome of T cell-mediated autoimmunity. Up to now, several studies have demonstrated a role of PPARγ endogenous ligands in local immune regulation during autoimmune inflammation. Emerson et al. demonstrated that ablation of 12/15 lipoxygenase exacerbated CNS autoimmunity[123], which substantiates the hypothesis that the presence of endogenous PPARγ ligands is crucial for limiting autoimmune inflammation. In line with this, several studies have shown that *in vivo* substitution of the main precursor of these ligands, i.e. linoleic acid, is protective in experimental colitis[124] and EAE[125] and furthermore, that treatment of mice with 15-deoxy-$\triangle^{12,14}$-prostaglandin J_2 during EAE resulted in amelioration of the clinical disease course[126]. Importantly, the T_H2 cytokine IL-4 has been described to induce not only PPARγ in macrophages but also expression of 12/15 lipoxygenase[82]. The latter is mediated via IL-4-induced binding of signal transducer and activator of transduction 6 (STAT6) to STAT6-responsive elements in the promoter region of 12/15 lipoxygenase[127]. Thus, it is conceivable that PPARγ-mediated induction of $CD8^+$ T cell tolerance as described in this study provides at least partial explanation for the anti-inflammatory effects observed after exposure to IL-4.

The here presented mechanism of $CD8^+$ T cell inactivation restricts excessive T cell responses and might be crucial during late stages of inflammation when the MR is upregulated and plays an important role in clearance of self-proteins that are elevated

during wound healing[97]. Although this question has not been investigated in this study, it could be speculated that endogenous ligands activate PPARγ at such late timepoints of inflammation which would result in PPARγ-induced upregulation of the MR for clearance of self-proteins. Without counterregulatory mechanisms, the increase in MR-expression and subsequent enhanced cross-presentation of endogenous antigens could potentially result in activation of self-reactive $CD8^+$ T cells and hence, tissue damage or autoimmunity. One such mechanism to interfere with induction of autoimmunity could be upregulation of B7H1 after PPARγ activation in DCs which results in protection of the organism from $CD8^+$ T cell-mediated pathology.

Interestingly, we observed the PPARγ-mediated inhibitory effect on cross-presentation solely for naive $CD8^+$ T cells as the antigen-specific reactivation of $CD8^+$ memory T cells by PIO-treated BM-DCs was not impaired (Figure 4d). Our observation is in line with other reports which demonstrated *in vitro* that reactivation of memory T cells depends primarily on signal 1, i.e. antigen presentation, and is independent on signal 2, i.e. costimulation[128]. Importantly, our data extend these findings by the observation that activation of memory T cells by professional APCs was independent of coinhibitory signaling mediated by upregulation of B7H1. This finding is especially important with regard to the development of treatment regimes that aim at dampening autoreactive $CD8^+$ T cell responses. Our data suggest that strategies which aim at inducing tolerance in $CD8^+$ T cells by PPARγ-mediated increase in B7H1 expression in DCs will prove useful in preventing initial priming of $CD8^+$ T cells whereas the reactivation of autoreactive memory T cells will not be impaired. In extension of the findings presented here, it will be interesting to investigate in conditional $PPAR\gamma^{KO}$ BM-DCs whether lack of PPARγ is associated with lower expression of B7H1 as reduced coinhibition might strongly increase the risk of developing T cell-mediated autoimmunity. In this regard it is interesting to note that the expression levels of PPARγ were decreased in peripheral blood mononuclear cells (PBMCs) isolated from MS patients compared to healthy controls and disease activity was inversely correlated to the expression of PPARγ[129]. With regard to the presented findings we hypothesise that reduced PPARγ levels possibly coincide with decreased coinhibition. This would imply that in MS patients, PBMCs are more prone to activate autoreactive T cells leading to aggravation of CNS autoimmune inflammation. Furthermore, high PPARγ activity in PBMCs might allow a

good prognosis for the disease course of MS whereas low PPARγ activity and hence low coinhibition might lead to high disease activity.

Taken together, the presented study demonstrates that PPARγ activation in DCs results in induction of $CD8^+$ T cell tolerance which is mediated by strongly increased cross-presentation of antigen and concomitant enhanced signaling via B7H1. This molecular mechanism of $CD8^+$ T cell inactivation might open new possibilities for the development of treatment regimes designed to impede $CD8^+$ T cell-mediated autoimmune diseases.

5.2 PPARγ is a regulator of myeloid cell immunogenicity and a potential candidate for treatment of MS

In the second part of this thesis we investigated the role of PPARγ in myeloid cells during EAE. Treatment with the PPARγ-agonist PIO resulted in amelioration of clinical and histopathological signs of EAE and we demonstrated that PPARγ in myeloid cells is important for limiting CNS inflammation during the effector phase of EAE. Importantly, we identified inflammatory monocytes as the central myeloid cell population regulated by PPARγ. *In vivo* PPARγ activation in CNS myeloid cells suppressed the upregulation of CD40 and MHC-II during the effector phase of EAE and in line with this we observed reduced $CD4^+$ T cell responses within the CNS of PIO-treated mice. Importantly, PPARγ in myeloid cells also suppressed the reciprocal activation of myeloid cells by autoreactive T cells resulting in diminished innate effector functions and thus, attenuated neuroinflammatory responses.

Daily treatment of EAE-diseased mice with the synthetic PPARγ agonist PIO resulted in a milder course of disease during the T cell-mediated induction phase and the effector phase (Figure 8a) during which inflammatory monocytes play a disease-promoting role by production of proinflammatory cytokines and proteolytic enzymes[63]. This is in line with previous findings which demonstrate that PPARγ agonists are effective in ameliorating disease in models of monophasic and relapsing EAE[74,90,126] and further underlines that PPARγ agonists provide therapeutic benefit in CNS autoimmunity.

During the effector phase, we observed a reduction in proinflammatory cytokines and iNOS in the CNS (Figure 8b) indicating that PIO-treatment beneficially alters the inflammatory milieu during EAE which contributes to amelioration of disease by

decreasing neuroinflammation. Among the investigated proinflammatory mediators, we observed a strong reduction in TNF-α and iNOS expression which strongly contribute to neurotoxicity[61]. TNF-α has been shown to be a major effector of immune-mediated demyelination as mice that constitutively express TNF-α within the CNS spontaneously develop a chronic inflammatory demyelinating disease[130]. As TNF-α and iNOS are primarily produced by CNS-resident microglia and infiltrating macrophages[49], PPARγ activation in myeloid cells has probably contributed to this reduction. Furthermore, IL-12 and IL-23, cytokines important for the reactivation of T_H1 and T_H17 cells, respectively[27,29], were found to be reduced in the CNS and concomitantly, we observed that levels of the T cell cytokine IFN-γ were diminished, thus indicating that *in vivo* PPARγ activation interfered with local T cell responses.

In addition, we could show that in the CNS of PIO-treated animals chemokines, including CCL2, CCL3, and CXCL10, were significantly reduced (Figure 11d) and in line with this, strongly reduced numbers of macrophages and T cells were present in the CNS at a late stage of EAE (Figure 11f). Chemokines play an important role during MS and EAE, as the production of chemokines within the CNS results in further recruitment of encephalitogenic T cells, B cells, and inflammatory monocytes which in turn leads to perpetuation of local inflammation and subsequent neurodegeneration. Interfering with chemokine-dependent immune cell recruitment has proven to be effective in amelioration of CNS inflammation[63,131-133] and strategies that have been developed include antibodies against chemokines, small molecules that prevent binding of the chemokine to its receptor, as well as mutant chemokines that act as chemokine receptor antagonists[131]. It is conceivable that treatment regimes that interfere with the recruitment of a range of immune cells will prove more effective than those that target just one cell population. Here, we identified PPARγ as an attractive candidate to modulate immune cell recruitment to the CNS during ongoing inflammation as PIO-treatment resulted in reduced expression of a variety of chemokines, which interferes with recruitment of monocytes, macrophages as well as activated T cells during already established CNS autoimmunity.

Among the investigated chemokines, especially CCL2 plays an important role in EAE. Mice that lack the CCL2 receptor CCR2 are resistant to EAE[134] and Mildner et al. identified $CCR2^+$ inflammatory monocytes to be essential for development of EAE and

crucial for cell-mediated pathology during the effector phase of EAE[63]. In active EAE, the expression of CCL2 correlates with disease severity[135] and CCL2-deficient mice show a delayed onset of disease as well as ameliorated clinical symptoms[136]. Furthermore, interference with CCL2-mediated recruitment of inflammatory monocytes has been shown to be beneficial during the effector phase of EAE[63] and in a model of west nile virus encephalomyelitis[118]. Importantly, we identified myeloid cells as a potential source for CCL2 in the CNS and demonstrated that PPARγ suppressed the production of CCL2 by myeloid cells upon interaction with activated T cells (Figure 15e). Hence, PPARγ in myeloid cells modulates innate immune responses during EAE not only in a qualitative but also in a quantitative manner. Interestingly, CCL20 which attracts T cells was only slightly reduced in PIO-treated animals. CCL20 has been shown to be constitutively expressed on epithelial cells of the choroids plexus in healthy mice which is important for the entry of CCR6-expressing T_H17 cells into the brain and the onset of EAE[55]. As the induction phase is also ameliorated in PIO-treated animals, it is possible that CCL20 is regulated by PPARγ but to an earlier timepoint, namely during the T cell-dependent phase when T_H17 cells are recruited to the CNS.

By employing myeloid cell-specific conditional knockout (LysM-PPARγ^{KO}) mice we demonstrated that PPARγ in myeloid cells, i.e. macrophages and microglia, is primarily important during the effector phase of EAE, as LysM-PPARγ^{KO} mice exhibited an aggravated disease course during the effector but not the induction phase when compared to wildtype mice (Figure 9b). This lack of effect during the induction phase is surprising as our group has previously shown that ablation of PPARγ in DCs results in enhanced $CD4^+$ T cell responses[79] and PPARγ^{KO} macrophages are involved in peripheral induction of T cell responses. This indicates that PPARγ in peripheral myeloid cells does not play a role in regulating initial T cell responses during EAE. However, it is also conceivable that APCs that are not targeted by LysM-Cre-mediated ablation of PPARγ, most probably DCs, are involved in initial T cell priming whereas LysM-expressing myeloid cells only play a minor role.

In a previous study we showed that conditional CD4-PPARγ^{KO} mice exhibit an aggravated disease course during the T cell-mediated induction but not the effector phase which was due to enhanced initial T_H17 responses[89]. Thus, by employing cell-

type specific ablation of PPARγ in different immune cells that play a role during EAE, we revealed that PPARγ interferes at different stages of CNS autoimmunity depending on the cell type involved. In T cells PPARγ plays a role in limiting the induction phase of EAE. In contrast, PPARγ in myeloid cells is an important regulator during the effector phase when it limits local inflammatory responses and hence, CNS pathology.

Importantly, we identified $CCR2^+$ inflammatory monocytes as the central myeloid cell population that is regulated by PPARγ during the effector phase of EAE. Upon depletion of $CCR2^+$ monocytes by administration of an αCCR2 antibody, we observed that EAE was ameliorated in both, wildtype and LysM-$PPAR\gamma^{KO}$ mice, as described before[63] and furthermore, that ablation of inflammatory monocytes resulted in abrogation of the differences observed between wildtype and LysM-$PPAR\gamma^{KO}$ mice during EAE (Figure 9d). This observation further underlines the importance of inflammatory monocytes for EAE pathogenesis in general and furthermore, demonstrates that inflammatory monocytes represent the key myeloid cell population regulated by PPARγ. Interestingly, our findings indicate that although $PPAR\gamma^{KO}$ microglia potentially contribute to the aggravation of disease, $PPAR\gamma^{KO}$ microglia alone are not sufficient to mediate the damage. There are two reasons why this might be the case. Firstly, infiltrating macrophages are important for full activation of microglia as the absence of blood-borne macrophages, e.g. after depletion by clodronate liposomes, was shown to result in impaired activation of microglia in several studies of EAE[49,60,68]. Hence, as in αCCR2-treated LysM-$PPAR\gamma^{KO}$ mice, numbers of infiltrating macrophages in the CNS are low[63], $PPAR\gamma^{KO}$ microglia might not have been appropriately activated which resulted in diminished microglial inflammatory responses and hence, abolished any microglia-mediated differences between LysM-$PPAR\gamma^{KO}$ and LysM-$PPAR\gamma^{WT}$ mice. Secondly, infiltrating Ly-$6C^{hi}$ monocytes have been shown to differentiate not only into CNS macrophages but also acquire a microglia-like phenotype under certain conditions such as in a model of West Nile virus encephalitis[118]. A prerequisite for this differentiation process is an overt blood-brain barrier disruption[137] whereas under steady-state conditions CNS-resident microglia reside in the CNS from birth where they self-renew rather than being replaced by bone marrow-derived progenitors[138]. Importantly, here we show by *in vivo* labelling of

Ly-6C^{hi}CCR2^{+} inflammatory monocytes and adoptive transfer of monocytes that during EAE, inflammatory monocytes invade the brain where they differentiate into macrophages and microglia. These data suggest that the absence of monocyte-to-microglia-differentiation processes in αCCR2-treated animals could also have contributed to the abrogated difference between LysM-PPARγ^{KO} and LysM-PPARγ^{WT} mice after depletion of inflammatory monocytes.

Several reports describe that the activation of PPARγ in macrophages and microglia results in inhibition of inflammatory responses upon activation *in vitro*[69,73,80,81]. In line with these, we observed that PPARγ in macrophages and microglia interfered with the production of neurotoxic factors like TNF-α, NO, and ROS as well as proinflammatory cytokines and importantly, suppressed inflammation-induced neurotoxicity (Figures 11,12). These *in vitro* findings mirrored our *in-vivo* observation that reduced levels of inflammatory mediators were present during the effector phase within the CNS of PIO-treated animals and further indicate that the observed reduction in neuronal damage in the CNS of PIO-treated animals was at least in parts due to a modulation of myeloid cell immunogenicity. The molecular mechanisms that mediate the antiinflammtory effects of PPARγ have not been subject to this study as this issue has already been extensively studied. The primary mechanism by which PPARγ mediates its antiinflammatory action is intranuclear crosstalk with other proinflammatory transcription factors, such as NF-κB, which results in inhibition of these transcription factors and hence, inhibition of gene transcription. This mechanism of action, i.e. the ability of a nuclear receptor to inhibit the activity of a promotor without directly binding to it, is referred to as transrepression[69]. Recently, Glass et al. identified the molecular pathway by which PPARγ is converted into a promotor-specific repressor of NF-κB target genes that regulate immunity and homeostasis. They revealed that ligand-dependent sumoylation directs PPARγ to the promoters of inflammatory genes where it inhibits transcription by stabilising NCoR-containing corepressor complexes at the promotor. As a result, these complexes are not cleared from the promoter and target genes are maintained in a repressed state[139].

During EAE, myeloid cells substantially contribute to neuropathology not only by exerting innate effector functions that induce neurotoxicity but also by reinforcing

adaptive immune responses as APCs. Here, we revealed that PPARγ in macrophages and microglia is important to limit $CD4^+$ T cell responses within the CNS as PIO-treatment resulted in reduced expression of MHC-II on macrophages and microglia as well as of the costimulatory molecule CD40 on macrophages (Figure 13). Importantly, this effect was PPARγ-dependent, as in PIO-treated LysM-$PPAR\gamma^{KO}$ mice we did not observe a reduction of CD40 or MHC-II expression on CNS-infiltrating macrophages.

Both, MHC-II and CD40, are crucial for local restimulation of encephalitogenic $CD4^+$ T cells within the CNS as MHC-II is important for presentation of self-antigens to autoreactive $CD4^+$ T cells[40,51] and CD40 has been demonstrated to critically influence the outcome of EAE[51,58,59]. Our data suggest that PPARγ-mediated suppression of MHC-II and CD40 expression on CNS macrophages and microglia is responsible for reduced reactivation of autoreactive T cells (Figure 14). Importantly, it has been shown that T cell-derived IFN-γ induces MHC-II expression on myeloid cells which contributes to perpetuation of local $CD4^+$ T cell responses[60,140-142]. Our data indicate that reduced reactivation of $CD4^+$ T cells and diminished IFN-γ production, respectively, in PIO-treated animals contributes to keeping MHC-II expression levels low and, hence, also presentation of self-antigens. Interestingly, also microglial MHC-II expression was strongly reduced by PIO-treatment although PIO has been shown to exhibit only limited permeability to cross the BBB under steady-state conditions[143]. Although it is conceivable that this permeability increases during ongoing CNS inflammation due to leakage of the BBB, microglial immune responses could also be modulated indirectly. As microglia are activated upon interaction with infiltrating macrophages[49,60,68] and activated T cells[56,57] which are both targeted in the periphery by oral PIO-treatment, infiltrating immune cells which exhibit a PPARγ-mediated less stimulatory phenotype, do not fully activate CNS-resident microglia. Furthermore, as we could show that inflammatory monocytes also exhibit a microglial phenotype after entry into the inflamed CNS (Figure 10), peripheral modulation of monocyte activation by PIO-treatment will also influence the immunogenicity of the microglial cell population within the CNS. Therefore, PIO is able to indirectly interfere with microglial immune responses despite its limited permeability to cross the BBB. The costimulatory molecule CD40 on CNS macrophages and microglia has been shown to be crucial for the amplification of CNS autoimmunity as CD40 knockout mice are resistant to EAE[58].

Furthermore, treatment of diseased mice with an antibody against CD40L on day 13 after immunisation results in amelioration of disease demonstrating that the interaction of CD40 and CD40L plays an important role in the initiation of EAE but also during the effector phase[58,59]. Hence, our data suggest that PIO-treatment interferes with local reactivation of encephalitogenic T cells also by suppression of myeloid cell costimulation. This leads to a decrease in T cell effector functions and thus, amelioration of disease.

In this line, we observed in the CNS of PIO-treated animals not only a reduction in expression levels of MHC-II and CD40 on CNS myeloid cells but moreover, decreased levels of IL-12 and IL-23, two cytokines that are important for local reactivation of T_H1 and T_H17 cells, respectively (Figure 8,13). Accordingly, we observed a reduction in both, IFN-γ-expressing T_H1 cells and IL-17A-expressing T_H17 cells during the effector phase of EAE demonstrating that autoreactive $CD4^+$ T cell responses were decreased in the CNS of PIO-treated mice. However, the reduction was more pronounced on T_H17 cells than T_H1 responses. This differential effect might be explained by additional direct actions of PPARγ on T_H17 development. We have previously shown that PPARγ acts as a cell-intrinsic regulator of T_H17 differentiation which suppressed T_H17 development *in vitro* and during EAE *in vivo*[89]. However, as the T_H1 response is reduced in the CNS of PIO-treated mice and moreover, autoreactive T cells need to be locally reactivated within the CNS[40], our data suggest that the PIO-mediated reduction in local T cell responses is largely mediated by modulation of CNS APCs and their cytokine milieu.

During CNS inflammation myeloid cells interact with T cells in two directions. On the one hand, myeloid cells provide necessary signals which lead to reactivation of encephalitogenic T cells[58]. On the other hand, myeloid cells reciprocally receive signals of activated T cells through soluble mediators like IFN-γ or GM-CSF[56,57] or cell-cell interactions e.g. via CD40L[58,59], which is referred to as T cell-mediated licensing. Importantly, in this study we identified that PPARγ in myeloid cells limits such T cell-mediated licensing which resulted in ameliorated immune responses, such as production of NO, TNF-α, IL-6, and CCL2 as well as reduced CD40 expression (Figure 15). We therefore hypothesise that PPARγ represents a cell-intrinsic brake that limits the inflammatory activation of myeloid cells by autoreactive T cells during CNS

autoimmunity and that interference with local T cell-mediated licensing of myeloid cells during EAE will ameliorate local innate immune responses within the CNS and hence disease progression.

Taken together, during ongoing CNS autoimmune inflammation the interaction of myeloid cells and encephalitogenic T cells is crucial for the perpetuation of disease. CNS myeloid cells locally reactivate encephalitogenic T cells to perform adaptive effector functions by antigen-presentation via MHC-II and providing sufficient costimulation by signalling through CD40 (Figure 16 (1)) while at the same time, T cell-mediated licensing of CNS myeloid cells elicits local innate immune responses which critically contribute to autoimmune inflammation and CNS damage (Figure 16 (2)). Both steps are not independent but rather fuel each other, resulting in an amplification and fortification of autoimmune inflammation during CNS autoimmunity. As interference with the immunogenic potential of CNS myeloid cells dampens both, T cell reactivation and T cell-mediated myeloid cell licensing, specific targeting of intrinsic myeloid cell activity represents a very effective strategy to interefere with reciprocal interaction of autoreactive T cells and CNS myeloid cells. Importantly, in this study we identified PPARγ as a promising candidate for such targeted modulation of CNS myeloid cell immunogenicity.

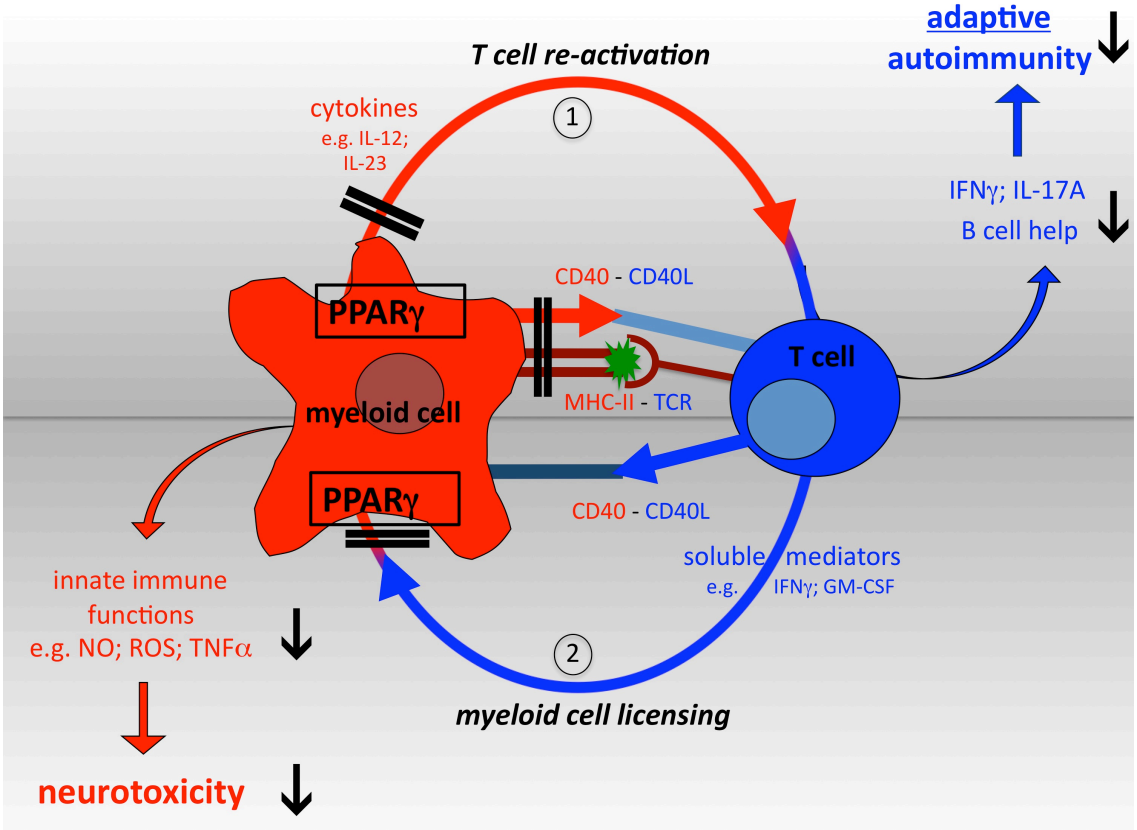

Figure 16 During EAE, PPARγ in myeloid cells interferes with both axes of myeloid : T cell interaction.

During EAE myeloid cells interact with encephalitogenic T cells via MHC-II and CD40 and through secretion of proinflammatory cytokines which results in local T cell reactivation and reinforcement of adaptive immune responses (1). Autoreactive T cells reciprocally license myeloid cells to perform innate effector functions, such as production of NO and ROS or secretion of proinflammatory cytokines including TNF-α, all of which results in neurotoxicity and hence, CNS pathology (2). Importantly, PPARγ in myeloid cells interferes at both steps of this vicious circle, i.e. T cell reactivation and innate neurotoxic responses by myeloid cells, which leads to amliorated CNS autoimmune inflammation.

Macrophages in MS or EAE lesions have been shown to exhibit a classically activated phenotype that has been linked to neurotoxicity due to high production of TNF-α, NO, ROS, and proinflammatory cytokines[61]. In this study we demonstrated that PPARγ activation in macrophages and microglia resulted in reduced expression of these inflammatory mediators in response to stimulation which resembles characteristics associated with the status of alternatively activated macrophages (aaMs). aaMs are induced by T_H2 cytokines IL-4 and IL-13, express several characteristic markers, such as arginase-I, YM1, and IGF-1, and play important roles in the maintenance of tissue homeostasis and wound healing[144]. Preliminary experiments showed that under steady-

state conditions, oral treatment with PIO resulted in increased expression of the aaM-associated markers arginase-I, Ym1, and FIZZ in peritoneal macrophages, splenic monocytes, and blood monocytes. These preliminary data suggest that pharmacological activation of PPARγ indeed induces an aaM-phenotype in myeloid cells rather than simply suppressing the expression of markers, such as TNF-α and iNOS, which have been associated with classically activated macrophages. This observation is especially interesting with regard to the development of novel treatment regimes as several reports have demonstrated beneficial roles for alternatively activated (aa) myeloid cells in immune modulation of CNS autoimmunity. Butovsky et al. demonstrated that the intraventricular injection of IL-4-treated microglia, which express markers of aaMs, significantly improves clinical symptoms of EAE and induces oligodendrogenesis in the CNS[145]. Furthermore, Weber et al. demonstrated that monocytes treated with glatiramer acetate, an approved drug for MS-treatment, promote the development of aa monocytes that suppress the development of T_H17 cells and induced both, T_H2 differentiation and expansion of regulatory T cells during EAE[146]. Therefore, it would be interesting to investigate in future experiments whether PPARγ activation in myeloid cells during EAE induces aa monocytes, macrophages, and microglia and to what extent this contributes to PIO-mediated amelioration of EAE. Importantly, several studies indicate that PPARγ is important for the development of aaMs[147]. Odegaard et al.[148] demonstrated in murine macrophages that PPARγ is required for acquisition and maintenance of the aa phenotype and that IL-4 induced expression of aa markers in a PPARγ-dependent manner. Importantly, Bouhlel et al.[149] reported that activation of PPARγ in human monocytes results in polarisation to an aa phenotype thus indicating that treatment with a PPARγ agonist during EAE might indeed be able to alter the phenotype of monocytes towards an aaM phenotype before they enter the inflamed CNS. However, more experiments need to be performed to further address this issue. Especially analysis of the expression profile of macrophages and microglia isolated from the CNS of PIO-treated EAE-diseased animals would be of interest to confirm a PPARγ-mediated induction of aa macrophages *in vivo* in the context of CNS autoimmunity.

5.3 Concluding remarks

It is known that PPARγ plays an important role in regulation of inflammatory responses by different immune cells including DCs, macrophages, and microglia[69]. In the first part of this study we extend previous findings which showed that activation of PPARγ in DCs induces $CD4^+$ T cell anergy[79] as we now demonstrate that PPARγ in DCs also regulates cross-priming of $CD8^+$ T cells resulting in impaired activation of naive $CD8^+$ T cells. Furthermore, we revealed that during EAE, PPARγ limits myeloid cell-mediated CNS pathology by interfering with the T cell reactivating capacity of CNS macrophages and microglia but also by suppressing innate immune responses upon T cell-mediated licensing of myeloid cells. Thus, both parts of the study further underline that PPARγ is an attractive pharmacological target to treat diseases which are mediated by excessive T cell responses or innate inflammation.

In DCs, PPARγ activation increased MR expression and MR-mediated uptake of the model antigen OVA. Despite significant elevated levels of cross-presented OVA, activation of naive OVA-specific $CD8^+$ T cells was impaired due to concomitant upregulation of the coinhibitory molecule B7H1 (Figure 16). This mechanism of action interferes with excessive $CD8^+$ T cell activation and might be crucial e.g. during late stages of inflammation when the MR is upregulated and plays an important role in the clearance of self-proteins that are elevated during wound healing[97]. MR-mediated increase of cross-presented self-antigen could favour the activation of self-reactive $CD8^+$ T cells and hence, tissue damage. However, concomitant upregulation of the coinhibitory molecule B7H1 interferes with such activation and protects the organism from $CD8^+$ T cell-mediated tissue damage and autoimmunity.

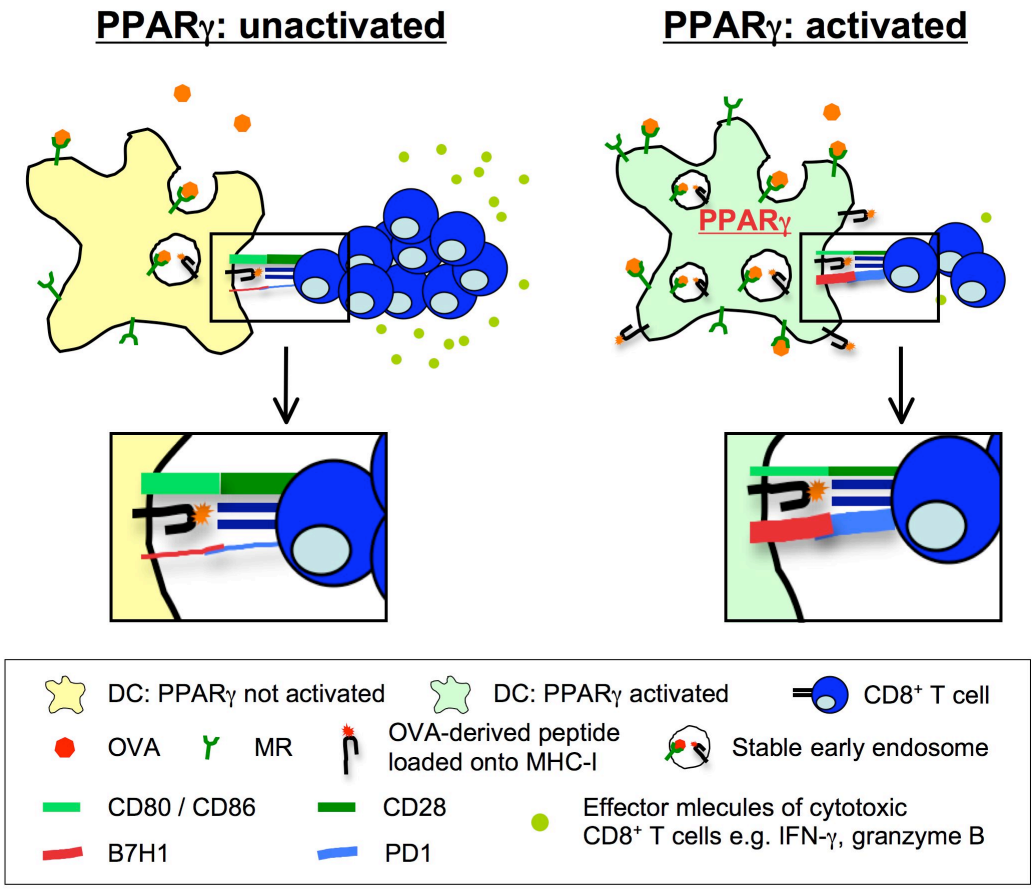

Figure 17 Increased antigen cross-presentation but impaired cross-priming after activation of PPARγ in DCs is mediated by upregulation of B7H1.

PIO-treatment results in increased expression of levels of the MR by DCs that results in enhanced MR-mediated uptake and cross-presentation of the model antigen OVA. Due to strongly increased expression of the coinhibitory molecule B7H1, activation of naive OVA-specific $CD8^+$ T cells is impaired.

In myeloid cells, PPARγ is important to limit local immune responses during the effector phase of EAE. We identified $CCR2^+$ inflammatory monocytes as the key population regulated by PPARγ which are recruited to the inflamed CNS during EAE where they differentiate into macrophages but also acquire a microglia phenotype (Figure 17, (1)). PPARγ suppresses reactivation of encephalitogenic T cells by decreasing MHC-II and CD40 expression on CNS myeloid cells as well as production of cytokines important for reactivation of T_H1 and T_H17 cells (Figure 17, (2+3)). Importantly, PPARγ also interferes with reciprocal licensing of myeloid cells by activated T cells resulting in decreased innate effector functions, such as production of proinflammatory cytokines and chemokines (Figure 17, (4)) and in consequence reduces

inflammation-induced neurotoxicity (Figure 17, (5)). Thus, pharmacological activation of PPARγ in myeloid cells during EAE controls the immunogenic capacity of CNS myeloid cells which contributes to amelioration of EAE in two ways: First, by impairing reactivation of autoreactive T cells by myeloid cells and second, by interfering with T cell-mediated licensing of myeloid cells. Hence, PPARγ represents a brake that limits the mutual interactions between myeloid cells and encephalitogenic T cells within the CNS.

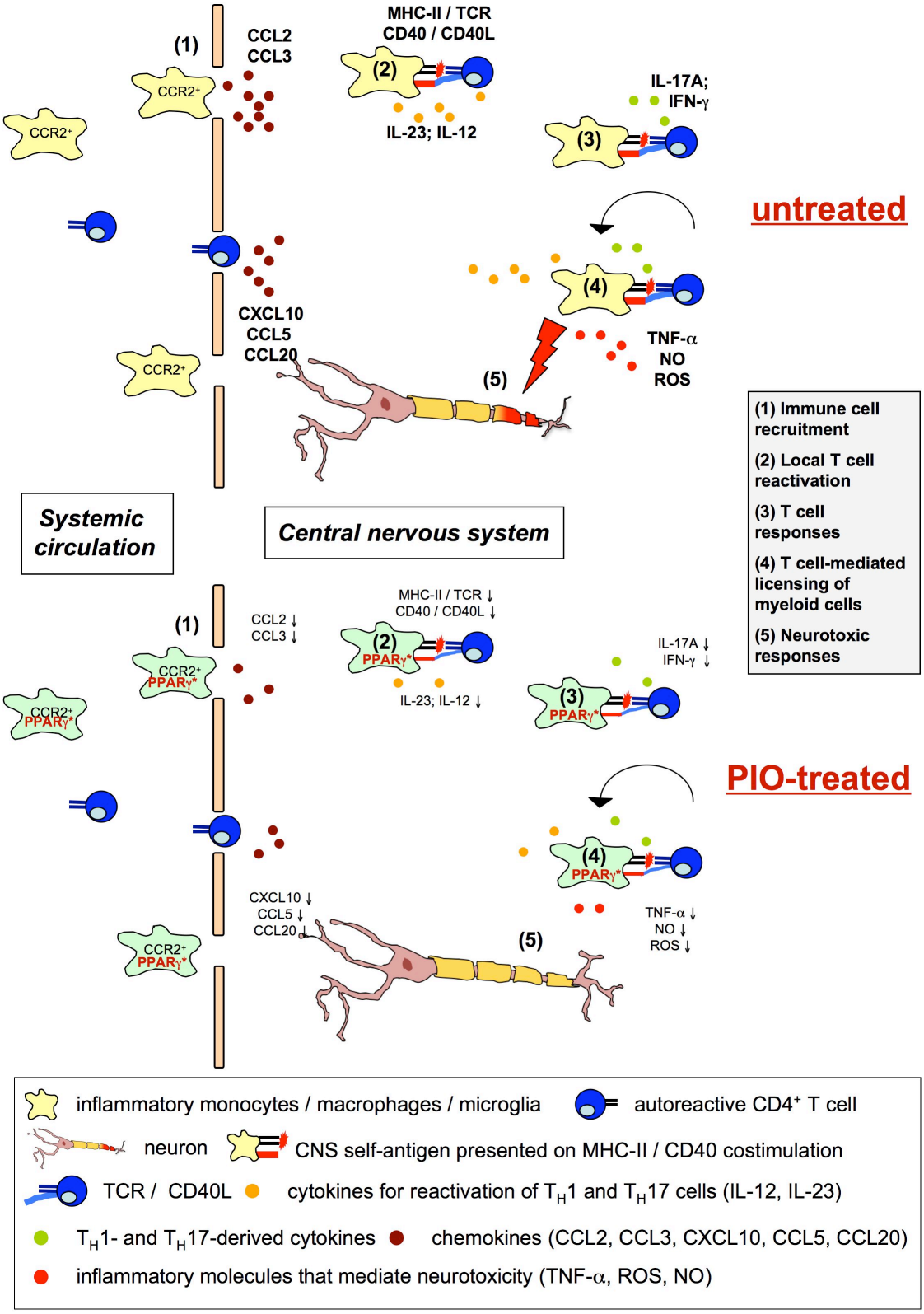
(1)
CCL2
CCL3
CCR2+
MHC-II / TCR
CD40 / CD40L
(2)
IL-23; IL-12
IL-17A;
IFN-γ
(3)
untreated
(4)
CXCL10
CCL5
CCL20
TNF-α
NO
ROS
(5)
Systemic circulation
Central nervous system
(1) Immune cell recruitment
(2) Local T cell reactivation
(3) T cell responses
(4) T cell-mediated licensing of myeloid cells
(5) Neurotoxic responses
CCL2 ↓
CCL3 ↓
MHC-II / TCR ↓
CD40 / CD40L ↓
PPARγ*
IL-17A ↓
IFN-γ ↓
IL-23; IL-12 ↓
PIO-treated
CXCL10 ↓
CCL5 ↓
CCL20 ↓
TNF-α ↓
NO ↓
ROS ↓
inflammatory monocytes / macrophages / microglia
autoreactive CD4+ T cell
neuron
CNS self-antigen presented on MHC-II / CD40 costimulation
TCR / CD40L
cytokines for reactivation of TH1 and TH17 cells (IL-12, IL-23)
TH1- and TH17-derived cytokines
chemokines (CCL2, CCL3, CXCL10, CCL5, CCL20)
inflammatory molecules that mediate neurotoxicity (TNF-α, ROS, NO)

Figure 18 PPARγ is an important regulator of myeloid cell-mediated CNS pathology during the effector phase of EAE.

During EAE, pharmacological activation of PPARγ by PIO-treatment results in amelioration of disease in several ways:
(1) Reduced levels of chemokines interfere with recruitment of inflammatory monocytes and autoreactive T cells.
(2) PIO-treatment reduced the potential of myeloid cells to reactivate autoreactive T cells due to reduced levels of MHC-II and CD40 expression which
(3) results in less T cell activation.
(4) Importantly, PPARγ suppresses T cell-mediated activation of myeloid cells.
(5) This dampens innate immune responses that mediate neurotoxicity, hence, mediating protection.

Taken together, both studies demonstrate that PPARγ in myeloid cells is an attractive pharmaceutical target for treatment of excessive immune responses such as those observed during autoimmunity. Furthermore, both studies show that activation of PPARγ in innate immune cells has beneficial effects on different stages of such (auto-)immune responses, i.e. PPARγ activation interferes with the initial T cell responses but also limits local reactivation of autoreactive T cells and innate effector functions. This is important with regard to treatment of already established T cell autoimmunity as this will allow treatment also after onset of disease. Importantly, in contrast to treatment regimes which aim at interfering with the activation or differentiation of certain autoreactive T cells and depend on antigen recognition, activation of PPARγ in innate APCs leads to antigen-independent amelioration of disease due to a general decrease of their inflammatory potential. Importantly, PPARγ-mediated dampening of innate effector functions mediates protection against innate immune cell-mediated tissue damage.

So far, PPARγ agonists currently approved for treatment of human type 2 diabetes, such as PIO or rosiglitazone, have been demonstrated to be beneficial in a number of autoimmune and other inflammatory diseases, including EAE, inflammatory bowel disease, or psoriasis. However, although PPARγ ligands are generally proved to be safe, they exhibit different undesired metabolic adverse effects, such as fluid retention, peripheral oedema, and heart failure[84]. As the metabolic action of PPARγ is mainly mediated by binding to PPAR response elements in the promotor region of target genes, the development of new PPARγ agonists should be promoted that specifically activate PPARγ to perform immunemodulatory actions that are preferentially mediated by negative interference with proinflammatory transcription factors[69]. The identification of

ligands that preferentially promote antiinflammatory actions could contribute to reducing the metabolic side effects. In line with this, as PIO has been shown to exhibit only limited permeability across the BBB[143], it would be of great importance to identify such PPARγ ligands that can easily cross the BBB to aim at amelioration during CNS autoimmunity.

Taken together, the presented data shed new light on PPARγ-mediated immune regulation and will further help to develop new therapeutic strategies to treat excessive immune responses such as those observed in autoimmune diseases.

6 References

1. Medzhitov, R. & Janeway, C., Jr. Innate immunity. *N Engl J Med* **343**, 338-44 (2000).
2. Janeway, C.A., Jr. & Medzhitov, R. Innate immune recognition. *Annu Rev Immunol* **20**, 197-216 (2002).
3. Abul K. Abbas, A.H.L. *Cellular and molecular immunology*, (Saunders, 2005).
4. Iwasaki, A. & Medzhitov, R. Toll-like receptor control of the adaptive immune responses. *Nat Immunol* **5**, 987-95 (2004).
5. Takeda, K., Kaisho, T. & Akira, S. Toll-like receptors. *Annu Rev Immunol* **21**, 335-76 (2003).
6. Banchereau, J. & Steinman, R.M. Dendritic cells and the control of immunity. *Nature* **392**, 245-52 (1998).
7. Sallusto, F. et al. Rapid and coordinated switch in chemokine receptor expression during dendritic cell maturation. *Eur J Immunol* **28**, 2760-9 (1998).
8. Tang, H.L. & Cyster, J.G. Chemokine Up-regulation and activated T cell attraction by maturing dendritic cells. *Science* **284**, 819-22 (1999).
9. Vyas, J.M., Van der Veen, A.G. & Ploegh, H.L. The known unknowns of antigen processing and presentation. *Nat Rev Immunol* **8**, 607-18 (2008).
10. Kalinski, P., Hilkens, C.M., Wierenga, E.A. & Kapsenberg, M.L. T-cell priming by type-1 and type-2 polarized dendritic cells: the concept of a third signal. *Immunol Today* **20**, 561-7 (1999).
11. Tokoyoda, K., Hauser, A.E., Nakayama, T. & Radbruch, A. Organization of immunological memory by bone marrow stroma. *Nat Rev Immunol* **10**, 193-200.
12. Wong, P. & Pamer, E.G. CD8 T cell responses to infectious pathogens. *Annu Rev Immunol* **21**, 29-70 (2003).
13. Mellman, I. & Steinman, R.M. Dendritic cells: specialized and regulated antigen processing machines. *Cell* **106**, 255-8 (2001).
14. Trombetta, E.S., Ebersold, M., Garrett, W., Pypaert, M. & Mellman, I. Activation of lysosomal function during dendritic cell maturation. *Science* **299**, 1400-3 (2003).
15. Bevan, M.J. Cross-priming for a secondary cytotoxic response to minor H antigens with H-2 congenic cells which do not cross-react in the cytotoxic assay. *J Exp Med* **143**, 1283-8 (1976).
16. Kurts, C. et al. Constitutive class I-restricted exogenous presentation of self antigens in vivo. *J Exp Med* **184**, 923-30 (1996).
17. Albert, M.L., Sauter, B. & Bhardwaj, N. Dendritic cells acquire antigen from apoptotic cells and induce class I-restricted CTLs. *Nature* **392**, 86-9 (1998).
18. Morgan, D.J., Kreuwel, H.T. & Sherman, L.A. Antigen concentration and precursor frequency determine the rate of CD8+ T cell tolerance to peripherally expressed antigens. *Journal of immunology (Baltimore, Md.* **163**, 723-7 (1999).
19. Huang, A.Y. et al. Role of bone marrow-derived cells in presenting MHC class I-restricted tumor antigens. *Science* **264**, 961-5 (1994).
20. Dudziak, D. et al. Differential antigen processing by dendritic cell subsets in vivo. *Science* **315**, 107-11 (2007).
21. Pooley, J.L., Heath, W.R. & Shortman, K. Cutting edge: intravenous soluble antigen is presented to CD4 T cells by CD8- dendritic cells, but cross-presented to CD8 T cells by CD8+ dendritic cells. *J Immunol* **166**, 5327-30 (2001).
22. Amigorena, S. & Savina, A. Intracellular mechanisms of antigen cross presentation in dendritic cells. *Curr Opin Immunol* **22**, 109-17.
23. Belizaire, R. & Unanue, E.R. Targeting proteins to distinct subcellular compartments reveals unique requirements for MHC class I and II presentation. *Proc Natl Acad Sci U S A* **106**, 17463-8 (2009).

24. Burgdorf, S. & Kurts, C. Endocytosis mechanisms and the cell biology of antigen presentation. *Curr Opin Immunol* **20**, 89-95 (2008).
25. Burgdorf, S., Kautz, A., Bohnert, V., Knolle, P.A. & Kurts, C. Distinct pathways of antigen uptake and intracellular routing in CD4 and CD8 T cell activation. *Science* **316**, 612-6 (2007).
26. Burgdorf, S., Lukacs-Kornek, V. & Kurts, C. The mannose receptor mediates uptake of soluble but not of cell-associated antigen for cross-presentation. *J Immunol* **176**, 6770-6 (2006).
27. Reis e Sousa, C. Dendritic cells in a mature age. *Nat Rev Immunol* **6**, 476-83 (2006).
28. Chen, L. Co-inhibitory molecules of the B7-CD28 family in the control of T-cell immunity. *Nat Rev Immunol* **4**, 336-47 (2004).
29. Bettelli, E., Korn, T., Oukka, M. & Kuchroo, V.K. Induction and effector functions of T(H)17 cells. *Nature* **453**, 1051-7 (2008).
30. Yen, D. et al. IL-23 is essential for T cell-mediated colitis and promotes inflammation via IL-17 and IL-6. *J Clin Invest* **116**, 1310-6 (2006).
31. Murphy, C.A. et al. Divergent pro- and antiinflammatory roles for IL-23 and IL-12 in joint autoimmune inflammation. *J Exp Med* **198**, 1951-7 (2003).
32. Westerberg, L.S., Klein, C. & Snapper, S.B. Breakdown of T cell tolerance and autoimmunity in primary immunodeficiency--lessons learned from monogenic disorders in mice and men. *Curr Opin Immunol* **20**, 646-54 (2008).
33. Sakaguchi, S. Naturally arising Foxp3-expressing CD25+CD4+ regulatory T cells in immunological tolerance to self and non-self. *Nat Immunol* **6**, 345-52 (2005).
34. Marrack, P., Kappler, J. & Kotzin, B.L. Autoimmune disease: why and where it occurs. *Nat Med* **7**, 899-905 (2001).
35. Ransohoff, R.M. & Perry, V.H. Microglial physiology: unique stimuli, specialized responses. *Annu Rev Immunol* **27**, 119-45 (2009).
36. Sadovnick, A.D., Ebers, G.C., Dyment, D.A. & Risch, N.J. Evidence for genetic basis of multiple sclerosis. The Canadian Collaborative Study Group. *Lancet* **347**, 1728-30 (1996).
37. Olerup, O. & Hillert, J. HLA class II-associated genetic susceptibility in multiple sclerosis: a critical evaluation. *Tissue Antigens* **38**, 1-15 (1991).
38. Gale, C.R. & Martyn, C.N. Migrant studies in multiple sclerosis. *Prog Neurobiol* **47**, 425-48 (1995).
39. Sibley, W.A., Bamford, C.R. & Clark, K. Clinical viral infections and multiple sclerosis. *Lancet* **1**, 1313-5 (1985).
40. Noseworthy, J.H., Lucchinetti, C., Rodriguez, M. & Weinshenker, B.G. Multiple sclerosis. *N Engl J Med* **343**, 938-52 (2000).
41. Murdoch, D. & Lyseng-Williamson, K.A. Subcutaneous recombinant interferon-beta-1a (Rebif): a review of its use in relapsing-remitting multiple sclerosis. *Drugs* **65**, 1295-312 (2005).
42. Prinz, M. et al. Distinct and nonredundant in vivo functions of IFNAR on myeloid cells limit autoimmunity in the central nervous system. *Immunity* **28**, 675-86 (2008).
43. Neuhaus, O. et al. Multiple sclerosis: comparison of copolymer-1- reactive T cell lines from treated and untreated subjects reveals cytokine shift from T helper 1 to T helper 2 cells. *Proc Natl Acad Sci U S A* **97**, 7452-7 (2000).
44. Duda, P.W., Schmied, M.C., Cook, S.L., Krieger, J.I. & Hafler, D.A. Glatiramer acetate (Copaxone) induces degenerate, Th2-polarized immune responses in patients with multiple sclerosis. *J Clin Invest* **105**, 967-76 (2000).
45. Aharoni, R., Teitelbaum, D., Sela, M. & Arnon, R. Copolymer 1 induces T cells of the T helper type 2 that crossreact with myelin basic protein and suppress experimental autoimmune encephalomyelitis. *Proc Natl Acad Sci U S A* **94**, 10821-6 (1997).
46. Jones, J.L. & Coles, A.J. New treatment strategies in multiple sclerosis. *Exp Neurol* **225**, 34-9.
47. McFarland, H.F. & Martin, R. Multiple sclerosis: a complicated picture of autoimmunity. *Nat Immunol* **8**, 913-9 (2007).

48. Gay, F.W., Drye, T.J., Dick, G.W. & Esiri, M.M. The application of multifactorial cluster analysis in the staging of plaques in early multiple sclerosis. Identification and characterization of the primary demyelinating lesion. *Brain* **120 (Pt 8)**, 1461-83 (1997).

49. Tran, E.H., Hoekstra, K., van Rooijen, N., Dijkstra, C.D. & Owens, T. Immune invasion of the central nervous system parenchyma and experimental allergic encephalomyelitis, but not leukocyte extravasation from blood, are prevented in macrophage-depleted mice. *J Immunol* **161**, 3767-75 (1998).

50. Cannella, B. & Raine, C.S. The adhesion molecule and cytokine profile of multiple sclerosis lesions. *Ann Neurol* **37**, 424-35 (1995).

51. Greter, M. et al. Dendritic cells permit immune invasion of the CNS in an animal model of multiple sclerosis. *Nat Med* **11**, 328-34 (2005).

52. Hemmer, B., Archelos, J.J. & Hartung, H.P. New concepts in the immunopathogenesis of multiple sclerosis. *Nat Rev Neurosci* **3**, 291-301 (2002).

53. McMahon, E.J., Bailey, S.L., Castenada, C.V., Waldner, H. & Miller, S.D. Epitope spreading initiates in the CNS in two mouse models of multiple sclerosis. *Nat Med* **11**, 335-9 (2005).

54. Paterson, P.Y. Transfer of allergic encephalomyelitis in rats by means of lymph node cells. *J Exp Med* **111**, 119-36 (1960).

55. Reboldi, A. et al. C-C chemokine receptor 6-regulated entry of TH-17 cells into the CNS through the choroid plexus is required for the initiation of EAE. *Nat Immunol* **10**, 514-23 (2009).

56. Ponomarev, E.D. et al. GM-CSF production by autoreactive T cells is required for the activation of microglial cells and the onset of experimental autoimmune encephalomyelitis. *J Immunol* **178**, 39-48 (2007).

57. Aloisi, F., De Simone, R., Columba-Cabezas, S., Penna, G. & Adorini, L. Functional maturation of adult mouse resting microglia into an APC is promoted by granulocyte-macrophage colony-stimulating factor and interaction with Th1 cells. *J Immunol* **164**, 1705-12 (2000).

58. Becher, B., Durell, B.G., Miga, A.V., Hickey, W.F. & Noelle, R.J. The clinical course of experimental autoimmune encephalomyelitis and inflammation is controlled by the expression of CD40 within the central nervous system. *J Exp Med* **193**, 967-74 (2001).

59. Ponomarev, E.D., Shriver, L.P. & Dittel, B.N. CD40 expression by microglial cells is required for their completion of a two-step activation process during central nervous system autoimmune inflammation. *J Immunol* **176**, 1402-10 (2006).

60. Benveniste, E.N. Role of macrophages/microglia in multiple sclerosis and experimental allergic encephalomyelitis. *J Mol Med* **75**, 165-73 (1997).

61. Hendriks, J.J., Teunissen, C.E., de Vries, H.E. & Dijkstra, C.D. Macrophages and neurodegeneration. *Brain Res Brain Res Rev* **48**, 185-95 (2005).

62. Heppner, F.L. et al. Experimental autoimmune encephalomyelitis repressed by microglial paralysis. *Nat Med* **11**, 146-52 (2005).

63. Mildner, A. et al. CCR2+Ly-6Chi monocytes are crucial for the effector phase of autoimmunity in the central nervous system. *Brain* **132**, 2487-500 (2009).

64. King, I.L., Dickendesher, T.L. & Segal, B.M. Circulating Ly-6C+ myeloid precursors migrate to the CNS and play a pathogenic role during autoimmune demyelinating disease. *Blood* **113**, 3190-7 (2009).

65. Hanisch, U.K. & Kettenmann, H. Microglia: active sensor and versatile effector cells in the normal and pathologic brain. *Nat Neurosci* **10**, 1387-94 (2007).

66. Davalos, D. et al. ATP mediates rapid microglial response to local brain injury in vivo. *Nat Neurosci* **8**, 752-8 (2005).

67. Berger, T. et al. Experimental autoimmune encephalomyelitis: the antigen specificity of T lymphocytes determines the topography of lesions in the central and peripheral nervous system. *Lab Invest* **76**, 355-64 (1997).

68. Huitinga, I., van Rooijen, N., de Groot, C.J., Uitdehaag, B.M. & Dijkstra, C.D. Suppression of experimental allergic encephalomyelitis in Lewis rats after elimination of macrophages. *J Exp Med* **172**, 1025-33 (1990).

69. Tontonoz, P. & Spiegelman, B.M. Fat and beyond: the diverse biology of PPARgamma. *Annu Rev Biochem* **77**, 289-312 (2008).

70. Varga, T. & Nagy, L. Nuclear receptors, transcription factors linking lipid metabolism and immunity: the case of peroxisome proliferator-activated receptor gamma. *Eur J Clin Invest* **38**, 695-707 (2008).

71. Bardot, O., Aldridge, T.C., Latruffe, N. & Green, S. PPAR-RXR heterodimer activates a peroxisome proliferator response element upstream of the bifunctional enzyme gene. *Biochem Biophys Res Commun* **192**, 37-45 (1993).

72. Jiang, C., Ting, A.T. & Seed, B. PPAR-gamma agonists inhibit production of monocyte inflammatory cytokines. *Nature* **391**, 82-6 (1998).

73. Ricote, M., Li, A.C., Willson, T.M., Kelly, C.J. & Glass, C.K. The peroxisome proliferator-activated receptor-gamma is a negative regulator of macrophage activation. *Nature* **391**, 79-82 (1998).

74. Yang, X.Y. et al. Activation of human T lymphocytes is inhibited by peroxisome proliferator-activated receptor gamma (PPARgamma) agonists. PPARgamma co-association with transcription factor NFAT. *J Biol Chem* **275**, 4541-4 (2000).

75. Cunard, R. et al. Repression of IFN-gamma expression by peroxisome proliferator-activated receptor gamma. *J Immunol* **172**, 7530-6 (2004).

76. Sakamoto, J. et al. Activation of human peroxisome proliferator-activated receptor (PPAR) subtypes by pioglitazone. *Biochem Biophys Res Commun* **278**, 704-11 (2000).

77. Racke, M.K. et al. Nuclear receptors and autoimmune disease: the potential of PPAR agonists to treat multiple sclerosis. *J Nutr* **136**, 700-3 (2006).

78. Nencioni, A. et al. Dendritic cell immunogenicity is regulated by peroxisome proliferator-activated receptor gamma. *J Immunol* **169**, 1228-35 (2002).

79. Klotz, L. et al. Peroxisome proliferator-activated receptor gamma control of dendritic cell function contributes to development of CD4+ T cell anergy. *J Immunol* **178**, 2122-31 (2007).

80. Storer, P.D., Xu, J., Chavis, J. & Drew, P.D. Peroxisome proliferator-activated receptor-gamma agonists inhibit the activation of microglia and astrocytes: implications for multiple sclerosis. *J Neuroimmunol* **161**, 113-22 (2005).

81. Gurley, C. et al. Microglia and Astrocyte Activation by Toll-Like Receptor Ligands: Modulation by PPAR-gamma Agonists. *PPAR Res* **2008**, 453120 (2008).

82. Huang, J.T. et al. Interleukin-4-dependent production of PPAR-gamma ligands in macrophages by 12/15-lipoxygenase. *Nature* **400**, 378-82 (1999).

83. Xu, J., Barger, S.W. & Drew, P.D. The PPAR-gamma Agonist 15-Deoxy-Delta-Prostaglandin J(2) Attenuates Microglial Production of IL-12 Family Cytokines: Potential Relevance to Alzheimer's Disease. *PPAR Res* **2008**, 349185 (2008).

84. Pershadsingh, H.A. Peroxisome proliferator-activated receptor-gamma: therapeutic target for diseases beyond diabetes: quo vadis? *Expert Opin Investig Drugs* **13**, 215-28 (2004).

85. Ellis, C.N. et al. Troglitazone improves psoriasis and normalizes models of proliferative skin disease: ligands for peroxisome proliferator-activated receptor-gamma inhibit keratinocyte proliferation. *Arch Dermatol* **136**, 609-16 (2000).

86. Saubermann, L.J. et al. Peroxisome proliferator-activated receptor gamma agonist ligands stimulate a Th2 cytokine response and prevent acute colitis. *Inflamm Bowel Dis* **8**, 330-9 (2002).

87. Yuan, Z. et al. Peroxisome proliferator-activated receptor-gamma ligands ameliorate experimental autoimmune myocarditis associated with inhibition of self-sensitive T cells. *J Cardiovasc Pharmacol* **43**, 868-75 (2004).

88. Yuan, Z. et al. Cardioprotective effects of peroxisome proliferator activated receptor gamma activators on acute myocarditis: anti-inflammatory actions associated with nuclear factor kappaB blockade. *Heart* **91**, 1203-8 (2005).

89. Klotz, L. et al. The nuclear receptor PPAR gamma selectively inhibits Th17 differentiation in a T cell-intrinsic fashion and suppresses CNS autoimmunity. *J Exp Med* **206**, 2079-89 (2009).

90. Feinstein, D.L. et al. Peroxisome proliferator-activated receptor-gamma agonists prevent experimental autoimmune encephalomyelitis. *Ann Neurol* **51**, 694-702 (2002).

91. Niino, M. et al. Amelioration of experimental autoimmune encephalomyelitis in C57BL/6 mice by an agonist of peroxisome proliferator-activated receptor-gamma. *J Neuroimmunol* **116**, 40-8 (2001).

92. Ansari, M.J. et al. The programmed death-1 (PD-1) pathway regulates autoimmune diabetes in nonobese diabetic (NOD) mice. *The Journal of experimental medicine* **198**, 63-9 (2003).

93. Karasuyama, H. & Melchers, F. Establishment of mouse cell lines which constitutively secrete large quantities of interleukin 2, 3, 4 or 5, using modified cDNA expression vectors. *Eur J Immunol* **18**, 97-104 (1988).

94. Stockinger, B., Zal, T., Zal, A. & Gray, D. B cells solicit their own help from T cells. *J Exp Med* **183**, 891-9 (1996).

95. Pang, Z.J., Zhou, M., Chen, Y. & Wan, J. Macrophage colony-stimulating factor reduces tert-butyl hydroperoxide induced oxidative injury to monocytes/macrophages. *Atherosclerosis* **147**, 33-40 (1999).

96. Karttunen, J., Sanderson, S. & Shastri, N. Detection of rare antigen-presenting cells by the lacZ T-cell activation assay suggests an expression cloning strategy for T-cell antigens. *Proc Natl Acad Sci U S A* **89**, 6020-4 (1992).

97. Lee, S.J. et al. Mannose receptor-mediated regulation of serum glycoprotein homeostasis. *Science* **295**, 1898-901 (2002).

98. Kurts, C. et al. CD4+ T cell help impairs CD8+ T cell deletion induced by cross-presentation of self-antigens and favors autoimmunity. *J Exp Med* **186**, 2057-62 (1997).

99. Dong, H. et al. B7-H1 determines accumulation and deletion of intrahepatic CD8(+) T lymphocytes. *Immunity* **20**, 327-36 (2004).

100. He, W. et al. Adipose-specific peroxisome proliferator-activated receptor gamma knockout causes insulin resistance in fat and liver but not in muscle. *Proc Natl Acad Sci U S A* **100**, 15712-7 (2003).

101. Clausen, B.E., Burkhardt, C., Reith, W., Renkawitz, R. & Forster, I. Conditional gene targeting in macrophages and granulocytes using LysMcre mice. *Transgenic Res* **8**, 265-77 (1999).

102. Bettelli, E. et al. Myelin oligodendrocyte glycoprotein-specific T cell receptor transgenic mice develop spontaneous autoimmune optic neuritis. *J Exp Med* **197**, 1073-81 (2003).

103. Klotz, L. et al. Increased antigen cross-presentation but impaired cross-priming after activation of peroxisome proliferator-activated receptor gamma is mediated by up-regulation of B7H1. *J Immunol* **183**, 129-36 (2009).

104. Coste, A. et al. PPARgamma promotes mannose receptor gene expression in murine macrophages and contributes to the induction of this receptor by IL-13. *Immunity* **19**, 329-39 (2003).

105. Burgdorf, S., Scholz, C., Kautz, A., Tampe, R. & Kurts, C. Spatial and mechanistic separation of cross-presentation and endogenous antigen presentation. *Nature immunology* (2008).

106. Houde, M. et al. Phagosomes are competent organelles for antigen cross-presentation. *Nature* **425**, 402-6 (2003).

107. Castellino, F. et al. Receptor-mediated uptake of antigen/heat shock protein complexes results in major histocompatibility complex class I antigen presentation via two distinct processing pathways. *J Exp Med* **191**, 1957-64 (2000).

108. Porgador, A., Yewdell, J.W., Deng, Y., Bennink, J.R. & Germain, R.N. Localization, quantitation, and in situ detection of specific peptide-MHC class I complexes using a monoclonal antibody. *Immunity* **6**, 715-26 (1997).

109. Sanderson, S. & Shastri, N. LacZ inducible, antigen/MHC-specific T cell hybrids. *International immunology* **6**, 369-76 (1994).

110. Karttunen, J., Sanderson, S. & Shastri, N. Detection of rare antigen-presenting cells by the lacZ T-cell activation assay suggests an expression cloning strategy for T-cell antigens. *Proceedings of the National Academy of Sciences of the United States of America* **89**, 6020-4 (1992).

111. Zeelenberg, I.S. et al. Targeting tumor antigens to secreted membrane vesicles in vivo induces efficient antitumor immune responses. *Cancer research* **68**, 1228-35 (2008).

112. Hogquist, K.A. et al. T cell receptor antagonist peptides induce positive selection. *Cell* **76**, 17-27 (1994).

113. Berg, M. et al. Cross-presentation of antigens from apoptotic tumor cells by liver sinusoidal endothelial cells leads to tumor-specific CD8+ T cell tolerance. *European journal of immunology* **36**, 2960-70 (2006).

114. Welch, J.S., Ricote, M., Akiyama, T.E., Gonzalez, F.J. & Glass, C.K. PPARgamma and PPARdelta negatively regulate specific subsets of lipopolysaccharide and IFN-gamma target genes in macrophages. *Proc Natl Acad Sci U S A* **100**, 6712-7 (2003).

115. Mack, M. et al. Expression and characterization of the chemokine receptors CCR2 and CCR5 in mice. *J Immunol* **166**, 4697-704 (2001).

116. Bruhl, H. et al. Targeting of Gr-1+,CCR2+ monocytes in collagen-induced arthritis. *Arthritis Rheum* **56**, 2975-85 (2007).

117. Tacke, F. et al. Immature monocytes acquire antigens from other cells in the bone marrow and present them to T cells after maturing in the periphery. *J Exp Med* **203**, 583-97 (2006).

118. Getts, D.R. et al. Ly6c+ "inflammatory monocytes" are microglial precursors recruited in a pathogenic manner in West Nile virus encephalitis. *J Exp Med* **205**, 2319-37 (2008).

119. Van Rooijen, N. & Sanders, A. Liposome mediated depletion of macrophages: mechanism of action, preparation of liposomes and applications. *J Immunol Methods* **174**, 83-93 (1994).

120. Sedgwick, J.D. et al. Isolation and direct characterization of resident microglial cells from the normal and inflamed central nervous system. *Proc Natl Acad Sci U S A* **88**, 7438-42 (1991).

121. Klotz, L. et al. Peroxisome proliferator-activated receptor gamma control of dendritic cell function contributes to development of CD4+ T cell anergy. *Journal of immunology (Baltimore, Md.* **178**, 2122-31 (2007).

122. den Haan, J.M., Lehar, S.M. & Bevan, M.J. CD8(+) but not CD8(-) dendritic cells cross-prime cytotoxic T cells in vivo. *J Exp Med* **192**, 1685-96 (2000).

123. Emerson, M.R. & LeVine, S.M. Experimental allergic encephalomyelitis is exacerbated in mice deficient for 12/15-lipoxygenase or 5-lipoxygenase. *Brain Res* **1021**, 140-5 (2004).

124. Bassaganya-Riera, J. et al. Activation of PPAR gamma and delta by conjugated linoleic acid mediates protection from experimental inflammatory bowel disease. *Gastroenterology* **127**, 777-91 (2004).

125. Harbige, L.S., Yeatman, N., Amor, S. & Crawford, M.A. Prevention of experimental autoimmune encephalomyelitis in Lewis rats by a novel fungal source of gamma-linolenic acid. *Br J Nutr* **74**, 701-15 (1995).

126. Diab, A. et al. Peroxisome proliferator-activated receptor-gamma agonist 15-deoxy-Delta(12,14)-prostaglandin J(2) ameliorates experimental autoimmune encephalomyelitis. *J Immunol* **168**, 2508-15 (2002).

127. Heydeck, D. et al. Interleukin-4 and -13 induce upregulation of the murine macrophage 12/15-lipoxygenase activity: evidence for the involvement of transcription factor STAT6. *Blood* **92**, 2503-10 (1998).

128. Mullbacher, A. & Flynn, K. Aspects of cytotoxic T cell memory. *Immunological reviews* **150**, 113-27 (1996).

129. Klotz, L. et al. Proinflammatory stimulation and pioglitazone treatment regulate peroxisome proliferator-activated receptor gamma levels in peripheral blood mononuclear cells from healthy controls and multiple sclerosis patients. *J Immunol* **175**, 4948-55 (2005).

130. Probert, L., Akassoglou, K., Pasparakis, M., Kontogeorgos, G. & Kollias, G. Spontaneous inflammatory demyelinating disease in transgenic mice showing central nervous system-specific expression of tumor necrosis factor alpha. *Proc Natl Acad Sci U S A* **92**, 11294-8 (1995).

131. Proudfoot, A.E., de Souza, A.L. & Muzio, V. The use of chemokine antagonists in EAE models. *J Neuroimmunol* **198**, 27-30 (2008).

132. Tsunoda, I., Lane, T.E., Blackett, J. & Fujinami, R.S. Distinct roles for IP-10/CXCL10 in three animal models, Theiler's virus infection, EAE, and MHV infection, for multiple sclerosis: implication of differing roles for IP-10. *Mult Scler* **10**, 26-34 (2004).

133. Chen, W. et al. In vivo administration of plasmid DNA encoding recombinant immunotoxin DT390-IP-10 attenuates experimental autoimmune encephalomyelitis. *J Autoimmun* **28**, 30-40 (2007).

134. Fife, B.T., Huffnagle, G.B., Kuziel, W.A. & Karpus, W.J. CC chemokine receptor 2 is critical for induction of experimental autoimmune encephalomyelitis. *J Exp Med* **192**, 899-905 (2000).

135. Glabinski, A.R., Bielecki, B., O'Bryant, S., Selmaj, K. & Ransohoff, R.M. Experimental autoimmune encephalomyelitis: CC chemokine receptor expression by trafficking cells. *J Autoimmun* **19**, 175-81 (2002).

136. Huang, D.R., Wang, J., Kivisakk, P., Rollins, B.J. & Ransohoff, R.M. Absence of monocyte chemoattractant protein 1 in mice leads to decreased local macrophage recruitment and antigen-specific T helper cell type 1 immune response in experimental autoimmune encephalomyelitis. *J Exp Med* **193**, 713-26 (2001).

137. Mildner, A. et al. Microglia in the adult brain arise from Ly-6ChiCCR2+ monocytes only under defined host conditions. *Nat Neurosci* **10**, 1544-53 (2007).

138. Ajami, B., Bennett, J.L., Krieger, C., Tetzlaff, W. & Rossi, F.M. Local self-renewal can sustain CNS microglia maintenance and function throughout adult life. *Nat Neurosci* **10**, 1538-43 (2007).

139. Pascual, G. et al. A SUMOylation-dependent pathway mediates transrepression of inflammatory response genes by PPAR-gamma. *Nature* **437**, 759-63 (2005).

140. Frei, K. et al. Antigen presentation and tumor cytotoxicity by interferon-gamma-treated microglial cells. *Eur J Immunol* **17**, 1271-8 (1987).

141. Williams, K., Ulvestad, E. & Antel, J. Immune regulatory and effector properties of human adult microglia studies in vitro and in situ. *Adv Neuroimmunol* **4**, 273-81 (1994).

142. Woodroofe, M.N., Hayes, G.M. & Cuzner, M.L. Fc receptor density, MHC antigen expression and superoxide production are increased in interferon-gamma-treated microglia isolated from adult rat brain. *Immunology* **68**, 421-6 (1989).

143. Maeshiba, Y. et al. Disposition of the new antidiabetic agent pioglitazone in rats, dogs, and monkeys. *Arzneimittelforschung* **47**, 29-35 (1997).

144. Mosser, D.M. & Edwards, J.P. Exploring the full spectrum of macrophage activation. *Nat Rev Immunol* **8**, 958-69 (2008).

145. Butovsky, O. et al. Microglia activated by IL-4 or IFN-gamma differentially induce neurogenesis and oligodendrogenesis from adult stem/progenitor cells. *Mol Cell Neurosci* **31**, 149-60 (2006).

146. Weber, M.S. et al. Type II monocytes modulate T cell-mediated central nervous system autoimmune disease. *Nat Med* **13**, 935-43 (2007).

147. Gales, A. et al. PPARgamma controls dectin-1 expression required for host antifungal defense against Candida albicans. *PLoS Pathog* **6**, e1000714.

148. Odegaard, J.I. et al. Macrophage-specific PPARgamma controls alternative activation and improves insulin resistance. *Nature* **447**, 1116-20 (2007).

149. Bouhlel, M.A. et al. PPARgamma activation primes human monocytes into alternative M2 macrophages with anti-inflammatory properties. *Cell Metab* **6**, 137-43 (2007).

7 Table of Figures

8 Abbreviations

aa	alternatively activated
aaM	alternatively activated macrophage
APC	antigen-presenting cell
APP	amyloid precursor protein
BBB	blood-brain barrier
BCR	B cell receptor
BM-DC	bone marrow-derived dendritic cell
BSA	bovine serum albumin
C	Celsius
CCL	chemokine ligand 2
CCR	chemokine receptor
CD	cluster of differentiation
CD40L	CD40 ligand
CFSE	carboxy-fluorescein diacetate succinimidyl ester
CMC	carboxymethylcellulose
CNS	central nervous system
CPRG	chlorophenol red-β-galactosidase
DC	dendritic cell
DMSO	dimethylsulfoxide
DZ	dendritische Zelle
EAE	experimental autoimmune encephalomyelitis
EDTA	ethylene diamine tetraacetic acid
FCS	fetal calf serum
FITC	Fluorescin-Isothiocyanat
g	gram
g	gravity

GBSS	Grey's balanced salt solution
GM-CSF	granulocyte macrophage colony-stimulating factor
h	hours
HLA	human leukocyte antigen
i.p.	intraperitoneal
i.v.	intravenous
IFN	interferon
Ig	immunoglobulin
IL	interleukin
iNOS	inducible nitric oxide synthase
IONO	ionomycin
KO	knockout
LFB	luxol fast blue
LysM	lysozyme M
M	molar
µ	micro
M-CSF	macrophage colony-stimulating factor
MFI	mean fluorescence intensity
mg	milligram
MHC	major histocompatibility complex
min	minutes
ml	millilitre
MR	mannose receptor
n	nano
NEAA	non-essential amino acids
NF-κB	nuclear factor-κB
ng	nanogram
NO	nitric oxide

OD	optical density
OVA	ovalbumin
PAMP	pathogen-associated molecular pattern
PBS	phosphate buffered saline
PFA	paraformaldehyd
PIO	pioglitazone
PMA	phorbol myristate actetate
pMg	primary microglia
PPARγ	peroxisome proliferator-activated receptor gamma
PRR	pattern recognition receptor
Rag-1	recombination-activating gene 1
rpm	rounds per minute
ROS	reactive oxygen species
S8L	OVA-derived peptide SIINFEKL (amino acids 257-264)
s.c.	subcutaneously
SEM	standard error of the mean
SSC	sideward scatter
STAT6	activator of transduction 6
TCR	T cell receptor
T_H1	T helper 1 cells
T_H2	T helper 2 cells
T_H17	T helper 17 cells
T_{reg}	regulatory T cells
TNF-α	tumor necrosis factor-alpha
TZD	thiazolidinediones
v/v	volume per volume
w/v	weight per volume
WT	wildtype

ZNS	zentrales Nervensystem